1-1-2013

Quantifying The Risks Of Soil Lead In Urban Community Gardens: Sampling To Account For Spatial Variability

Lauren Elizabeth-Korgol Bugdalski
Wayne State University,

QUANTIFYING THE RISKS OF SOIL LEAD IN URBAN COMMUNITY GARDENS: SAMPLING TO ACCOUNT FOR SPATIAL VARIABILITY

by

LAUREN E. BUGDALSKI

THESIS

Submitted to the Graduate School

of Wayne State University,

Detroit, Michigan

in partial fulfillment of the requirements

for the degree of

MASTER OF SCIENCE

2013

MAJOR: GEOLOGY

Approved By:

_____

Advisor Date

DEDICATION

To my parents,

Clifford and Lillian Bugdalski

Without your love and self-sacrifice, I would never be where I am today.

ACKNOWLEDGMENTS

First, I want to convey my deepest gratitude to my advisor, Dr. Lawrence Lemke, for his unwavering support, patience, and commitment to my growth as a scientist. Throughout the course of my undergraduate and graduate research, he has profoundly impacted my development as both a scientist and a person, for which I am grateful.

I would also like to thank my thesis committee members, Dr. Shawn McElmurry and Dr. Mark Baskaran for their contributions to this document as well as all they have taught me over the course of my studies.

This research would not have been possible without financial support through a Wayne State University research assistantship and a Geology Department Teaching assistantship, and I am very grateful for both of these opportunities.

I wish to thank my lab mates for their support over the years. In particular, I want to thank Gianluca Sperone for his assistance with GIS analysis, and more importantly for his friendship, advice and encouragement. I also want to thank Lena Pappas and Brendan O'Leary for their friendship.

I would like to thank all the undergraduate and graduate students who assisted with field and laboratory activities: Laura Leix, Mollie Monaghan, James Piaskeci, Rachel Malburg, Josiah Clemence, Jonathan Espinoza, Paula Lancaster, and Damon Sims. I would also like to thank Patrick Crouch of Earthworks Urban Farm and Edith Floyd of Growing Joy Gardens for graciously providing access to their community gardens.

Finally, I would like to thank my family and boyfriend Jon for their tireless encouragement, love, and support. I could not ask for better people to share my life and future with.

TABLE OF CONTENTS

LIST OF TABLES

LIST OF FIGURES

Chapter 1

Introduction

1.0 Introduction

Many urban areas across the United States face legacy contamination resulting from historical uses of lead in paint, gasoline additives, and past and present industrial activities (USEPA, 1998). Lead based paint has been banned in the United States since 1978. Leaded gasoline was first used in 1922, and was banned in an amendment to the Clean Air Act enacted in 1990, which allowed 5 years for the petroleum industry to phase leaded gasoline additives out of their products. Industry emissions have recently been more strictly regulated by amendments to the USEPA's National Ambient Air Quality Standards, which reduced the permissible amount of lead emitted in industry production from 1.0 ton/year to 0.5 ton/year and mandated air quality monitoring in urban areas with more than 500,000 residents (USEPA, 2010).

These regulations have contributed to a considerable reduction in the number of children with elevated blood lead levels nationwide. In 1978, the median blood lead level in children between the ages of one and five was 13.5 µg/dL. By 2008, this level had fallen to 1.5 µg/dL (USEPA, 2013). Elevated blood lead levels in children can lead to severe adverse health effects, including learning impairments, lower IQ, and slowed growth (ATSDR, 2007; Demayo et al., 1982). Adults can be affected by elevated blood lead levels as well, but to a lesser degree than children (ATSDR, 2007). Recent work has shown that significant nervous system damage can occur in children at levels well below the previous Centers for Disease Control (CDC) child "blood lead level of concern" of 10 µg/dL (Canfield et al., 2003; Jusko et al., 2008; Lanphear et al., 2005). As a result, the CDC recently lowered its child blood lead level reference value to 5 µg/dL (CDC, 2012).

Despite measures taken to decrease child blood lead levels, many children in urban areas still have blood lead levels greater than 10 µg/dL, potentially due to soil lead contamination in these areas (Filippelli and Laidlaw, 2010). Soil is one of the most significant, yet overlooked, exposure pathways of lead into the human body (Filippelli and Laidlaw, 2010; Mielke and Reagan, 1998). Soil derived material constitutes 20-80% of dust in urban homes (Paustenbach et al., 1997), and these fine soil particles can be easily ingested or inhaled. Contaminated soil can also be ingested through direct consumption by children (Stanek et al., 2012; USEPA, 1997b), or consumption of produce grown in contaminated soil (Finster et al., 2003; USEPA, 1997a).

Of the total lead contained in soil, a substantial fraction is considered bioavailable, or able to be absorbed by the human body (Ruby et al., 1999). The remainder of the total soil lead is too strongly bound to soil components to be readily extracted in the human digestive system. The U.S. EPA estimates the bioavailable fraction of lead in soil at 30% for children (USEPA, 2007). Based on this bioavailable fraction, the amount of soil likely to be ingested by children, and the past child blood lead level of concern of 10 µg/dL, the U.S. EPA set the maximum contaminant level for soil lead at 400 mg/kg (ppm) for bare soils where children play and 1200 ppm elsewhere (USEPA, 2001). The CDC's recent reduction of the child "blood lead level of concern" from 10 to 5 µg/dL may prompt further reductions in these maximum contaminant levels. While many states use the 400 ppm hazard standard, some states, including Minnesota and California, have lowered this hazard standard at the state level. California currently has the strictest guidelines in the country, with an 80 ppm standard (OEHHA, 2009).

Risks associated with exposure to contaminated soils are increasing as urban agricultural activities gain popularity throughout urban areas in the United States. Urban farming can be a source of fresh, locally grown food that is otherwise inaccessible to citizens of cities like Detroit,

Michigan (Gallagher, 2010). However, the ubiquitous nature of lead as an urban contaminant increases the difficulty associated with finding suitable sites on which to garden. Adequate and complete soil testing is required on these gardens to ensure any produce grown is safe for consumption (Turner, 2009).

1.1 Background

Legacy contamination in Detroit, Michigan is more severe than many other urban areas. Detroit had the fourth highest amount of lead aerosols deposited during the leaded gasoline era of all cities in the United States (Mielke et al., 2011) which may contribute to the city having the fourth highest incidence of child lead poising cases in the United States (Raymond et al., 2010). A recent Detroit Public Schools and Detroit Department of Health and Wellness Promotion study found 25% of Detroit Public School students had blood lead levels over 10 µg/dL, and 99% of the student population had a blood lead level of at least1 µg/dL (Raymond et al., 2010). The same study showed a marked decrease in standardized testing performance with increasing blood lead level. In the controlled study group of 39,176 Detroit children, an overwhelming 22,755, or 58%, were found to have blood lead levels greater than 5 µg/dL.

The severity of legacy lead contamination in urban areas like Detroit necessitates thorough sampling of potential urban gardens. Soil sampling is complicated by the heterogeneous nature of soil; more specifically, variability in soil mineralogy, particle size distributions, and soil chemistry (Coppola et al., 2012; Gustafsson et al., 2011). Complex site histories involving past residence demolitions and addition of fill soil prior to initiation of gardening activities further complicates soil sampling (Boudreault et al., 2010). For example, areas of high concentration, termed “hotspots”, can occur along the drip lines of homes; however, on reclaimed urban lots, it may be difficult to locate the drip line position of

demolished structures. Hotspots can also occur in areas where lead based paint chips have fallen, potentially during demolition, and in prior driveways or alleys where cars utilizing leaded gasoline might have idled frequently. To avoid missing these hotspots, and consequently mischaracterizing urban sites, land use histories and inherent spatial variability should be taken into account when sampling urban soils. Such information is often unavailable, however, and sampling schemes must be developed without the benefit of *a priori* information.

Currently, U.S. EPA guidance for sampling residential lots smaller than 465 m^2 (5000 ft^2) recommends that as few as two composite samples be taken for adequate site characterization(USEPA, 2000, 2003). Sieving of soil samples to obtain the soil size fraction less than 250 µm prior to analysis is also recommended because this size fraction is most likely to be ingested and inhaled (USEPA, 2003). According to one recommendation, two averaged composite samples with a relative percent difference (RPD) of less than 50% are taken to be representative of the average soil lead concentration across an entire lot (USEPA, 2000). Alternatively, two five point composite samples can be used to characterize the site, incorporating preferential sampling in areas with a higher probability of high soil lead concentrations (e.g. the drip line of an existing structure) (USEPA, 2003). Urban gardeners commonly have limited, if any, information on site histories and are thus faced with soil sampling questions such as how many samples should be taken and what sampling pattern should be used.

1.2 Previous Studies

Previous investigators have examined large scale spatial variability of soil lead concentrations using geostatistics. Several studies used kriging or stochastic simulation to assess

risk associated with contaminated soils at neighborhood to city scales in urban areas. For example, Cattle et al. (2002) employed multiple indicator kriging to generate probability maps of contaminated urban residential sites in Sydney, Australia, using random sampling within grid blocks ranging from 2500 to 10,000 m^2. More recently, Milillo et al. (2012) concluded that ordinary kriging and cokriging were stronger methods of soil lead hotspot detection and delineation than inverse distance weighting and other deterministic methods in a 240,000 m^2 industrial residential neighborhood located in Buffalo, New York. Shinn et al. (2000) demonstrated variability at scales as small as an urban block within a four block residential area of Chicago. Schwarz et al. (2012) documented soil lead concentrations variability among 61 residential parcels in Baltimore, Maryland.

Considerably less study has been devoted to the spatial variability of soil metal content on urban gardens and single residential properties. A study of urban gardens in Oakland, California found soil lead concentrations below 400 ppm on average, but also found that the concentrations were highly spatially variable, with higher concentrations usually attributable to site history (McClintock, 2012). Bugdalski et al. (2013) found spatial variability on a Detroit urban garden plot at scales as small as one meter.

This degree of site specific variability in urban soil leads to a need for soil spatial variability to be analyzed at a smaller scale than previously studied. If soil lead concentrations and chemistry differ from site to site, it can be inferred that spatial variability will also differ from site to site, necessitating that geostatistical studies at the scale of individual sites, as opposed to block, or even city, scales.

Most work surrounding urban agriculture has focused on the effects of eating produce grown in lead contaminated soil on the human body, and more specifically on children. Although

consumption of produce grown in contaminated soil is not the primary exposure pathway, it is nevertheless quantifiable, and contributes to the total lead body burden of children living in urban areas (Clark et al., 2008). Most plants take up small amounts of lead, usually less than 10 ppm per plant on a dry mass basis, but the amount of lead ingested from consuming plants can still contribute to adverse health effects, especially if produce is not washed extremely well prior to consumption (Finster et al., 2003). Another study found that certain hyper-accumulating plants, like mustard, collard greens and sunflowers could take up as many as 47 ppm of lead from the soil on a dry mass basis (Clark et al., 2006).

1.3 Study Motivation and Objectives

The motivation for this study originated with a small pilot study at Earthworks Urban Farms in Detroit, completed as part of a Wayne State Undergraduate Research Project. That study documented small scale soil lead variability at a single urban garden plot Bugdalski et al. (2013). Because the degree of spatial variability can vary from site to site, it is important to compare results at other urban gardens to the results from Earthworks. The overarching goal of this thesis was to expand upon the Earthworks analysis in an attempt to generalize its results by employing similar sampling designs and measurements at two additional urban garden plots in Detroit.

A specific objective of this study was to assess and quantify the risks and benefits associated with composite sampling strategies. Spatial variability of lead in soil can significantly affect the results of soil sampling campaigns and subsequent risk assessments. EPA guidance documents for soil lead sampling recommend composite sampling to increase sample support and to aide in contaminant detection (USEPA, 2000, 2003). However, compositing

samples can lead to an averaging effect, potentially masking high concentration subsamples with lower concentration subsamples. Consequently, this averaging effect can lead to failure to detect potential hotspots on these sites.

A related objective of this work was to explore the potential effect that the reduced CDC child blood lead level reference value could have on risk assessment associated with a composite sampling strategy. Using the EPA Integrated Exposure Uptake and Biokinetic (IEUBK) model, and a value of 5 µg/dL instead of the default of 10 µg/dL, the soil Preliminary Remediation Goal (PRG) is reduced from 418 ppm, the basis for the current EPA guideline, to 153 ppm (USEPA, 1994a). A reduction of this magnitude will have a considerable impact on risk analyses associated with urban residential sites.

A further objective of this work was to generate maps depicting the soil lead concentration and probability of exceeding a specified regulatory threshold at each the three study sites. Probability maps are useful tools because they provide information for regulators and gardeners on areas that are most likely to exceed a threshold concentration, and therefore help in detecting and delineating hotspots, as well as designing appropriate remediation strategies. Moreover, these probability maps can be compared to an acceptable exceedance probability to determine the probability of site misclassification associated with differing sampling designs. Such analyses can form the basis for recommendations on sampling patterns and densities for urban garden sites that may minimize the probability of site misclassification.

1.4 Hypotheses

The primary goal of this study is to expand the Bugdalski et al. (2013) study to include two additional urban gardens in Detroit, with the intention of generalizing one or more of the results. Three hypotheses were developed related to this goal.

1. *All three gardens will display a similar degree of spatial variability, although site-specific spatial patterns may be present.*

   The three sites included in this study have similar site histories involving residential buildings, demolition, and backfilling. Therefore, a common degree of spatial variability is expected at all three sites. However, because of unique site histories, it is unlikely that the same spatial patterns are present at each site because of differing sources and degrees of lead contamination.

2. *Error rates (false negative or false positive) at each site will depend upon: (1) the sampling objective (global average concentration versus hot spot detection), (2) the sampling method (design versus model based sampling), (3) the number of samples taken, (4) the averaging method (i.e., compositing) employed, and (5) the chosen soil lead hazard standard.*

   The number and spacing of composite samples are important considerations in the design of every sampling campaign, as are the sampling goals. Results from the Earthworks pilot study demonstrated that compositing was beneficial if the sampling goal on the site were estimation of a global average concentration because it decreased the probability of type I (false positive) errors (i.e. remediating an uncontaminated site) (Bugdalski et al., 2013). However, if the sampling goal were hotspot detection, compositing caused an increase in type II (false negative) errors (i.e. failing to detect a hotspot on a site). Design-based sampling methods involve random sampling, while model-based methods

involved grid sampling and subsequent geostatistical analysis. The model-based approach is expected to lower the risk of failing to detect hotspots. Similar results are expected at each lot included in this study; however, the choice of soil lead hazard standard can have a considerable influence on the results. If the hazard standard falls below the median soil lead concentration of the site, the error relationships may be reversed, so that compositing will result in an increase in the percent of false positive error and a decrease in the percent of false negative error. Thus, depending on the configuration of soil lead concentrations, error rates should depend upon a combination of the factors hypothesized here.

3. *The risk of misclassification will be minimized at a probability threshold close to the marginal probability of contamination of each site.*

   An important decision in remediation studies is the choice of an acceptable exceedance probability threshold (an acceptable probability that any location on a site exceeds the hazard standard). At low exceedance probability thresholds, the risk of false positives increases and could lead to unnecessary cleanup costs. At high exceedance probability thresholds, the risk of false negative error can become unacceptably high from a human health perspective. Therefore, the overall risk of misclassification (the combined rate of false negatives and positives) should be minimized near the marginal probability of contamination (i.e. the global exceedance probability) on the site (Saito and Goovaerts, 2002). Consequently, the choice of probability threshold, as well as the number of samples and sampling design, is expected to have a considerable impact on the risk of site misclassification.

1.5 Thesis Structure

This chapter provides the context for the study by introducing the problem of soil lead contamination in Detroit and the issues associated with managing risk at urban gardens. Chapter 2 covers the sampling design and lab methodologies. Geostatistical and risk assessment methods are described in Chapter 3. Results of sampling, spatial analyses, and risk assessments are reported in Chapter 4 and discussed in Chapter 5 along with conclusions and recommendations for future research.

Chapter 2

Field Sampling and Laboratory Analysis Methods

2.0 Introduction

In this study, three gardens were sampled in Detroit, Michigan. The first was sampled as part of a pilot study, and the second and third gardens were sampled two years later in an extension of the initial study. These three gardens were chosen for their ease of accessibility, minimal cultivation, and perceived differences in soil types. The pilot study garden is part of Earthworks Urban Farm, located in southeastern Detroit. Gardens in northeastern part of the city were chosen for subsequent sampling to extend the study to a different area of Detroit (Figure 2.1).

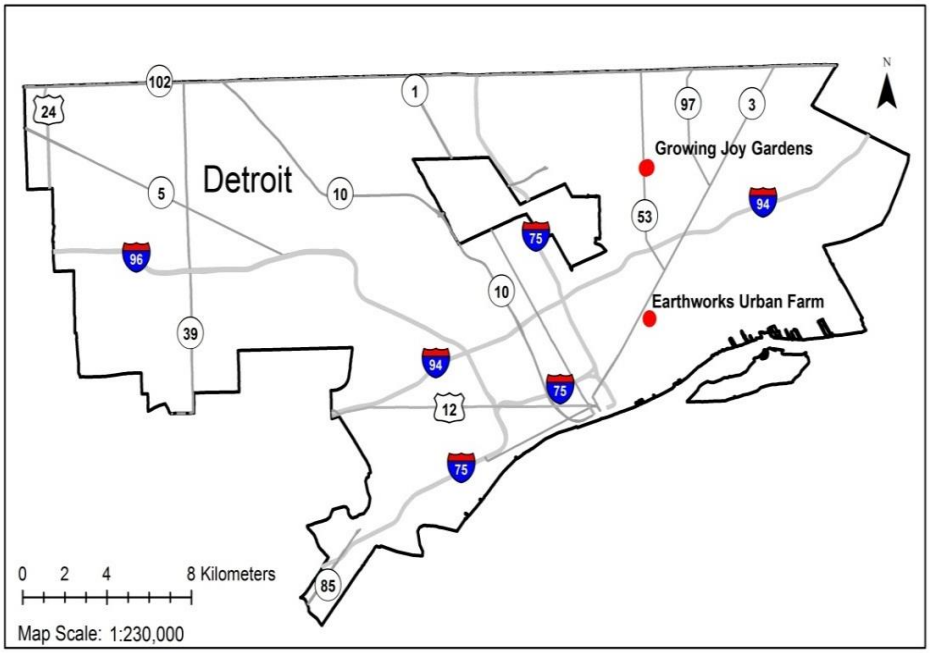

Figure 2.1: Location of study areas

Laboratory methods used for total soil lead analyses in this study were based on current USEPA analytical methods, and the bioaccessible lab methods follow the Urban Soil

Bioaccessibility Lead Test (see Section 2.3.2 and 2.3.3). This chapter provides background information on all three study areas, followed by a detailed description of field and laboratory methods employed.

2.1 Study Areas

2.1.1 Earthworks Urban Farm

The Earthworks garden is a 450 m^2 plot situated on two former residential lots in southeast Detroit (Figure 2.2). Historical Sanborn fire insurance maps show three buildings on the site as recently as 1951, two of which were multi-family homes, and the third identified as a paint shop. Exact demolition dates of these structures are unknown, but the garden manager estimates the demolition occurred approximately 10 years ago. According to the garden manager, gardening commenced on this site in 2009. Prior to planting, the garden was tilled to a depth of 7.5-10 cm and organic compost was applied. The garden was tilled again prior to sampling in 2010, but compost was not applied until after the sampling campaign was finished. The northern third of the site is not under cultivation because of excessive rubble (e.g. concrete slabs, wood scraps), presumably from demolition of the structures that previously stood on the site.

2.1.2 Growing Joy Gardens

In the summer of 2012, two sites in northeastern Detroit, at a group of gardens referred to as Growing Joy Gardens, were added to the study (Figure 2.3). According to the Growing Joy Garden manager, these sites were tilled to a depth of 7.5-10 cm and received an organic compost application in 2011, but no tilling or composting had been done in 2012 prior to sampling. Both

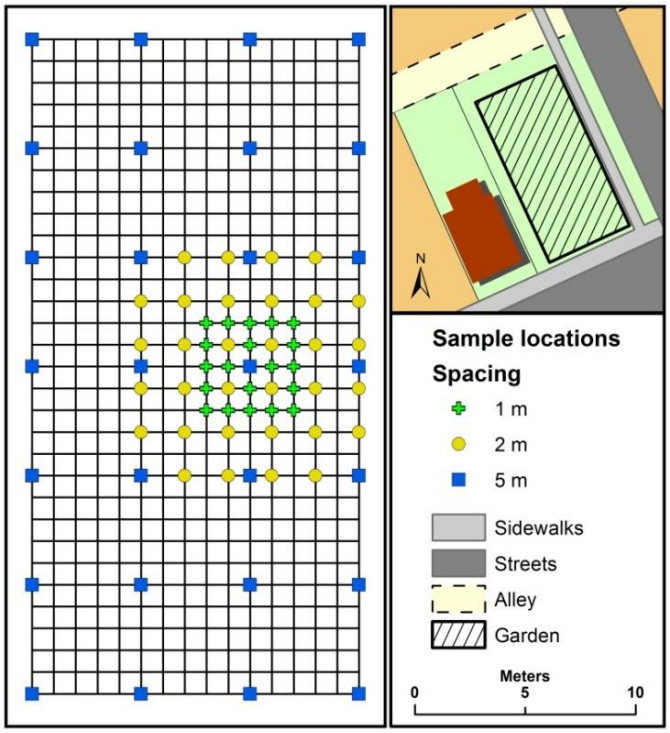

Figure 2.2: Sampling design and location map for the Earthworks plot

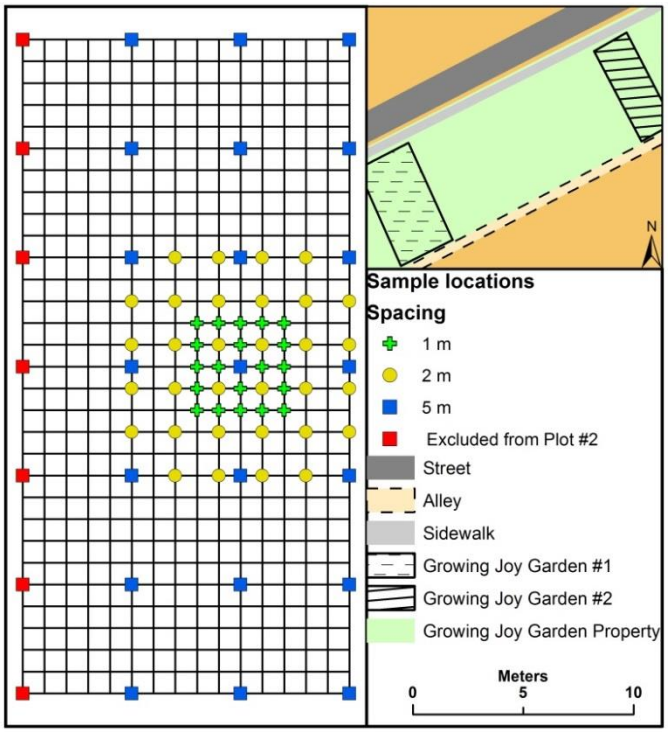

Figure 2.3: Sampling design and location map for Growing Joy gardens

sites are former residential lots, with recent demolition of the homes that previously stood on the sites, although exact demolition dates are unknown. Historical Sanborn fire insurance maps show all of Growing Joy Gardens as residential or undeveloped in 1951. The first site has an area of 450 m^2 and the second an area of 300 m^2. The two gardens are situated about 100 feet apart from one another. The first site had been cultivated once prior to sampling and was used primarily for growing tomatoes. The second lot was difficult to garden due to its clay rich soil matrix. Small amounts of rubble (e.g., glass, scrap metal) present on both sites did not interfere with gardening or sampling. However, the upper boundary of both lots is bordered by an alley containing accumulations of debris, including wood and metal scraps and piles of old tires.

2.2 Field Sampling Methods

All three sites were sampled using a model-based approach (Gruijter et al., 2006) intended to provide information needed to estimate variogram structures. The sample design was constrained by the cost of sample analyses and accessibility while the gardens were under cultivation. 73 to 80 samples spaced five, two, or one meter apart, were taken at each lot (see Figures 2.2 and 2.3). Samples were taken using a nested, grid-based sampling pattern with no preferential sampling. The nested grid design aided in geostatistical analysis by providing a large number of samples that were taken near one another, providing a more accurate assessment of small scale spatial variability. However, an undesirable result of the clustering of sample points in the center of these sites was a possible biasing of the site statistics. Data declustering was therefore employed to assign lower weights to closely spaced points than samples taken further apart (see Section 3.1).

A consistent sampling design was used at all three garden plots, although seven fewer samples were taken at the second Growing Joy garden because it is five meters narrower than the other two gardens. Approximately 50 g of soil was composited from five subsamples surrounding each sample location. One subsample was collected at a depth of 7.5 cm at each grid node and four additional subsamples, at the same depth, were taken at a distance of 10% of the sample spacing north, south, east and west of each sampled node (Figure 2.4a). Replicates were collected at 10% of the sample locations, chosen randomly (see Appendix D for replicate locations). Replicate samples were composited in the same manner with one subsample collected at the grid node and four additional subsamples collected at a distance of 10% of the sample spacing; however, the location where additional subsamples were collected was shifted 45 degrees to positions northeast, southeast, northwest and southwest of each sampled node (Figure 2.4b).

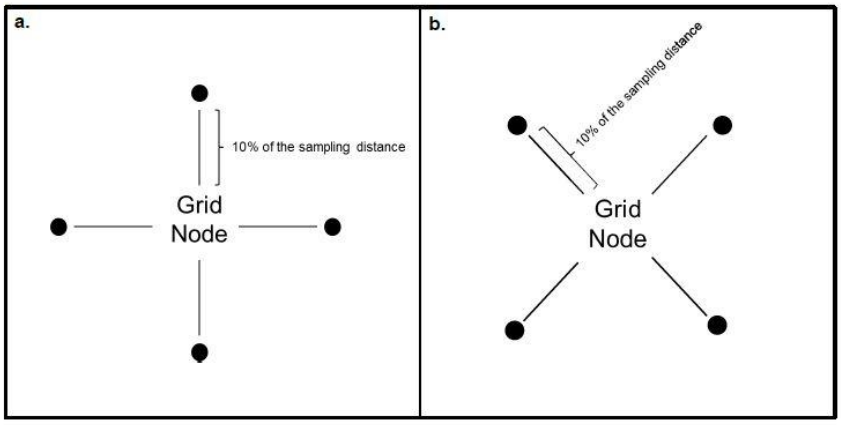

Figure 2.4: Composite sampling design for a) samples taken at each grid node and b) replicate samples

2.3 Laboratory Analysis

2.3.1 Sample Preparation

A standard sample preparation procedure was developed during the pilot study. Samples were air dried prior to all analyses. 0.5 g of unsieved soil was taken from each sample and analyzed during a first round of measurements, hereafter referred to as *unsieved total lead*. The remainder of each sample was passed through a 250 μm sieve prior to a second and third round of analyses, hereafter referred to as *sieved total lead* and *bioaccessible lead*, respectively. This approach was adopted because particle size fractions < 250 μm (No. 60 sieve) have been established as the critical soil-particle size when assessing exposure (Que Hee et al., 1985; TRW, 2000). Furthermore, soil fractions < 250 μm were used to calibrate the U.S. EPA IEUBK model (USEPA, 1994b), which was designed to evaluate bioaccessible lead exposure risk (Casteel et al., 1997; Maddaloni et al., 1998; Ruby et al., 1996).

Preparation for the Growing Joy garden samples was identical to the method described above, except that analyses were restricted to sieved total and bioaccessible lead to reduce sampling cost and workload. However, because most gardeners do not have access to soil sieves, 25% of the samples on each of the two Growing Joy gardens were analyzed prior to sieving (i.e. unsieved total lead) to establish a correlation between sieved and unsieved lead on each site.

2.3.2 Total Lead

Total unsieved and sieved lead analyses were performed following U.S. EPA method 3051a (U.S. EPA, 2007). Approximately 0.5 g of soil and 10 mL of concentrated trace metal grade nitric acid (68% v/v) was placed in a Teflon tube, and heated to 175°C in a CEM Mars Xpress microwave digestion unit. Samples were then diluted to ~40 mL, centrifuged and the

supernatant was analyzed for lead by flame atomic absorption (Flame AA; Perkin-Elmer, AA200) following Standard Method 3111b (Clesceri et al., 1998). Additionally, blank samples and standard reference materials (NIST, 2008) with known lead concentrations were tested to ensure method reproducibility.

2.3.3 Bioaccessible Lead

Bioaccessible lead analysis was performed using the Urban Soil Bioaccessibility Lead Test (USBLT) method (Zia et al., 2010), which is a revised version of the original *in vitro* method developed by Drexler and Brattin (2007). This method has been found to correlate to human bioavailability observed in standard soils (i.e., Joplin, Missouri control soils), costs 1/8 to 1/20 as much as existing methods, and can be performed using Flame AA. Analysis by flame AA also helps to mitigate possible interferences from other more abundant metals (e.g. Fe) that may be observed using other techniques (McBridge et al., 2011).

For the USBLT method, approximately 4 g of soil and 40 mL of 0.4 M glycine/HCL (38% v/v) solution (pH adjusted to2.5 ± 0.05) was placed in a 50 mL centrifuge tube and shaken by a wrist-action shaker at 100 rpm for two hours. In cases where the size fraction less than 250 μm (i.e., the soil to be analyzed) weighed less than 6 g, 2 g of soil and 20 mL of 0.4 M glycine were used instead. The samples were then centrifuged and the supernatant analyzed for bioaccessible lead by Flame AA (Perkin-Elmer, AA200) following Standard Method 3111b (Clesceri et al., 1998).

Chapter 3

Geostatistical Analysis and Risk Assessment

3.0 Introduction

The spatial component of geostatistics sets it apart from traditional statistical methods. Geostatistics is based on the principle that variables are auto-correlated in space or time, so that samples that are spatially or temporally closer together are more likely to be similar than those that are further apart (Isaaks and Srivastava, 1989). The covariance structure among samples is represented by a variogram, which models the change in variability with increasing distance between samples. In practice, discontinuous experimental variograms derived directly from sample data are fit with continuous variogram model functions that capture the covariance structure for use in kriging estimates of the variable over the entire study area. This chapter describes the geostatistical methods and modeling used to evaluate the hypotheses for this thesis (Section 1.4).

Recent studies have documented the use of Monte Carlo simulation to evaluate risk associated with different exposure models but comparatively little work has been done applying Monte Carlo simulation techniques to assess and optimize small scale soil sampling strategies. The Monte Carlo methods used to assess risk associated with different soil sampling designs and test the remaining hypotheses of this thesis (Section 1.4) are also discussed in this chapter.

3.1 Data Transformations

The nested grid sampling design (Section 2.2) included a higher density of soil lead measurements near the center of each site. This spatial bias was eliminated by declustering the data, so that lesser weight was given to measurements in more densely sampled areas, while a greater weight was given to measurements in more sparsely sampled areas (Deutsch and Journel,

1998). Data were declustered using the GSLIB program DECLUS (Deutsch, 1989). A cell size of seven meters was selected to correct for preferential sampling of lower concentrations near the center of each site by maximizing the declustered mean. An example DECLUS parameter file is included in Appendix A.

Because normally distributed data are assumed for ordinary kriging algorithms, it was necessary to transform the sieved total lead, hereafter simply referred to as *total lead*, and bioaccessible lead data for each of the three gardens to meet this assumption. A normal score transform was applied using the GSLIB program NSCORE and the weighted output files from the DECLUS program (see Appendix A for example parameter files). In a normal score transform, data are ranked from lowest to highest. These ranks are matched with a corresponding rank in the standard normal distribution to generate the transformed dataset. Backtransformations from normal score to the original sample space were implemented using the GSLIB program BACKTR (see Appendix A for parameter file) after variography and ordinary kriging were completed (described below). Each of the six datasets (total lead and bioaccessible lead for each of the three garden plots examined) were normal score transformed prior to variography.

3.2 Variography

Experimental semi-variograms (also referred to as sample variograms or experimental variograms) were generated to illustrate the covariance structure at each of the three garden sites. An experimental variogram is calculated as half the mean squared difference between values separated by a specified distance or lag *(Isaaks and Srivastava, 1989):*

$$\gamma(h) = \frac{1}{2N(h)} \sum_{(i,j)} \left(v_i - v_j\right)^2 \qquad (3.1)$$

where *N(h)* represents the total number of data pairs separated by the lag distance *h*, and v_i and v_j represent the individual components of a single data pair at locations *i* and *j*. Experimental variograms were then fit with variogram models to define a continuous spatial covariance model for input into a selected kriging algorithm.

SGeMS (Remy et al., 2009) was used to generate experimental variograms and, subsequently, to fit each experimental variogram with a variogram model. Declustered data were evaluated for anisotropy (directional dependence at 45 degree azimuthal increments); however, omnidirectional experimental variograms were found to sufficiently describe spatial variability. Omnidirectional experimental variograms were constructed using a 1 m lag spacing with a 0.5 m lag tolerance. Variogram models typically include a nugget effect to account for discontinuities at the origin arising from small scale spatial variability, a lack of data pairs at short distances, or measurement error. The nugget effect was estimated using the variance of the field replicate concentrations for each data set. Experimental variograms were then fit with one of three positive definite variogram models:

spherical,

$$\gamma(h) = c\left[1.5\,\frac{h}{a} - 0.5\left(\frac{h}{a}\right)^3\right], \tag{3.2}$$

exponential,

$$\gamma(h) = c\left[1 - exp\left(-\frac{3h}{a}\right)\right], \tag{3.3}$$

or Gaussian

$$\gamma(h) = c\left[1 - exp\left(-\frac{(3h)^2}{a^2}\right)\right], \tag{3.4}$$

where γ is the variance at lag increment *h*, and *a* is the range in the case of the spherical model or the effective range corresponding to the distance at which γ reaches 95% of the positive sill contribution, *c*, in the exponential and Gaussian models (Goovaerts, 1997). Emphasis was placed on fitting experimental variograms at lag distances less than 5m to best represent short-scale variability in each garden plot. Each of the models were adjusted to achieve the best visual fit.

3.3 Ordinary Kriging

Kriging refers to a family of methods used to generate optimized estimates at unsampled locations (Isaaks and Srivastava, 1989). All kriging algorithms are based on a generalized linear regression estimator. The values in a particular dataset are assigned weights at every unsampled location to generate point estimates. These weights are assigned in a manner which minimizes the error variance. Ordinary kriging is one of the more commonly employed kriging methods, and, like all types of kriging, is considered to be a "best linear unbiased estimator," or BLUE (Deutsch and Journel, 1998). Unlike simple kriging, which assumes a constant global mean for the entire study area, ordinary kriging assumes a constant local mean in the search neighborhood near the estimation point .

In this study, ordinary kriging was employed to create interpolated soil lead concentration maps that were subsequently used to assess spatial patterns and conduct risk assessment. Ordinary kriging maps were generated using total and bioaccessible data from each of the three garden plots. Kriging maps were created on a 10 cm x 10cm grid using SGeMS for kriging estimation and ArcGIS 10.0 for map editing.

Although ordinary kriging produces useful images for visualizing spatial patterns of data values, use of the ordinary kriging variance as an error estimator, and subsequently as a method for generating probability maps, is not recommended because the ordinary kriging variance is dependent upon only the spatial arrangement of the data, not the data themselves. This is an effect of the assumption of homoscedasticity, or similar variances between populations (Goovaerts, 1997). This assumption, however, is rarely met in practice because the local variance commonly changes across the study area (Goovaerts, 1997). In multiple indicator kriging, homoscedasticity is not assumed, and kriging variances are based on the magnitude of the data themselves, as well as the data configuration. Multiple indicator kriging is therefore generally considered a more robust error estimator, as discussed in the following section.

3.4 Multiple Indicator Kriging and Exceedance Probability Estimation

The primary disadvantages of using ordinary kriging variances in uncertainty estimation arise from the homoscedastic nature of the ordinary kriging variances and the assumed normality of the raw data (Goovaerts, 1997). Alternatively, indicator kriging is non-parametric and does not assume homoscedasticity, so that error estimates are based on both the data themselves as well as their spatial configuration. This makes indicator kriging a much more robust choice for generating probability maps, which are based heavily on kriging variance estimates.

The principal difference between ordinary and indicator kriging lies in the transformation of data into their indicator transform equivalent. In indicator coding, data are transformed into either ones or zeros, indicating whether a given data point lies respectively above or below a specified threshold. This function of indicator kriging provides the facility to build a local conditional cumulative distribution function (ccdf) at every estimation point in the study area,

and the variance derived from this ccdf is a more reliable approximation of estimation error than the ordinary kriging variance.

Multiple indicator kriging generates local ccdfs by specifying a number of thresholds and performing indicator transforms for each threshold. As threshold values increase, the cumulative frequency increases as well, building the beginnings of a ccdf. Finally, interpolation between these discrete ccdf points generates a continuous local ccdf that can be used to map the probability of exceeding a given threshold on the site. Extrapolation of the ccdf tails is also required for most applications.

Multiple indicator kriging was used to create maps estimating the probability of exceeding a given threshold (e.g. a specific soil lead hazard standard) at each of the three garden plots in this study. Only total soil lead was mapped using indicator kriging because hazard standards that can serve as a practical threshold value for bioaccessible lead have not been established. Nine cutoff values corresponding to the deciles of the declustered raw data were chosen as the indicator thresholds used to generate local ccdfs. The raw sieved total lead concentration measurements were transformed into binary indicator data and variogram analysis was performed for each site. Variogram parameters were determined for each indicator dataset (nine indicator datasets per garden for a total of 27 datasets) (see Appendix B). Indicator kriging was performed using the GSLIB program ik3d (Deutsch and Journel, 1998) on a 10 cm grid, consistent with the resolution of previously generated ordinary kriging maps and indicator kriging probability maps. Full indicator kriging was used rather than median indicator kriging because median indicator kriging assumes a similar structure for all indicator variograms across all thresholds, but considerable variation in indicator variogram parameters was observed between thresholds. A representative ik3d parameter file is included in Appendix A.

The GSLIB program POSTIK was used to generate maps of probabilities of exceeding 400 ppm, the current soil lead hazard standard, and 150 ppm, a potential revised soil hazard standard estimated using the IEUBK model (Section 1.3). POSTIK is an indicator kriging post-processor that can be used to generate an E-type estimate (i.e. the mean of the ccdf), an exceedance probability for a specified threshold, or a conditional probability quantile from the indicator kriging results (Deutsch and Journel, 1998). POSTIK is also used to generate a continuous local ccdf from the discrete ccdf generated by the indicator program ik3d using a variety of interpolation strategies. POSTIK was employed in this study to linearly interpolate the indicator kriging results and calculate a local probability of exceeding either 400 or 150 ppm at every estimated point of each study site. POSTIK output was converted to Surfer .grd files using a customized Fortran program called SURFGRD (see Appendix C) and mapped in Surfer and ArcGIS. An example POSTIK parameter file is included in Appendix A.

3.5 Simulated Random Sampling and Risk Assessment

3.5.1 Background

Uncertainty associated with decisions concerning sampling goal and sampling design (e.g. sampling pattern, number and distribution of samples) was quantified using Monte Carlo simulations with varying sampling schemes. Monte Carlo simulation involves utilizing a large number of trials with random sampling components to generate a probability distribution of potential outcomes (McKillup and Dyar, 2010). If the true soil concentration distribution is known, the simulated Monte Carlo sample output distribution can be analyzed using specified soil hazard standards to generate an estimate of the site misclassification risk associated with any sampling design specified in the simulation. For the purposes of this study, the SGEMS ordinary

kriging maps were treated as exhaustive "known" datasets that were resampled using alternative methodologies in a series of Monte Carlo simulations described below.

3.5.2 Risk Assessment Associated with EPA Residential Sampling Strategies

Two EPA sampling strategies for residential properties less than 465 m^2 were assessed in this study.

The first EPA method is based on calculations of a relative percent difference (RPD). In this method, two samples, each comprised of three, four, or five composites, are selected randomly over the sampling site, and an RPD is calculated using the two composite samples according to the following formula:

$$RPD = \frac{C_1 - C_2}{(C_1 + C_2)/2} \quad (3.5)$$

where C_1 and C_2 are the concentrations of the two composite samples. If the RPD is less than or equal to 50%, the site is considered to have been acceptably characterized. If the RPD is greater than 50%, the site is resampled until an RPD of less than 50% is achieved (USEPA, 2000).

The second EPA sampling method, designed for Superfund sites, involves dividing a site roughly in half to create two sampling zones, with one zone including the front yard of the home and the other zone the backyard. One random composite sample is then taken in each of the two zones. If applicable, a third zone is established around the drip line of the home based on the assumption that lead concentrations resulting from atmospheric deposition or lead based paint will be higher in those areas (USEPA, 2003). One additional random composite sample is then taken within this third zone. On urban gardens, however, a third zone cannot be established because the homes have been demolished. In these cases, the site would be divided into only two sampling zones.

To assess the EPA methods, ordinary kriging estimates of total lead were treated as exhaustive data sets in this phase of the analysis. Monte Carlo simulation programs EPA2000 and EPA2003 (see Appendix C), written using FORTRAN and the Compaq Visual Fortran compiler (Compaq, 1999), were developed for each EPA sampling strategy. CDFs were created for the results of 10,000 trials in each simulation so that the probability of exceeding 150 or 400 ppm could be quantified.

Program EPA2000 was designed to implement the USEPA (2000) recommendations. Two samples were assembled, each of which was comprised of 3 to 5 random composites, which were averaged together. An RPD was then calculated for the two samples using equation 3.5. If the RPD was less than or equal to 50%, the two samples were averaged and recorded as the result for that trial. If the RPD was greater than 50%, the program selected additional pairs of random, composited samples until an RPD less than 50% for a pair of two samples was encountered. At that point, all prior samples were arithmetically averaged to determine the result for that sampling trial.

Program EPA2003 (see Appendix C) was written to randomly sample the exhaustive datasets with 2, 3, 4, 5, or 6 samples averaged (i.e. composited) for each trial, similar to the sampling recommendations for Superfund residential sites (USEPA, 2003). Because there is currently no home on any of these urban garden plots, EPA 2003 was not designed to split the site into zones based on the location of the home, but rather randomly sampled to assess the effect of compositing in such a situation.

3.5.3 Risk Assessment Associated with Sampling Design, Number of Samples, and Soil Hazard Standard

Monte Carlo simulations were also designed to assess risk associated with varying sampling designs, the number of samples and subsamples, and the chosen soil lead hazard standard. The three main parameters varied among the different simulations were sampling design (i.e. implementing a random or grid based scheme), the number of samples and subsamples/composites, and the soil hazard standard used to determine whether a site is contaminated.

To facilitate a comparison between the detection probability when using random sampling (i.e. a design-based approach) and grid sampling (i.e. a model based approach) an additional Monte Carlo simulation program called GRIDSAMP (see Appendix C) was written to sample the exhaustive kriging data set using a grid based sampling pattern. Specifically, the program divided the site into a specified number of equal sized blocks, with one random sample taken within each block to adhere to the random aspect of Monte Carlo simulation. The blocks were distributed evenly over the entire site to simulate sampling using a grid based design. Output from this program included an average concentration per trial (to assess the effects of compositing) and a binary detection flag that was triggered and recorded as 1 if the sampled concentration at any of the blocks in a trial was greater than the soil hazard standard and 0 otherwise. These binary detection flags were then averaged over the 10,000 trials to calculate a detection probability for the simulation. Output from this program was compared to the results from EPA2003 (USEPA, 2003) (see Section 3.5.2), after modification of that program to include a detection flag for each trial. This modified program (RANDSAMP) is presented in Appendix C.

The number of samples per trial was also varied in each simulation to assess the effect that sample quantity and compositing have on risk. Initially, a total of 4, 10, 20, or 50 random samples per trial were averaged (i.e. composited). These values were selected to encompass a variety of possible numbers of samples per site, ranging from a cost-effective and realistic number of samples to a quantity of samples assumed large enough to be sufficient for site characterization based on current sampling recommendations. In the grid-based simulation, the site was divided into 4, 10, 20, or 50 blocks of equal size, with one random sample per block. These samples were also averaged over each trial. To better assess the hotspot detection probability, one to eight additional samples and blocks were used to refine the graphs presented in Figure 4.10.

Finally, the soil hazard standard was varied in each program to assess differences in detection probability with different soil hazard standards. Programs RANDSAMP and GRIDSAMP were coded to set a detection flag if any concentration in a trial exceeded a threshold value of either 150 ppm or 400 ppm. Trials containing at least one sample greater than the threshold were flagged with a value of 1, while trials without any samples greater than the threshold were assigned a detection value of 0.

3.6 Misclassification Risk and Probability Thresholds

The ordinary kriging maps and the probability maps generated using multiple indicator kriging were used to calculate and map the probability of type I (false positive) and type II (false negative) error when detecting and delineating hotspots. A four step process was employed to accomplish this assessment.

First, the ordinary kriging maps were transformed such that all values greater than the soil hazard standard were assigned a value of 1, and all values less than or equal to the soil hazard standard were assigned a value of 0.

Second, the probability maps were transformed in a similar way, using a range of probability thresholds (p=0.05, 0.35, 0.50, 0.65, and 0.95 at a minimum) of exceeding the soil hazard standard. These transformations result in two sets of maps. The first set of maps displays transformed ordinary kriging estimates, and a value of 1 indicates a location greater than the soil hazard standard (i.e. 400 or 150 ppm), and a value of zero a location less than or equal to the soil hazard standard. The second set of maps displays the transformed probability maps, where a value of 1 indicates a location greater than the probability threshold (e.g., 0.05, 0.35, etc.), and a value of 0 indicates a location less than or equal to the probability threshold.

Third, the transformed maps were then compared using ArcGIS Map Algebra and Raster Calculator tools. The transformed ordinary kriging map was subtracted from the transformed probability map. With respect to this calculation, a value of zero on the resulting maps indicates that there is no error between the two transformed maps (i.e., the transformed ordinary kriging and probability maps both have the same transformed value). If the result of the raster algebra was +1, the probability map was greater than the transformed kriging map. This means the experimental data suggest the site is contaminated when the exhaustive data set indicates it is not contaminated. This was classified as type I error. A value of -1 indicated that the transformed probability map value was lower than the transformed ordinary kriging map value. This means if the transformed ordinary kriging estimates are considered reality, and the transformed probability maps are generated from experimental data, then the experimental data indicate that the site is uncontaminated, whereas the exhaustive data set (i.e. reality) indicates it is

contaminated. This was classified as type II error. The potential results of this analysis are summarized in Table 3.1.

Table 3.1: Summary of possible error map calculations and results

Calculation	Result
Probability map - Ordinary kriging map = **0**	No error
Probability map - Ordinary kriging map = **+1**	Type I error
Probability map - Ordinary kriging map = **-1**	Type II error

Finally, these raster maps were color-coded resulting in a display of the areas where type I, type II, and no error are present. The proportion of each raster map attributed to type I and type II error was also calculated to determine the total percent misclassification on each site.

Chapter 4

Results

4.0 Introduction

The results of the analyses described in the two preceding chapters are presented in the sections below. A brief description of the laboratory analysis results, including summary statistics and transformations, is presented in Section 4.1. The results of geostatistical analyses are described in Section 4.2. Finally, Monte Carlo simulation and risk assessment results are presented in Section 4.3. A discussion of these results follows in Chapter 5 of this thesis.

4.1 Sample Data Description

Analysis of unsieved soil lead measurements was restricted to the basic statistical analyses presented in this section. Therefore, the convention in this thesis is to refer to sieved total lead simply as “total lead”, except in instances where it is necessary to distinguish between unsieved and sieved soil lead.

Histograms of the declustered results are shown in Figure 4.1 and basic statistics of the raw and declustered results are given in Table 4.1. Total and bioaccessible lead data from each of the three gardens are highly non-normal. This non-normality can be visualized in Figure 4.1, but was quantified using the Shapiro-Wilk normality test. In the Shapiro-Wilk test, a p value of less than 0.05 indicates non-normality (i.e. the null hypothesis is a normal distribution) at a 95% confidence level. Shapiro-Wilk p-values for total and bioaccessible lead on each of the three sites were less than 2.2E-05, indicating highly non-normal distributions (see Table 4.1). Each of the six distributions were also right-skewed, with greater means than medians (Table 4.1).

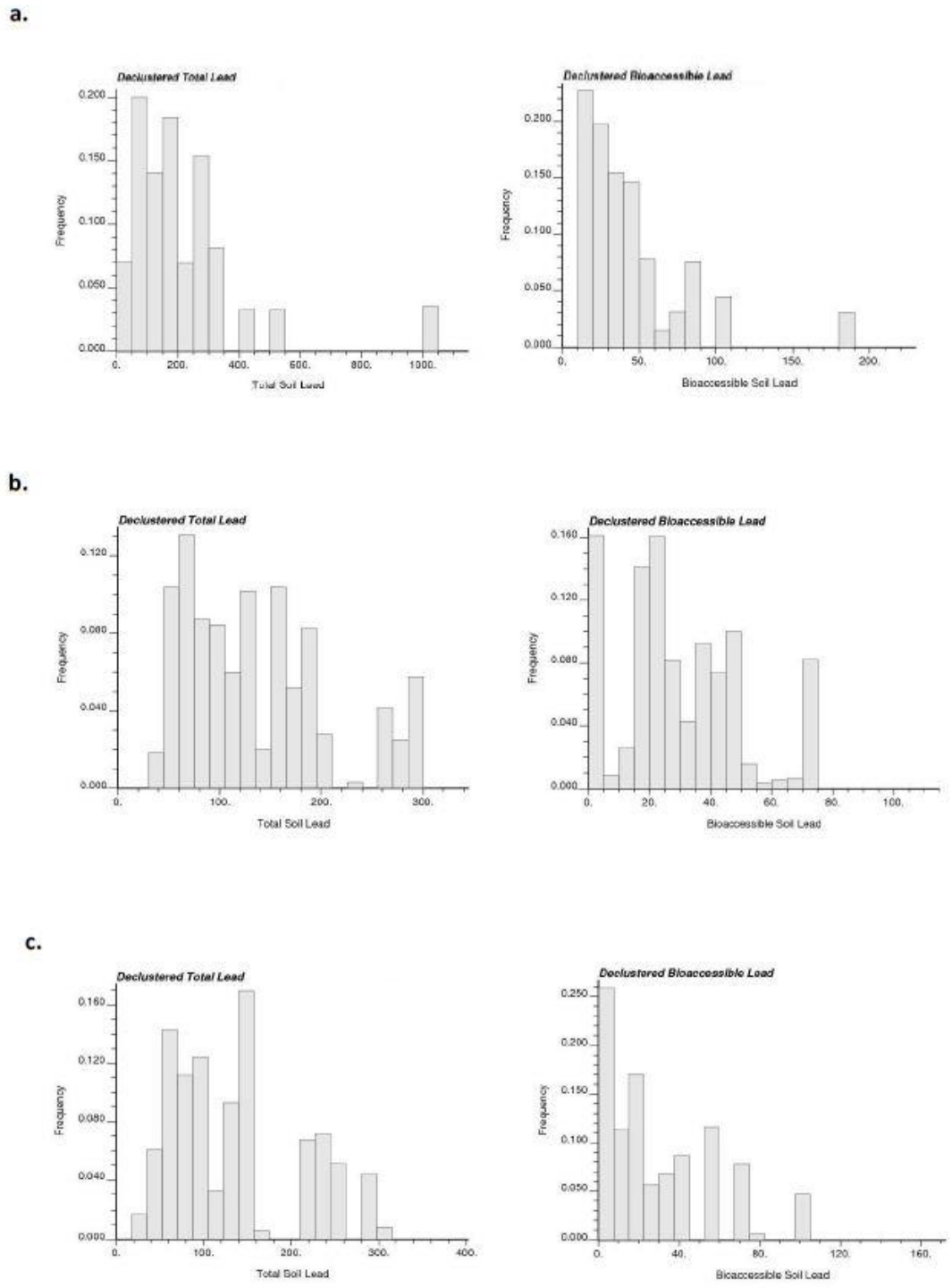

Figure 4.1: Histograms of declustered total and bioaccessible lead concentrations (ppm) of a) Earthworks (N = 80), b) Growing Joy #1 (N = 80), and c) Growing Joy #2 (N=73)

Table 4.1: Summary statistics of raw and declustered soil lead concentrations

	Earthworks Plot			Growing Joy Plot #1			Growing Joy Plot #2	
	Total	*Bioaccessible*		*Total*	*Bioaccessible*		*Total*	*Bioaccessible*
Number of samples	80			80			73	
Minimum (mg/kg)	32	11		43	3		28	5
Mean (mg/kg)	181	34		118	28		90	16
Median (mg/kg)	154	27		106	25		74	7
Maximum (mg/kg)	1,532	182		298	73		307	96
Variance (mg^2/kg^2)	30,350	612		3,117	304		2,923	314
Coefficient of Variation	0.96	0.73		0.47	0.62		0.60	1.1
Declustered Mean (mg/kg)	237	44		135	29		133	31
Declustered Median (mg/kg)	176	36		125	25		121	22
Declustered Variance (mg^2/kg^2)	73,984	1,225		5,041	361		5,184	676
Shapiro-Wilk p-value	2.05E-15	9.03E-12		1.21E-05	0.0022		2.16E-10	3.88E-12

Total lead concentrations on both Growing Joy lots were generally lower than the Earthworks garden. Earthworks had a maximum concentration of 1,532 ppm. By comparison, the maximum observed concentrations on the two Growing Joy gardens were 298 and 307 ppm, respectively. Although these maximum concentrations were below the current soil lead hazard standard (400 ppm), they exceeded the anticipated revised soil lead hazard standard of 150 ppm.

After declustering, the mean total soil lead concentration of the pilot study and the first and second Growing Joy gardens increased from 181 ppm to 237 ppm, 118 to 135 ppm, and 90 to 133 ppm, respectively (Table 4.1). This increase in mean soil lead concentrations supports the interpretation that the data were clustered in areas of low concentration. An increase in bioaccessible lead average concentrations was also observed after declustering.

On the Earthworks garden plot, 4% of the sieved lead samples exceeded 400 ppm, and 53% exceeded 150 ppm (Table 4.2). None of the Growing Joy sieved lead samples exceed 400 ppm, but 24% of samples from Growing Joy Plot #1 and 10% of samples from Growing Joy Plot #2 exceed 150 ppm (Table 4.2).

Table 4.2: Soil lead hazard exceedance percentages (raw data)

	Earthworks Plot	Growing Joy Plot #1	Growing Joy Plot #2
Raw Data Exceeding 150 ppm	53%	24%	10%
Raw Data exceeding 400 ppm	4%	0%	0%

Bioaccessibility concentrations were consistently lower than total soil lead concentrations; specifically, the average bioaccessible fraction (percent of sieved total lead concentration determined to be bioaccessible) on all three sites ranged from 16 to 22% of the sieved total lead concentration (Table 4.3).

Table 4.3: Relationships between unsieved total lead, sieved total lead, and bioaccessible lead

	Earthworks Plot	Growing Joy Plot #1	Growing Joy Plot #2
Bioaccessible fraction	0.20	0.22	0.16
Bioaccessible vs. Sieved Correlation (r)	0.91	0.88	0.92
Unsieved vs. Sieved Correlation (r)	0.90	0.94	0.94

Sieved total lead and bioaccessible lead Pearson correlation coefficients were high for all three gardens and ranged from 0.88 to 0.92 (Table 4.3). Sieved to unsieved lead correlations were also high, ranging from 0.90 to 0.94 (Table 4.3). On the Earthworks plot, sieved total lead concentrations were consistently higher than unsieved total lead concentrations, as would be expected because smaller particles have a greater proportion of surface area available for adsorption of lead ions per mass of soil particle (Abouelnasr, 2009). However, on both Growing Joy plots, the relationship was approximately one to one (Figure 4.2). This is an unexpected result that will be discussed further in Chapter 5.

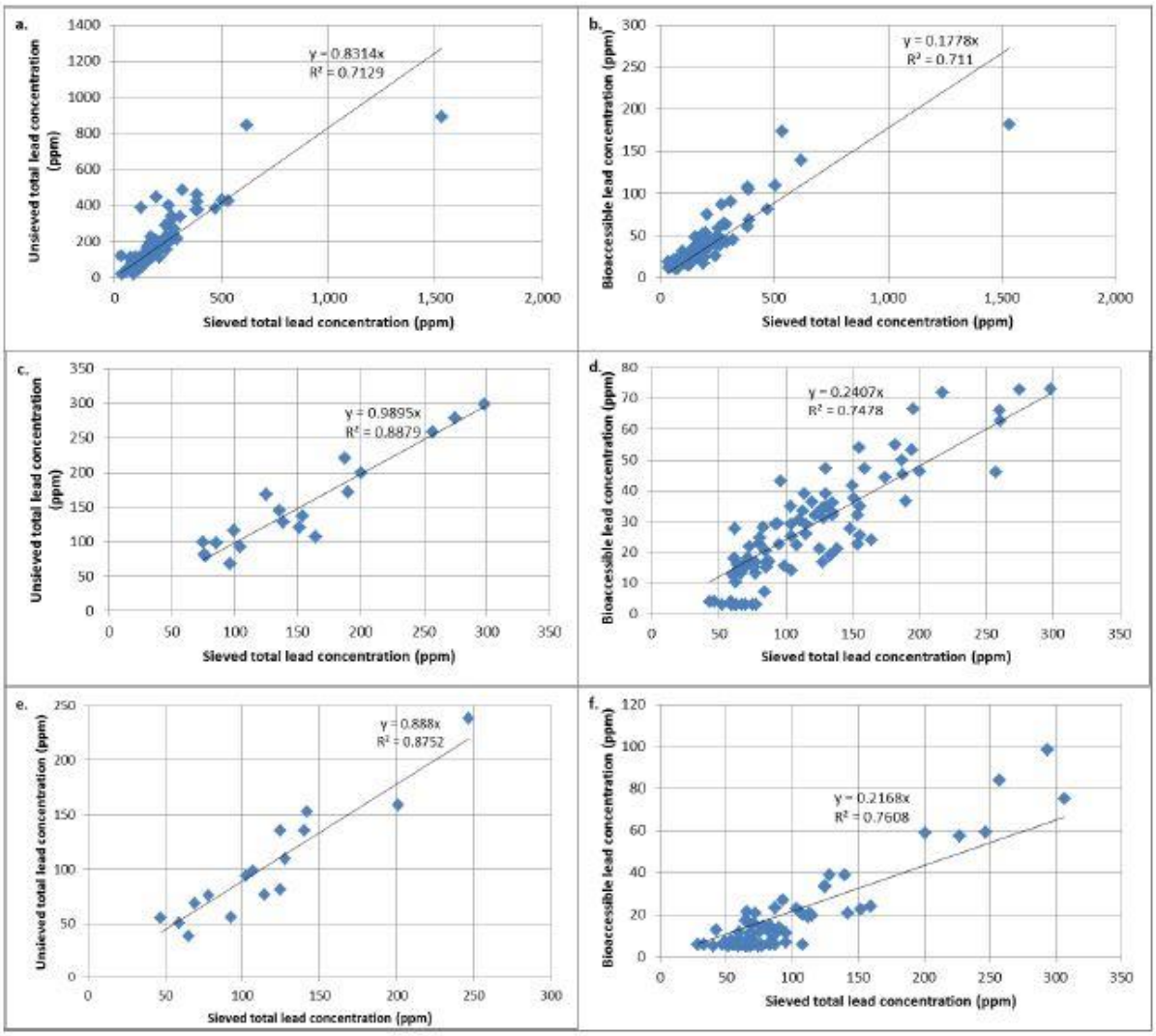

Figure 4.2: Scatterplots comparing sieved total lead to either unsieved total lead or bioaccessible lead for a) and b) Earthworks, c) and d), Growing Joy Plot #1 and e) and f), Growing Joy plot #2

4.2 Geostatistical Analysis

4.2.1 Variography

The three sites in this study exhibited differing degrees of spatial variability. Lead concentration data were normal score transformed prior to variography (Section 3.1). No significant anisotropy was detected prior to the modeling efforts, so all models were fit to omnidirectional experimental variograms. Both total and bioaccessible experimental variograms

for the Earthworks and second Growing Joy plots were fit with spherical models and the total and bioaccessible experimental variograms for Growing Joy plot #1 were fit with exponential models. These models were chosen based on best visual fit.

The total and bioaccessible experimental variograms for each garden plot are similar (Figure 4.3).Variogram model ranges of the Earthworks plot total and bioaccessible lead were 20 and 16 m, respectively, both of which are greater than the smallest sample spacing, but smaller than the maximum dimensions of the garden plot (Figure 4.3a. and b.). On Growing Joy plot #1, the total and bioaccessible soil lead variogram model ranges were 16 and 8 m, respectively (Figure 4.3c. and d.); on Growing Joy plot #2 they were 25 and 18 m (Figure 4.3e. and f.). All variogram model parameters are shown in Table 4.4.

Table 4.4: Total and bioaccessible soil lead variogram model parameters

	Earthworks Plot			**Growing Joy Plot #1**			**Growing Joy Plot #2**	
	Total	*Bioaccessible*		*Total*	*Bioaccessible*		*Total*	*Bioaccessible*
Model Type	Spherical	Spherical		Exponential	Exponential		Spherical	Spherical
Nugget Effect	0.01	0.03		0.25	0.5		0.2	0.1
Relative Nuggest	1%	3%		31%	48%		12%	8%
Range/Practical Range (m)	20	16		16	8		25	18
Sill Contribution (mg^2/kg^2)	0.85	0.85		0.55	0.55		1.5	1.2

4.2.2 Ordinary Kriging

Kriged concentrations across all of the plots in this study show spatial variability at scales as small as one meter. Nevertheless, there is a similarity in spatial pattern between kriged maps associated with total and bioaccessible soil lead concentrations for each plot. The same prominent hotspot in the upper left corner of the Earthworks garden is visible in both the total and bioaccessible kriged concentration maps (Figure 4.4). Both the total and bioaccessible soil lead concentration maps of Growing Joy plot #1 show an area of elevated concentrations directly

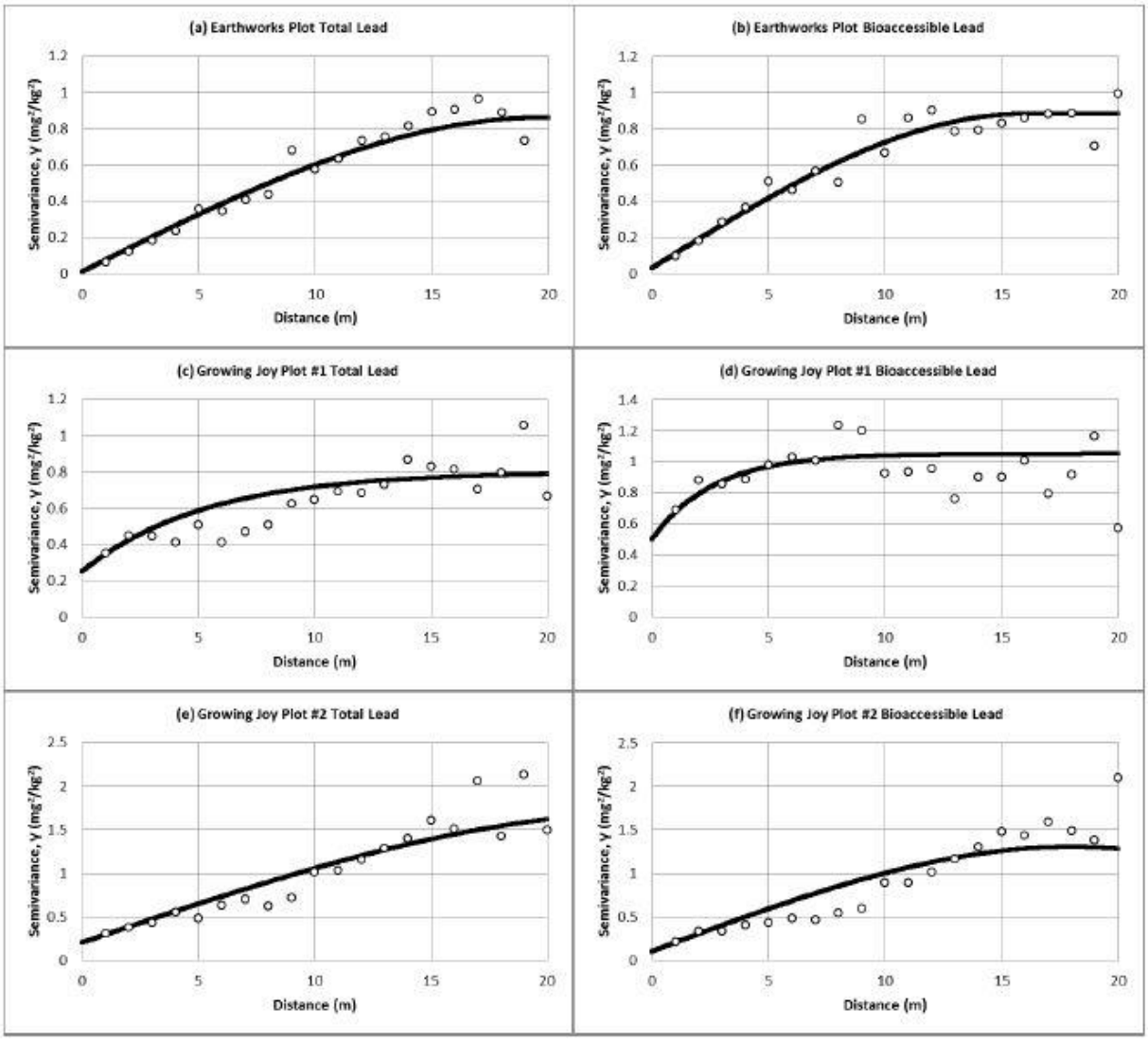

Figure 4.3: Normal score transformed experimental variograms (points) and variogram models (curves)

along the southwest (left hand) edge of the site. The Growing Joy plot #2 has areas of elevated total and bioaccessible soil lead concentrations along the upper and lower site boundaries (Figure 4.4). Kriged mean total and bioaccessible soil lead concentrations (Table 4.5) were higher than the raw data means (Table 4.1). Kriging means were lower than the declustered means on each plot, however, and ranged from 11% lower on Growing Joy Plot #2 to 15% lower on the

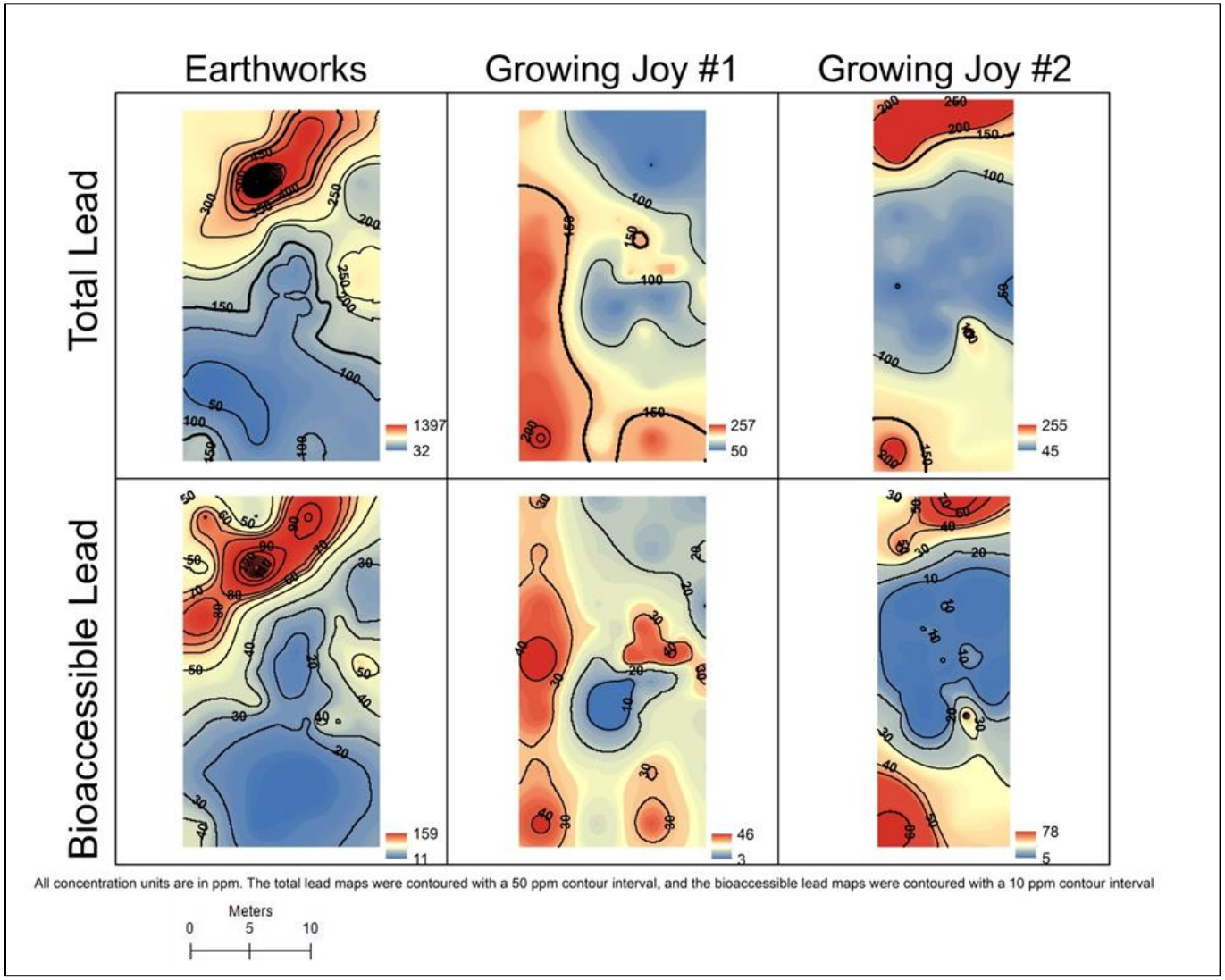

Figure 4.4 Ordinary kriging estimates of total and bioaccessible soil lead on Earthworks, Growing Joy #1 and Growing Joy #2 garden plots

Earthworks plot. The maps shown in Figure 4.4 depict the exhaustive data sets used for simulated sampling during the Monte Carlo simulations.

Table 4.5: Summary statistics of ordinary kriging estimates

	Earthworks Plot			Growing Joy Plot #1			Growing Joy Plot #2	
	Total	*Bioaccessible*		*Total*	*Bioaccessible*		*Total*	*Bioaccessible*
Mean (mg/kg)	202	38		124	25		118	25
Variance (mg^2/kg^2)	18,887	418		1,487	52		2,489	330
Minimum (mg/kg)	32	11		51	3		46	5
Median (mg/kg)	173	35		127	24		118	22
Maximum (mg/kg)	1,397	97		258	46		255	79

4.2.3 Multiple Indicator Kriging and Probability Maps

Indicator variogram model parameters corresponding to each decile of the declustered data are reported in Appendix B. The highest decile was not used as an indicator class, because indicator variograms based on the most extreme threshold are typically built using relatively few pairs (Goovaerts, 1997). Although the tenth decile provided a reasonable indicator variogram estimate with respect to the Earthworks garden, the other two plots yielded poorly behaved indicator variograms of the tenth decile. For consistency of analysis among the three garden plots, the tenth decile was therefore excluded and the remaining nine indicator classes were used in indicator variogram calculations.

Indicator variogram model parameters varied considerably between deciles for each garden. The variogram ranges varied from 4 m to 19 m on the Earthworks plot, from 4 to 20 m on the first Growing Joy lot, and from 4 to 26 m on Growing Joy plot #2 (see Appendix B). Nevertheless, the spatial patterns of the probability maps generated using multiple indicator kriging (Section 3.4) were similar to the ordinary kriging maps. Maps showing the probability of exceeding 400 ppm on the Earthworks plot reveal two hotspots (Figure 4.5a). The largest hotspot

is located in the northwest corner of the site with exceedance probabilities between 79 and 89 percent. An additional small hotspot is located on the easternmost site boundary. When the exceedance threshold was reduced to 150 ppm, the two hotspots merge and the area with probability above 89% expands to cover the northern half of the lot (Figure 4.5b). Maps utilizing a 400 ppm exceedance threshold were not generated for either Growing Joy plot, because sample concentrations greater than 400 ppm were not observed on these lots. The exceedance probability map corresponding to a 150 ppm threshold for Growing Joy plot #1 showed the highest probabilities (about 70%) along the leftmost site boundary (Figure 4.5c). The map for Growing Joy plot #2 showed the highest exceedance probabilities (about 85%) at the uppermost site boundary and the lower left hand corner (Figure 4.5d).

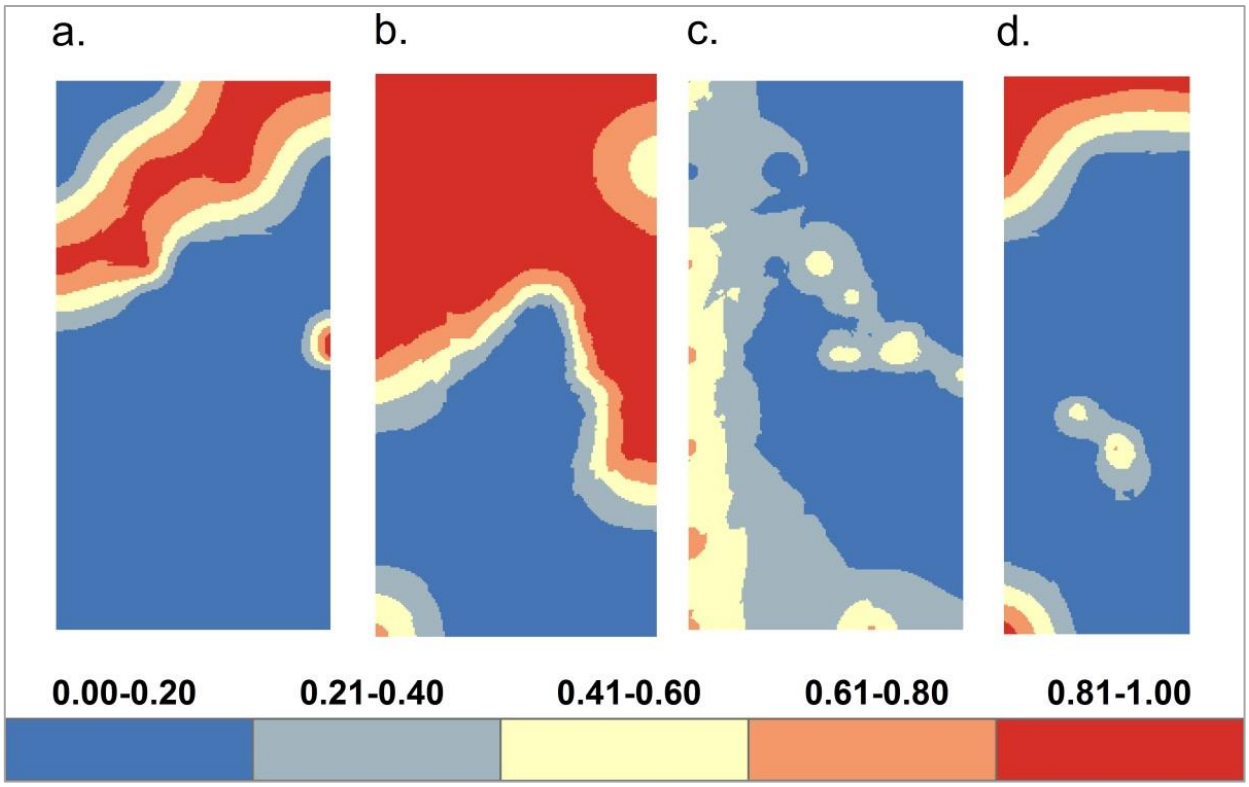

Figure 4.5: Probability maps of a) Earthworks using a 400 ppm threshold, b) Earthworks using a 150 ppm threshold, c) Growing Joy Plot #1 using a 150 ppm threshold, and d) Growing Joy Plot #2 using a 150 ppm threshold

4.3 Simulated Random Sampling

4.3.1 EPA Sampling Methodologies

Two Monte Carlo simulations were completed to assess current U.S. EPA soil sampling methods for residential and past residential lots (Section 3.5.2). For the purpose of each of the four scenarios evaluated in this study, the probability of exceeding 400 ppm or 150 ppm observed in the ordinary kriging estimates was treated as the "correct" threshold exceedance probability, and Monte Carlo simulation results were compared to this value. Threshold exceedance probabilities were calculated using cumulative frequencies from ordinary kriging estimate CDFs (solid black curves on Figures 4.6-4.9). The cumulative frequency value at the soil hazard standard was subtracted from 1.0 (i.e. 100% exceedance probability) to arrive at a percentage of values that were greater than the soil hazard standard (i.e. the threshold exceedance probability). For the Earthworks plot, the probability of exceeding 400 ppm (i.e. the "correct" threshold exceedance probability for the purposes of risk assessment) was 9%, and the probability of exceeding 150 ppm was 66%. The first and second Growing Joy plots had threshold exceedance probabilities for 150 ppm of 29% and 18%, respectively.

Table 4.6: Percent of kriging estimates exceeding 150 ppm or 400 ppm

	Earthworks Plot	**Growing Joy Plot #1**	**Growing Joy Plot #2**
Kriging estimates exceeding 150 ppm	66%	29%	18%
Kriging estimates exceeding 400 ppm	9%	0%	0%

Results of the simulations associated with program EPA2003 are shown in Figure 4.6. These simulations were designed following EPA guidelines (USEPA, 2003) that involve taking as few as two composite samples to characterize the global mean of a site (Section 3.5.2). Two, three, four, five, or six samples were averaged per trial, and this process was repeated 10,000 times. Results from these trials were plotted as CDFs along with the ordinary kriging estimate

CDF (Figure 4.6). If a 400 ppm threshold is applied to the Earthworks plot, the exceedance probability decreases from 9% in the ordinary kriging estimate to 3% when two samples were averaged. If six samples are averaged, there is virtually a 0% exceedance probability (Figure 4.6a). On the same plot, however, using a 150 ppm threshold has the opposite effect. There is a 66% exceedance probability at 150 ppm, and as more samples are averaged, the exceedance probability increases, first to 70% when two samples are averaged, and continuing to increase until, when six samples are averaged, the exceedance probability is about 83% (Figure 4.6a). This change in behavior between thresholds has an important effect on risk assessment, and is discussed in Chapter 5.

Results on the Growing Joy plots applying the 150 ppm threshold behaved similarly to the 400 ppm Earthworks results. Growing Joy plot #1 shows a rapid decrease in exceedance probability from 29% to 20% after averaging (i.e. compositing) two samples (Figure 4.6b.). This trend continues as more samples are averaged, but after averaging six samples a 5% probability of exceeding 150 ppm remains. On Growing Joy plot #2, averaging two samples results in the same exceedance probability as the kriging estimates, or 18% (Figure 4.6c). As the number of samples increases, there is a slight decrease in exceedance probability, but it is less extreme than the increase in the first plot. In fact, when six samples are averaged, a 6% exceedance probability remains, slightly higher than that of Growing Joy plot #1.

The second EPA sampling scheme assessed here relies upon the calculation of a relative percent difference, or RPD. In this simulation (program EPA2000), two samples, each composed of three to five composite samples, were selected until an RPD of less than 50% was achieved, then all prior samples were averaged (see Section 3.5.2). In general, this simulation produced

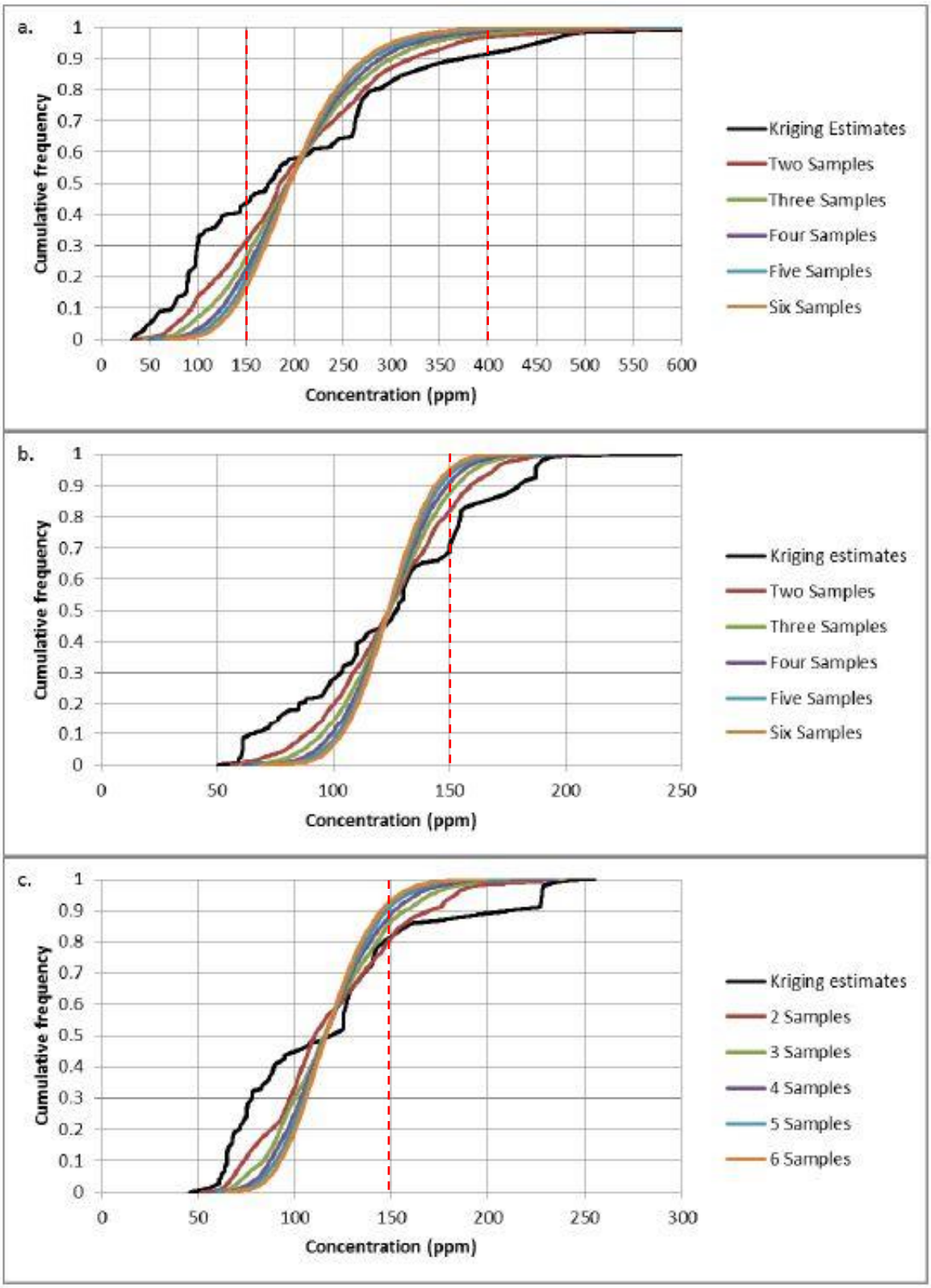

Figure 4.6: Results of Monte Carlo simulation using EPA2003 for a) Earthworks, b) Growing Joy #1 and c) Growing Joy #2 garden plots

more uniform CDFs (Figure 4.7), and the associated change in the exceedance probability of each trial was greater than in the previous simulation.

Simulations conducted using data from the Earthworks plot produced opposing results at the two thresholds (400 ppm and 150 ppm). Using the kriging estimates, there is about a 9% exceedance probability at 400 ppm, and this falls to less than 1% when three, four or five composites per sample are averaged (Figure 4.7a). Conversely, the 66% exceedance probability at 150 ppm increases to 90% when three composites are used, and reaches almost 100% when five composites are used (Figure 4.7a). Again, the effect this change has on risk assessment is discussed further in the next chapter.

Results of Growing Joy plots for the same simulation are shown in Figures 4.7b and c. The three composite trial on Growing Joy Plot #1 resulted in a decrease in the threshold exceedance probability from 29% to about 6% (Figure 4.7b). When five composites were averaged, less than a 1% probability of exceeding the soil hazard standard remained. The behavior on the second Growing Joy garden was similar, with the exceedance probability decreasing from 18% to 6% with three composites to an exceedance probability of about 1% when five composites were averaged per sample (Figure 4.7c).

4.3.2 Sampling Design, Number of Samples and Soil Hazard Standard

Results of simulations comparing differing sampling strategies and number of samples (programs RANDSAMP and GRIDSAMP) are shown in Figure 4.8 and 4.9. To assess the effect of sampling design, number of samples, and soil hazard standard, more general sampling designs (i.e., grid based or random sampling) were used instead of specific EPA methods. Samples were selected both randomly from the entire plot (RANDSAMP) or randomly within an evenly spaced

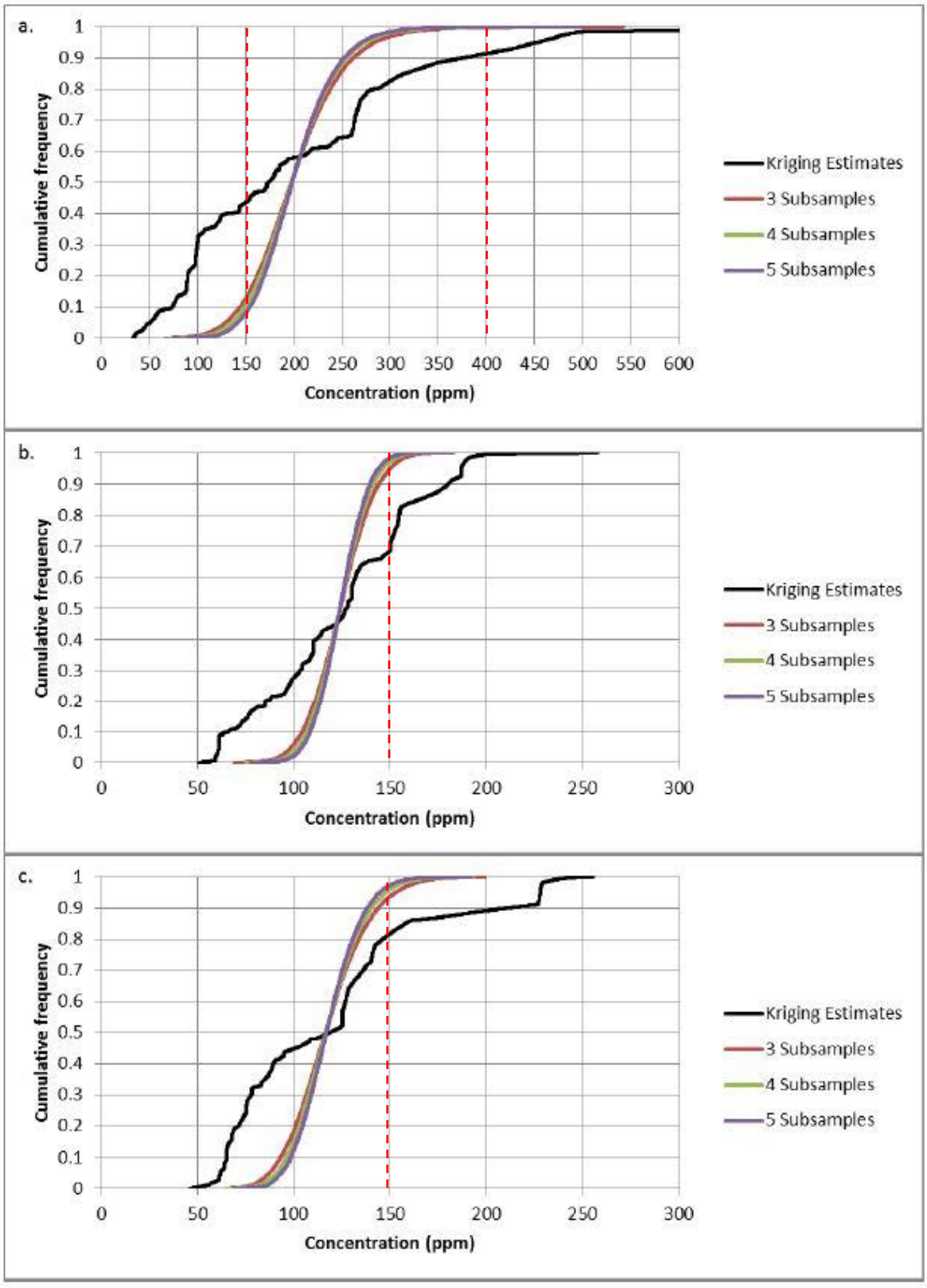

Figure 4.7: Results of Monte Carlo simulation using EPA2000 for a) Earthworks, b) Growing Joy Plot #1 and c) Growing Joy Plot #2 garden plots

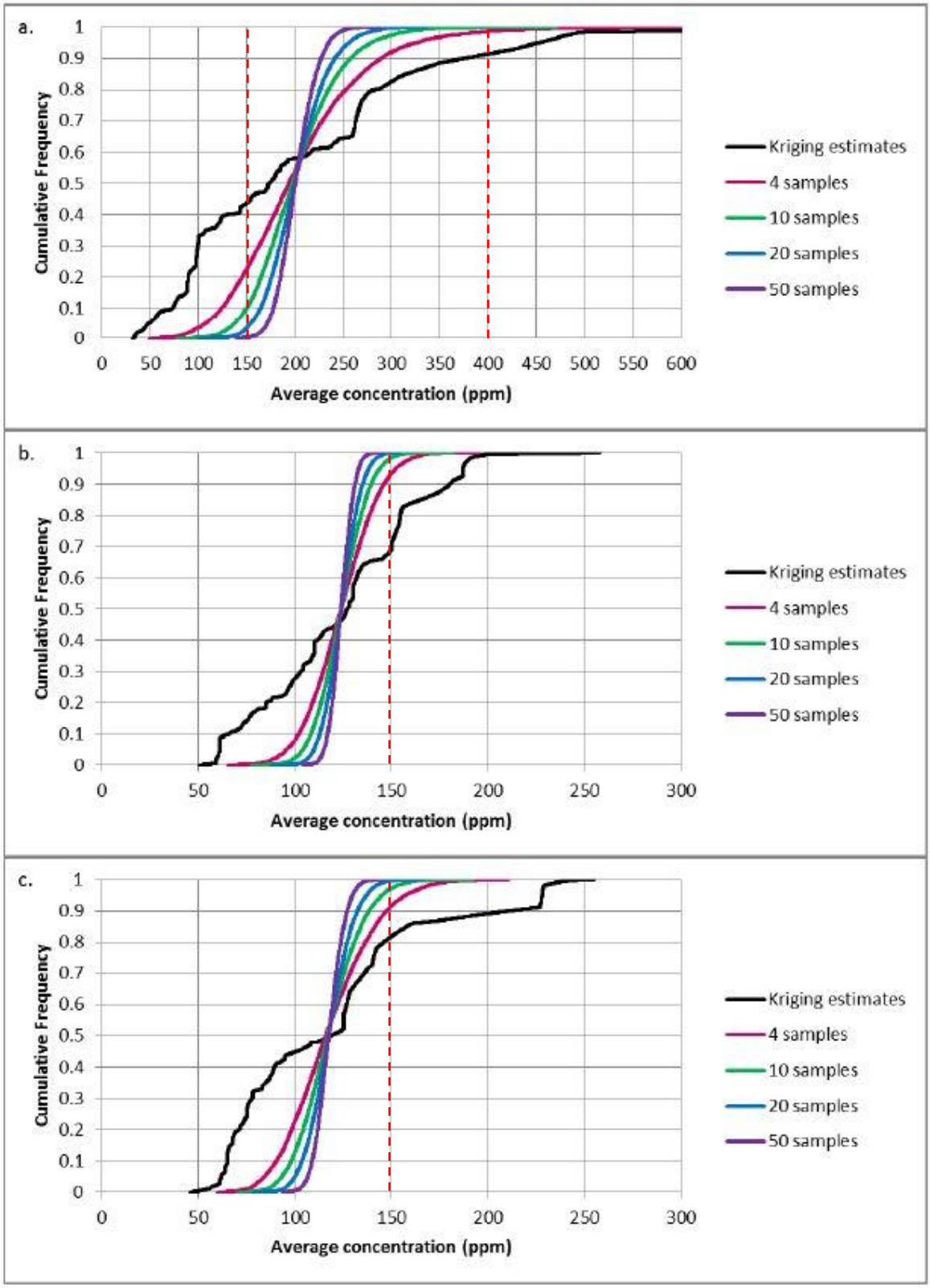

Figure 4.8: Results of Monte Carlo simulation using RANDSAMP for a) Earthworks, b) Growing Joy Plot #1 and c) Growing Joy Plot #2 garden plots

grid across each plot (GRIDSAMP), while varying the number of samples per trial and soil hazard standard.. The number of samples averaged together in each trial was varied from 4 to 10, 20 or 50 samples (or blocks with one sample per block, for GRIDSAMP), and the soil hazard standard was varied between 400 ppm (where applicable) and 150 ppm. The programs RANDSAMP and GRIDSAMP generated an average concentration per trial (to assess the effects of compositing) and a binary detection flag that was triggered if the concentration at any of the blocks in a trial was greater than the soil hazard standard. The number of trials with binary detection flags was divided by10,000 total trials to calculate a hotspot detection probability for each Monte Carlo simulation.

In the random RANDSAMP simulations of the Earthworks plot, the probability of exceeding 400 ppm was about 1% for 4 samples and effectively 0% for 10, 20 or 50 samples (Figure 4.8a). The probability of exceeding 150 ppm ranged from 95% with 4 samples to 100% with any number of samples greater than four (4.8a). On Growing Joy plot #1 (Figure 4.8b), there was an 8% chance of exceeding 150 ppm with 4 samples, 2% with 10 samples, and 0% with more than 10 samples. On Growing Joy plot #2 (Figure 4.8c), there was a 10% chance of exceeding 150 ppm with 4 samples, 2% with 10 samples, and 0% with either 20 or 50 samples.

The grid based GRIDSAMP simulations yielded similar results (Figure 4.9). On the Earthworks plot (Figure 4.9a), there was essentially no chance of exceeding 400 ppm with four or more samples. With respect to a 150 ppm standard, there was a 90% probability of exceedance with 4 samples, and a 100% probability of exceedance with 10, 20 or 50 samples. On Growing Joy #1 (Figure 4.9b), there was a 1% chance of exceeding 150 ppm with 4 samples, and virtually no chance of exceedance with 10, 20 or 50 samples. On Growing Joy plot #2 (Figure 4.9c), there was a 10% chance of exceeding 150 ppm with 4 samples per trial, but virtually no chance of

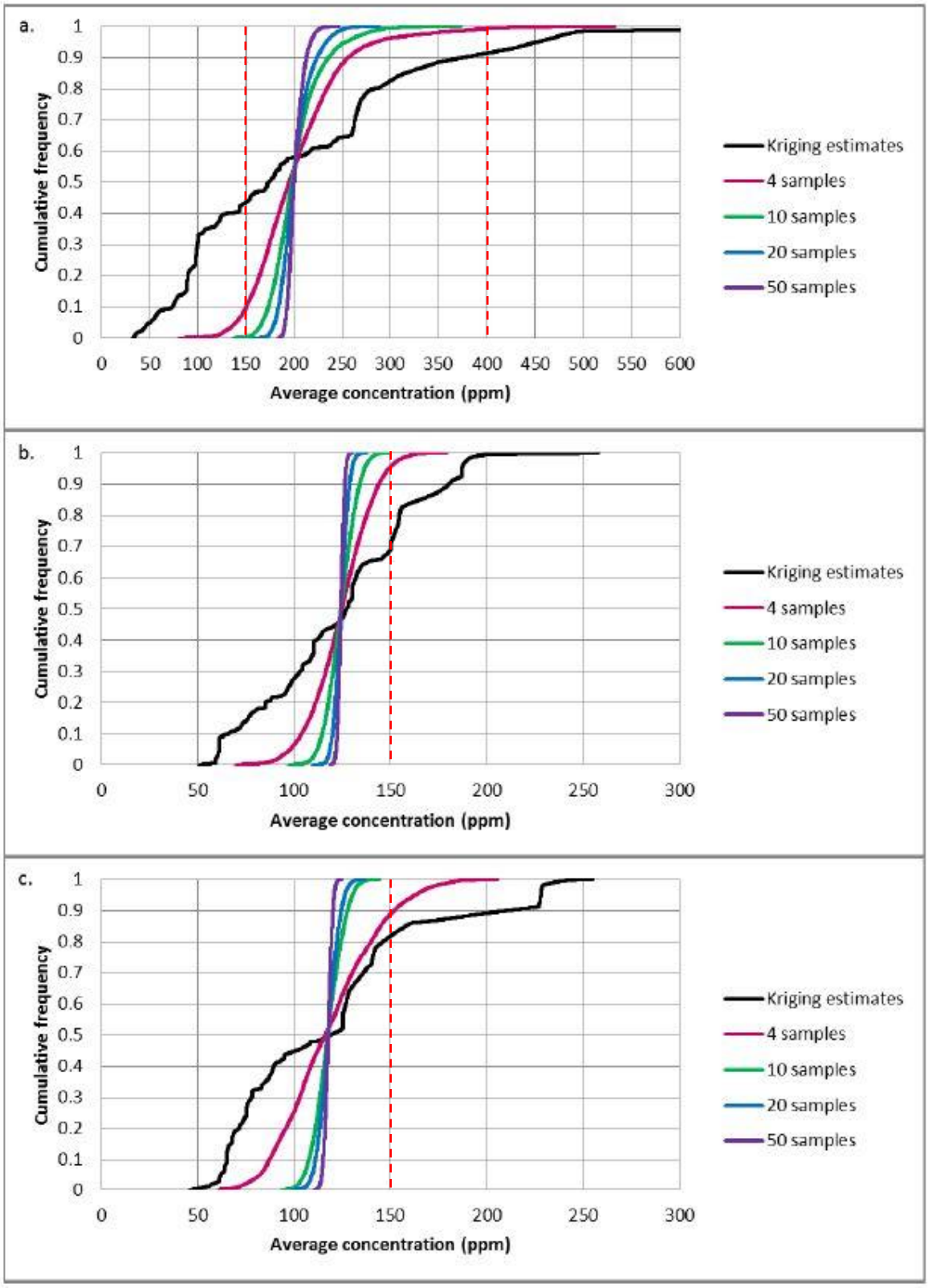

Figure 4.9: Results of Monte Carlo simulation using GRIDSAMP for a) Earthworks, b) Growing Joy Plot #1 and c) Growing Joy Plot #2 garden plots

exceedance with 10 or more samples. A strong smoothing was observed on all simulation CDFs when compared to the CDF of the ordinary kriging estimates.

In addition to calculating an average concentration per trial, the hotspot detection probability (i.e. the probability of detecting at least one sample greater than the threshold) was calculated for each random and grid based Monte Carlo simulation (Figure 4.10). As expected, the grid based sampling pattern consistently required fewer samples to achieve 90% or 95% probability that a hotspot was detected. Using a 400 ppm soil hazard standard on the Earthworks plot, 18 and 22 samples were required, respectively, to achieve 90% or 95% hotspot detection probability with the gird sampling pattern. This compares to 25 and 35 samples, respectively, with the random sampling pattern (Figure 4.10a). When a 150 ppm soil hazard standard is applied at the Earthworks plot, little difference is seen between random or gridded sampling. With both sampling designs, 3 and 4 samples were needed to achieve 90 or 95% confidence in detection (Figure 4.10b). On the Growing Joy plot #1, 6 and 8 samples were required to achieve 90% or 95% confidence with a grid based design, compared to 8 and 9 with the random sampling design (Figure 4.10c). Finally, on Growing Joy plot #2, a grid based sampling design required 9 or 10 samples to achieve 90% or 95% confidence in detection, whereas a random sampling design required 11 or 17 samples, respectively (Figure 4.10d). These results are summarized in Table 4.7.

Table 4.7: Summary of hotspot detection results

	Earthworks Plot					**Growing Joy Plot #1**			**Growing Joy Plot #2**	
Soil Hazard Standard	**400 ppm**		**150 ppm**			**150 ppm**			**150 ppm**	
Sampling Design	*Grid*	*Random*	*Grid*	*Random*		*Grid*	*Random*		*Grid*	*Random*
Samples required for 90% confidence	18	25	3	3		6	8		9	11
Samples required for 95% confidence	22	35	4	4		8	9		10	17

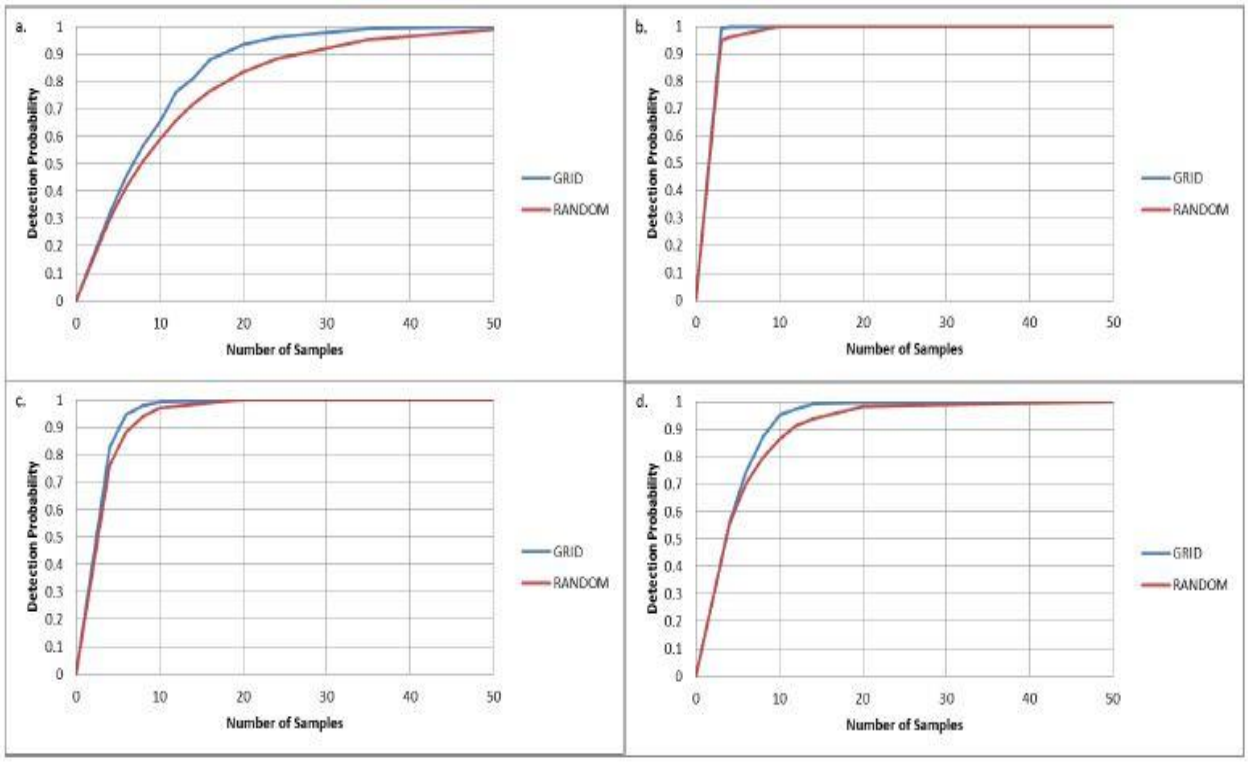

Figure 4.10: Detection probability using either a grid or random sampling design for a) Earthworks using a 400 ppm threshold, b) Earthworks using a 150 ppm threshold, c) Growing Joy Plot #1 using a 150 ppm threshold, and d) Growing Joy Plot #2 using a 150 ppm threshold

4.4 Misclassification and Probability Threshold

Results related to the effect of probability threshold on site misclassification are presented in Figure 4.11. A minimum of five different probability thresholds, corresponding to exceedance probabilities from the original probability maps (Figure 4.5), were examined: p = 0.05, 0.35, 0.50, 0.65, and 0.95. Additional probability thresholds (p=0.30 and 0.40), were also examined if five thresholds were not enough to confidently define a probability of misclassification minimum. On the Earthworks plot, the risk of misclassification (i.e. the sum of false positive and false negative error), is minimized near p = 0.65 for a soil hazard standard of 400 ppm (Figure 4.11a). The misclassification risk is minimized near p = 0.50 when a 150 ppm soil hazard standard is used instead (Figure 4.11b). Growing Joy Plot #1 required additional

probability thresholds for accurate characterization, and generated a minimal misclassification risk near p = 0.35 (Figure 4.11c). The lowest risk of misclassification for Growing Joy Plot #2 occurs near p = 0.50 (Figure 4.11d).

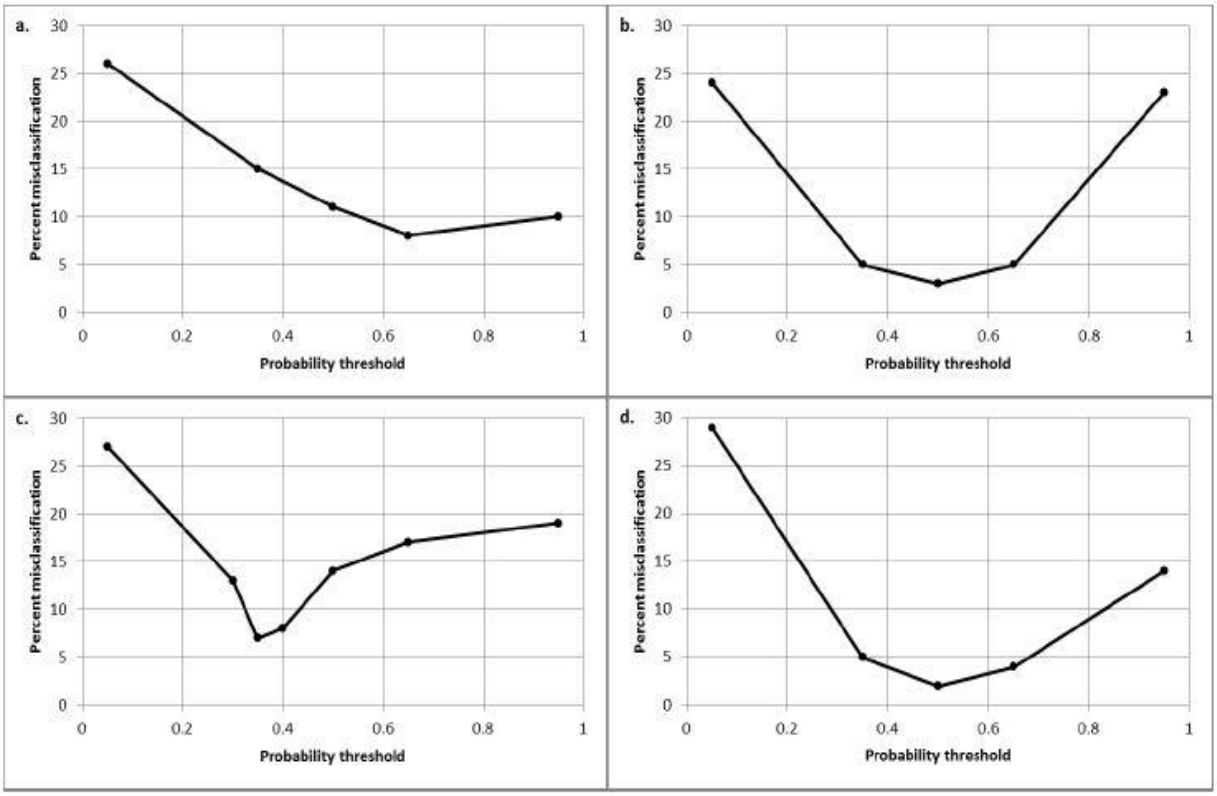

Figure 4.11: Effect of probability threshold on the probability of site misclassification for a) Earthworks using a 400 ppm threshold, b) Earthworks using a 150 ppm threshold, c) Growing Joy Plot #1 using a 150 ppm threshold, and d) Growing Joy Plot #2 using a 150 ppm threshold

The effect of probability threshold on false positive and false negative error is observable in the error maps presented in Figure 4.12. Regardless of the site or the chosen soil hazard standard, the risk of false positive error is highest at the lower probability thresholds, while the risk of false negative error is higher at the higher probability thresholds (Figure 4.12). When a 400 ppm hazard standard was used on the Earthworks plot, there was a much higher incidence of type I error than type II error overall. Spatially, most of the error surrounded the hotspot in the

upper left hand corner of the site (Figure 4.12a). When a 150 ppm soil hazard standard was used on the Earthworks plot, the error was again grouped around the hotspot (Figure 4.12b). Unlike the 400 ppm Earthworks error map, however, the 150 ppm maps had a roughly equal incidence of type I and type II error overall. Error maps for Growing Joy Plot #1showed a considerably higher incidence of type I error at the 0.05 probability threshold (Figure 4.12c) than any of the other plots. Similar to the other plots, as probability threshold increased, the incidence of type II error increased and the incidence of type I error decreased. Error maps of Growing Joy Plot #2 (Figure 4.12d) also contained areas of false positive and negative error adjacent to the edges of hotspots, as well as a slightly higher incidence of type I error than type II error.

Figure 4.12a

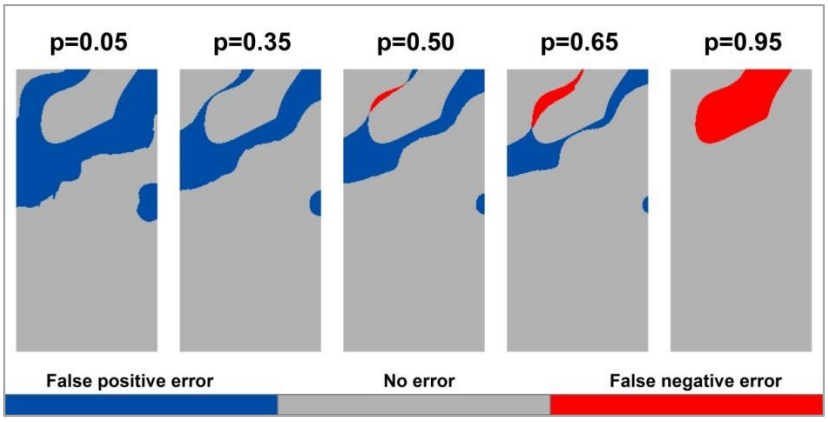

Figure 4.12b

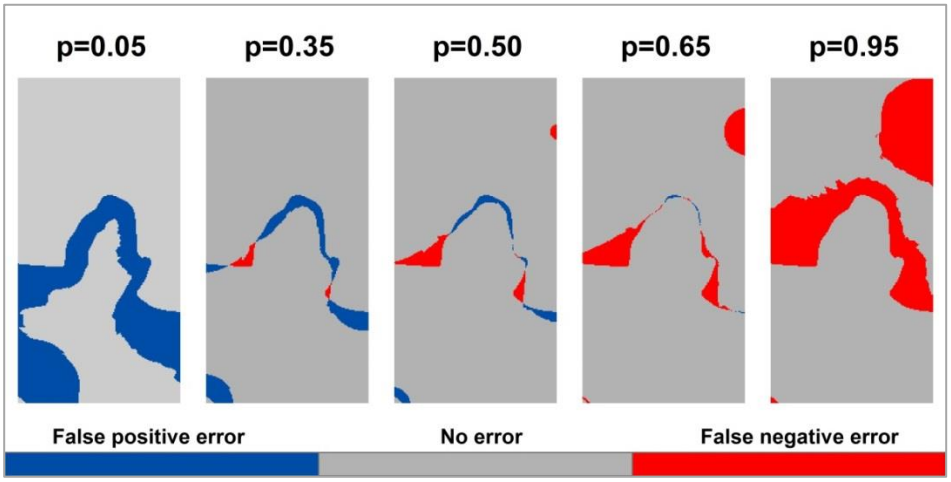

Figure 4.12c

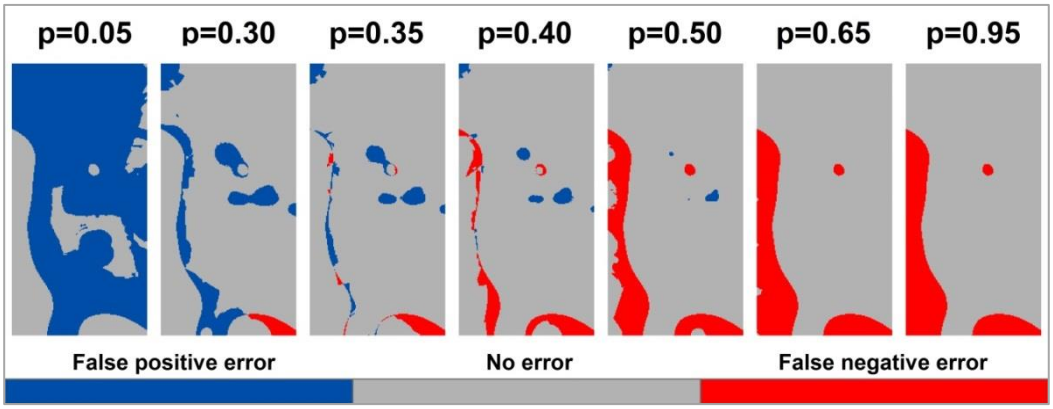

Figure 4.12d

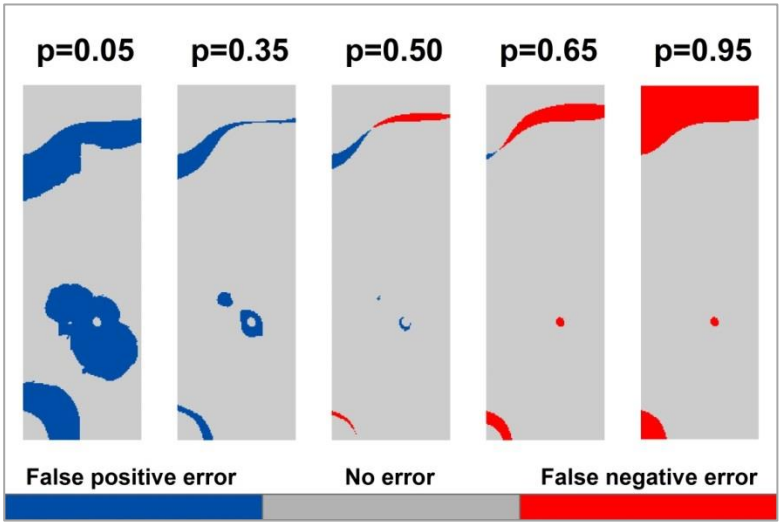

Figure 4.12: Misclassification error maps for a) Earthworks using a 400 ppm threshold, b) Earthworks using a 150 ppm threshold, c) Growing Joy Plot #1 using a 150 ppm threshold, and d) Growing Joy Plot #2 using a 150 ppm threshold

Chapter 5

Discussion

5.0 Introduction

The purpose of this thesis was to assess risk associated with various soil sampling strategies designed for residential and past residential sites, specifically in the context of urban gardening. A desired outcome was the formulation of recommendations for soil lead sampling on urban gardens. Three working hypotheses were developed to assess the effect of spatial variability and sampling design on soil sampling recommendations. This chapter presents a discussion of the results reported in Chapter 4, as well as a study limitations, conclusions, and directions for future research.

5.1 Sample Data Description and Laboratory Analyses

Basic statistics of the sample data are presented in Section 4.1. Soil lead measurements collected at each garden were highly non-normal and right-skewed (i.e. the distribution had a higher mean than median). This result is typical of environmental data, because with the exception of extremely polluted sites, there is usually a greater likelihood of a sample distribution containing many low concentrations with fewer outlying higher concentrations.

Most of the measured soil lead concentrations on the gardens sampled in this study fell below the current regulatory standard of 400 ppm. None of the samples at either Growing Joy garden plot analyzed had concentrations higher than 400 ppm. The Earthworks garden had one sample with a maximum concentration of 1,532 ppm, well over regulatory standards, and two additional samples with concentrations between 400 and 500 ppm. The three garden plots were former residential sites with similar gardening and tilling histories. The primary differences

between the Earthworks plot and both Growing Joy plots are visible in historic Sanborn maps of both properties. In 1951, the Earthworks plot had a paint shop located in the northwest corner as well as two homes on the property. The Growing Joy gardens contained only individual residential structures. The paint shop on the Earthworks plot may have contributed to the elevated soil lead observed concentrations there.

If 150 ppm were specified as the hazard standard instead of 400 ppm, a much greater portion of all three sites would be considered contaminated (Figure 4.4). On the Earthworks plot, many of the samples in the upper half of the site exceed 150 ppm. On Growing Joy Plot #1, the samples along left edge of the site and two samples in the center of the site exceeded 150 ppm. On Growing Joy Plot #2, samples collected along the northern and southern site boundaries exceeded 150 ppm.

Total unsieved to sieved lead correlations were calculated for each site (see section 4.1). Pearson correlation coefficients exceeded 0.90, indicating a strong correlation. On the Earthworks plot, sieved total lead concentrations were consistently higher than total lead concentrations, as would be expected because smaller particles have a greater proportion of surface area available for adsorption of lead ions per mass of soil particle (Abouelnasr, 2009). A similar relationship was observed on the first Growing Joy plot. On the second Growing Joy plot, the unsieved to sieved relationship was approximately one to one; that is to say, the unsieved and sieved concentrations were roughly equal (Figure 4.2). A potential explanation for this is the high clay content of the Growing Joy soils, which is dominated by fine-fraction particles. If most of the soil lead is found in the fine fraction, which is present in both sieved and unsieved soil samples, the fine fraction concentration could dominate both concentrations and a one to one

correlation could result. Testing this explanation involves more rigorous lead measurements for various soil particle size fractions that are outside of the scope of this thesis, however.

After sieving and analysis, a bioaccessible to total sieved soil lead correlation was also calculated. These Pearson correlations were high as well (ρ = 0.88-0.92, see Section 4.1), indicating a strong correlation as expected. The bioaccessible fractions (i.e. the fraction of total soil lead that can be readily absorbed by the human digestive system) on the three sites ranged from 0.16 to 0.22. These bioaccessible fractions are lower than the assumed bioavailability of 30% used in calculations involving the EPA's IEUBK model (USEPA, 1994a).

The results of declustering the data support the conclusion that the measurements were preferentially clustered in areas of low concentrations at each site. Declustered means on each garden plot were notably higher than their clustered counterparts (Table 4.1).

5.2 Geostatistical Analysis

5.2.1 Variography

Experimental variograms and variogram models for total and bioaccessible lead for each site are described in Section 4.2.1. The total and bioaccessible lead variogram structures were similar to each other at each garden, which was expected given the high total to bioaccessible lead correlations discussed in the previous section. Prior to normal score transforms, Gaussian variogram models generated the best visual fit for most of the experimental variograms (Bugdalski et al., 2013). Homogenization of the site resulting from tilling is a potential explanation for this fit. However, after the normal score transform, better fits were obtained with either a spherical or exponential variogram model. This change could be caused by the normal score transform altering the skewness of the distribution and therefore the spatial continuity of

the data, especially at low concentrations. After the normal score transform, data are less skewed and the tail of the distribution associated with low concentrations is longer. This leads to less short scale continuity at these low concentrations, and therefore the Gaussian model, which is used to model very strong short scale continuity, is no longer an appropriate fit for the experimental variograms.

Spatial variability exists on each plot at scales smaller than a typical residential lot or urban garden. With the exception of the Growing Joy Plot #1 bioaccessible lead variogram, the variogram ranges were greater than 15 meters, which was greater than any of the sample spacings used in this study but smaller than the site dimensions. Spatial variability at this scale is typically considered minimal in the design of sampling campaigns. These results suggest, however, that soil lead distributions are not as continuous at small scales as previously assumed. This is potentially a function of grain size variability on urban sites and the uneven distribution of lead between different grain size fractions. The similarity in variogram model range, and therefore spatial variability, between the three gardens *supports the first hypothesis of this thesis: All three gardens will display a similar degree of spatial variability, although site-specific spatial patterns may be present.*

5.2.2 Ordinary Kriging

Although each site had similar lead concentration distributions arising from likely similar lead sources, the spatial patterns of ordinary kriging estimates differ among the three sites (Section 4.2, Figure 4.4), which also *supports the first hypothesis of this thesis*. A strong similarity between the spatial patterns of total and bioaccessible soil lead was observed on each of the plots (see Figure 4.4), which suggests that in addition to strongly correlated laboratory

measurements, total and bioaccessible concentrations were also well correlated in space. Differences among the spatial distribution of bioaccessible lead are also clearly evident among the three plots (Figure 4.4), however.

In general, the highest concentrations on each of the three sites lay along the site boundaries. This could be caused by adjacent roadways, alleyways, or homes with exterior lead based paint affecting the spatial patterns (i.e. areas of high and low concentration), suggesting that proximity and land use of neighboring properties can have a discernable effect on soil lead concentrations in urban residential lots.

Because of the declustering effect of kriging, kriging means were consistently higher than raw data means at each site. However, kriging means were also lower than the declustered means by 9-17% (Table 4.1 and Table 4.4). This result is likely attributable to the much greater number of data averaged to calculate a mean kriging estimate as compared to a declustered mean.

In addition to hotspots identifiable on ordinary kriging maps (Figure 4.4), two different types of hotspot signatures are evident on CDFs of ordinary kriging estimates for the three sites. These signatures are most evident when the kriging estimates are generated from declustered normal score transformed data, because smoothing effects imparted by clustering are removed from the CDF. The first type of signature indicates the presence of a hotspot composed of a small number of estimates at the tail of the distribution that exceed the other estimates on the site. For example, on the CDF of the Earthworks plot kriging estimates (the solid black line in Figures 4.6a-4.9a) there is a gradual increase in cumulative frequency from about 350 to 500 ppm, and an even more gradual increase from 500 to 600 ppm. As the concentration is increasing quickly, the cumulative frequency is increasing slowly, indicating that relatively few estimates account for a large change in concentration. The second type of hotspot signature is composed of a group

of samples of the same or similar concentration that are above the regulatory threshold. For example, in Figures 4.6c-4.9c, the CDF is nearly vertical at about 225 ppm, indicating that there is little change in concentration as the cumulative frequency increases. This means there is a set of similar estimates greater than the 150 ppm threshold, or in other words, a hotspot, that covers approximately 8% of the site. This corresponds to the hotspot visible in the lower left hand corner of Growing Joy plot #2 (see Figure 4.4).

5.2.3 Multiple Indicator Kriging and Probability Maps

Probability maps generated using multiple indicator kriging are shown in Section 4.2.3 (Figure 4.5). Ordinary kriging maps and probability maps on each site were similar. The probability maps in this study were generally less smooth than their ordinary kriging counterparts, which was a function of the small range of some of the indicator variograms and the less pronounced smoothing effect of indicator kriging compared to ordinary kriging. No attempt was made to smooth these maps because their main function was to serve as an exhaustive data set used to generate error maps, and smoothing would have resulted in less detailed maps. The probability map for the Earthworks plot with 150 ppm as the hazard standard (Figure 4.5b) was the only map where the exceedance probability ranges from 0.0 to 1.0, or 0 to 100%. The elevated concentrations leave little uncertainty of exceeding 150 ppm in certain areas of the site. Most of the probability maps did not reach a value of 1.0 in the areas identified as hotspots, indicating that an element of uncertainty associated with these estimates remains.

5.3 Risk Assessment

5.3.1 The Effect of Sampling Goal

Designing a soil sampling campaign involves a series of decisions based on site specific goals and conditions (Figure 5.1). The first, and often overriding, decision is the goal of the sampling campaign. The two major sampling goals considered here are global mean estimation and hotspot detection or delineation. These two goals can lead to different interpretations of the same data. For example, if we consider the kriging estimates (i.e. the exhaustive data set) of the Earthworks plot, , there is a 9% exceedance probability for a hazard standard of 400 ppm (see Section 4.3.1). The mean of the kriging estimates, however, is 202 ppm. If the goal of the sampling campaign is to characterize a global mean, this site appears safe, because the mean is less than 400 ppm. However, if the sampling goal is hot spot detection, then the exhaustive data indicates the site has a hotspot, because 9% of the estimates are greater than 400 ppm, and this site would be classified as contaminated. Thus, the differing sampling goals result in opposite determinations with respect to the safety and contamination of the same site. The sampling goal is therefore the first decision that should be made in the course of a sampling campaign. This result *supports hypothesis 2.1 of this thesis: Error rates (false negative or false positive) at each site will depend upon: (1) the sampling objective (global average concentration versus hot spot detection).*

Assessing the effects of decisions subsequent to the determination of the sampling objectives described above, including sampling according to a design-based or model-based approach, the number of samples and subsamples, and the soil hazard standard (Figure 5.1) is the focus of the second hypothesis of this thesis, which is discussed in detail in the following subsections. First, the effects of decisions made when the sampling goal is global mean

characterization are assessed in 5.3.2, followed by an assessment of the effects of decisions made when the sampling goal is hotspot detection in 5.3.3.

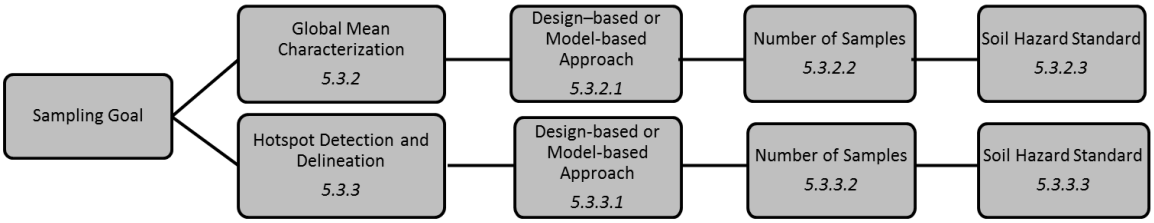

Figure 5.1: Sampling design decisions

5.3.2 Characterization of a Global Mean

5.3.2.1 Design-based vs. Model-based Approach

The effects of changes in the sampling decisions discussed hereafter are derived from results of the Monte Carlo simulations described in Section 4.3. A design-based approach evaluates uncertainty by repeated, controlled random sampling under the assumption that the distribution of concentrations is fixed, whereas a model-based approach involves repeated sampling with fixed locations (e.g., a grid), within varying spatial patterns of concentrations (de Gruijter et al., 2006). Classical random sampling methods are examples of design-based approaches, whereas using a gridded sampling pattern and geostatistical methods are examples of a model-based approach (de Gruijter et al., 2006). In the context of the following discussion, design-based methods will refer to random sampling, and model-based methods will refer to sampling on a regular grid.

When characterization of a global mean is the sampling goal, two EPA random sampling strategies were considered in addition to a basic random sampling campaign. The results of

simulations associated with these strategies are presented in section 4.3.1 and 4.3.2. On the Earthworks plot, the exhaustive data mean of the kriging estimates is 202 ppm, well below the regulatory 400 ppm regulatory standard. The exhaustive data means of the Growing Joy plots are 124 and 118 ppm respectively, below the potential 150 ppm soil hazard standard. With both EPA methods, there is a chance of type I error (i.e. the probability of classifying a site as unsafe when it is safe in reality), because concentrations greater than the hazard standard are present on the site, even though the global mean is less than the hazard standard. In other words, there is chance the mean concentration obtained from partial sampling of any of these sites might be greater than the true global mean soil lead concentration. This chance of type I error decreases with increasing number of samples. Therefore, taking and compositing a larger number of samples is beneficial when global mean characterization is the sampling goal because it lowers the risk of type I error. Sampling goal and choice of EPA sampling design have a considerable influence on the incidence of type I error when using a design-based approach to characterize a global mean concentration; thus, *supporting hypotheses 2.2 of this thesis: Error rates (false negative or false positive) at each site will depend upon: (2) the sampling method*. Both EPA methods are subject to potential type I error, but the effect is more pronounced in the RPD-based sampling strategy (Figure 4.7).

If model-based approaches are employed, there is little change in the chance of false positive error as an increasing number of samples are averaged (compare Figure 4.8 and 4.9). For example, on the Earthworks plot, the probability of exceeding 400 ppm when four samples are averaged, and therefore probability of type I error, was about 1% when both random and grid based sampling designs were used. This result is consistent across each site, suggesting that when the sampling goal is global mean characterization, the sampling approach has little effect,

because averaging samples tends to mask potential differences in concentration. When grid-based methods are used to characterize a global mean concentration, results using the data sets examined here *do not support hypothesis 2.2 of this thesis*.

5.3.2.2 Number of Samples and Subsamples

The effect of the number of samples was assessed by varying the number from 4 to 50 in each simulation. As more samples are averaged, the probability of exceeding either 150 or 400 ppm, and therefore the probability of Type I error, decreases (see Figures 4.6-4.9). Therefore, when the sampling goal is global mean characterization, more than four samples are consistently enough to effectively eliminate probability of type I error on the plots examined herein.

The effect of the number of subsamples (i.e. composites) is shown in the EPA RPD-based sampling strategy simulation results (Figure 4.7). In these simulations, taking two samples, each of which is comprised of 3 subsamples, leads to a 0% probability of type I error. From the perspective of global mean characterization, taking two three-point composite samples is enough to virtually eliminate the chance of type I error on any of these gardens. The tendency of an increased number of samples and subsamples to decrease the chance of type I error *supports hypotheses 2.3 and 2.4 of this thesis*: *Error rates (false negative or false positive) at each site will depend upon: (3) the number of samples taken, and (4) the averaging method (i.e., compositing) employed.*

5.3.2.3 Soil Hazard Standard

The relationship between the soil hazard standard and the mean concentration also has a considerable effect on the incidence of type I error at every site. If the soil hazard standard is

greater than the site mean, the type I error decreases as more samples are averaged. However, if the soil hazard standard is less than the site median (e.g., 150 ppm standard on the Earthworks plot), this behavior is reversed, and as more samples are averaged, the exceedance probability increases along with the chance of type I error (see Figure 4.8a). The choice of soil hazard standard has the potential, therefore, to produce opposing results with respect to risk assessment, *supporting hypothesis 2.5 of this thesis: Error rates (false negative or false positive) at each site will depend upon: (5) the chosen soil lead hazard standard.*

The difference between the 400 ppm and 150 ppm soil hazard standards cannot be assessed on the Growing Joy Garden plots because there were no samples greater than 400 ppm on either plot. However, it is likely that a similar change would be observed at concentrations lower than the median concentration on each of the Growing Joy plots. If the soil hazard standard were lower (the 80 ppm California guideline, for example), similar behavior would be seen on the Growing Joy Garden plots when assessing the difference between the 150 ppm and 80 ppm standard, because 80 ppm is less than the median concentration of both sites.

5.3.3 Hotspot Detection and Delineation

5.3.3.1 Design-based vs. Model-based Approach

The simulation results with respect to detection probability are shown in Figure 4.10. The number of samples needed to achieve 90 or 95% confidence in hotspot detection is consistently lower when the site is sampled on a grid instead of randomly. The strong effect of sampling design when hotspot detection is the goal *supports hypothesis 2.2 of this thesis*. The most significant difference between random and grid sampling occurred on the Earthworks plot using a 400 ppm hotspot threshold (Figure 4.10a). The smallest difference between the grid and

random methods is on the Earthworks plot when 150 ppm is used as the standard. In this instance, the "hotspot" comprised more than half of the garden plot, and therefore few samples were required for detection regardless of sampling strategy.

A similar result was seen between the two Growing Joy plots. Growing Joy Plot #1 had a higher exceedance probability in the exhaustive data set (29%) than Growing Joy Plot #2 (18%), and the choice of sampling design has less impact on the number of samples needed for detection on Growing Joy Plot #1. Again, this is because almost one third of Growing Joy Plot #2 is a hotspot (when 150 ppm is the hazard standard), so fewer samples are required for detection regardless of sampling strategy. Growing Joy Plot #2 still has a relatively high exceedance probability, however unlike Growing Joy Plot #1, the hotspots on this site are isolated from one another, making detection more difficult and requiring a larger number of samples. This result suggests that while the choice of sampling design has a strong effect on the number of samples needed for hotspot detection, this effect is more pronounced when the hotspot(s) on the site are smaller and/or isolated from one another.

5.3.3.2 Number of Samples and Subsamples

The number of samples needed to achieve 90 or 95% confidence in hotspot detection is also annotated in Table 4.6. The number of samples needed is highly site specific, and ranges from 3 to 18 samples needed to achieve 90% confidence. Only three samples were needed on the Earthworks plot (when 150 ppm is the threshold) because such a large portion of concentrations on the site were above the 150 ppm soil hazard standard. This situation, where over half the plot exceeds the soil hazard standard, is expected to be atypical for most urban gardens on past residential sites. Therefore in most cases, between 6 and 18 samples (the range in number of

samples needed for hotspot detection in the other data sets) likely describes a more realistic sampling situation.

With respect to subsamples, combining even two subsamples causes a considerable decrease in exceedance probability with respect to a given threshold concentration lying above the median of the CDF (see Figure 4.7). When hotspot detection is the sampling goal, this decrease in exceedance probability represents the decreased chance of detecting a hotspot. Therefore, a decrease in exceedance probability leads to an increase in type II error, or the chance of failing to detect a hotspot that exists on a site. Conversely, when global mean characterization is the sampling goal, compositing samples decreases type I error rates (see Section 5.3.2), again demonstrating the strong effect of both the number of samples and subsamples on risk assessment and *supporting hypotheses 2.3 and 2.4 of this thesis*. Because of the increased probability of type II error, compositing samples is not recommended when hot spot detection is the sampling goal.

5.3.3.3 Soil Hazard Standard

The effect of soil hazard standard can be evaluated by studying the differences in hotspot detection when a 400 ppm or 150 ppm standard is used on the Earthworks plot (see Figure 4.10a and b). When 400 ppm is used as the hazard standard, 18 samples are needed to achieve 90% confidence in detection. When 150 ppm is used as the hazard standard instead, only 3 samples are needed to achieve 90% detection. Again, this results from the large portion of the site exceeding 150 ppm. Because so few samples are necessary to detect a hotspot when the soil hazard standard is 150 ppm, there is a low risk of type II error. The 18 samples needed when a 400 ppm hazard standard is used likely exceed the typical cost-effective number of samples

affordable for urban garden plots. Consequently, the site would likely be under-sampled leading to a higher chance of type II error. The difference between the 400 ppm and 150 ppm soil hazard standards cannot be quantified because there were no samples greater than the 400 ppm soil hazard standard on the Growing Joy plots. However, if the soil hazard standard were lowered to the 80 ppm California soil hazard standard, for example, then a similar difference in the number of samples needed to detect a hotspot would be expected. These results again illustrate the considerable effect that the choice of soil hazard standard can have on risk assessment and *support hypothesis 2.5 of this thesis.*

5.3.4 Probability Threshold and Site Misclassification

A set of varying probability thresholds and probability maps were generated to evaluate the final hypothesis of this thesis (Section 4.4). An intermediate probability threshold is associated with the lowest percent misclassification in each data set (Figure 4.11a-d). Percent misclassification on Growing Joy Plot #1 was minimized at a probability threshold of approximately 0.35, while misclassification was minimized on the other sites near p=0.50 or p=0.65. Using these intermediate probability thresholds serves to minimize both type I and type II error. However, the risk of misclassification was not always minimized at the marginal probability of contamination (i.e. the percentage of the site that exceeded a given threshold), which *refutes the third hypothesis of this thesis*. For the Earthworks plot when 400 ppm is the hazard standard, the percent misclassification is minimized at p=0.65, and the marginal probability of contamination is 0.09. This finding holds on the remaining sites as well, although to a lesser degree. This suggests that the assertion that site misclassification is minimized at a

probability threshold near the marginal probability of contamination proposed by (Saito and Goovaerts, 2002) is overly generalized.

In each case examined here, false positive error dominates at low probability thresholds and false negative error dominates at the higher thresholds (Figure 4.12). The incidence of type I error was also higher than the incidence of type II error in the 400 ppm Earthworks data set and the both Growing Joy data sets. However, when a 150 ppm soil hazard standard was applied to the Earthworks plot, the two types of error are nearly equal (see Figure 5.2b). Figure 5.2 illustrates the degree to which type I and type II error contribute to the total percent misclassification. Again, Earthworks with 150 ppm as the hazard standard was the only site with roughly equal contributions of type I and type II error to the total percent misclassification. This effect is likely caused by the site median concentration being close to the 150 ppm soil hazard standard. The assertion that the misclassification risk is minimized near the marginal probability of contamination is not appropriate for soil lead on urban garden plots, *refuting the third hypothesis of this thesis*. The misclassification risk is, however, typically minimized at an intermediate, though site specific, probability threshold.

Figure 5.2a

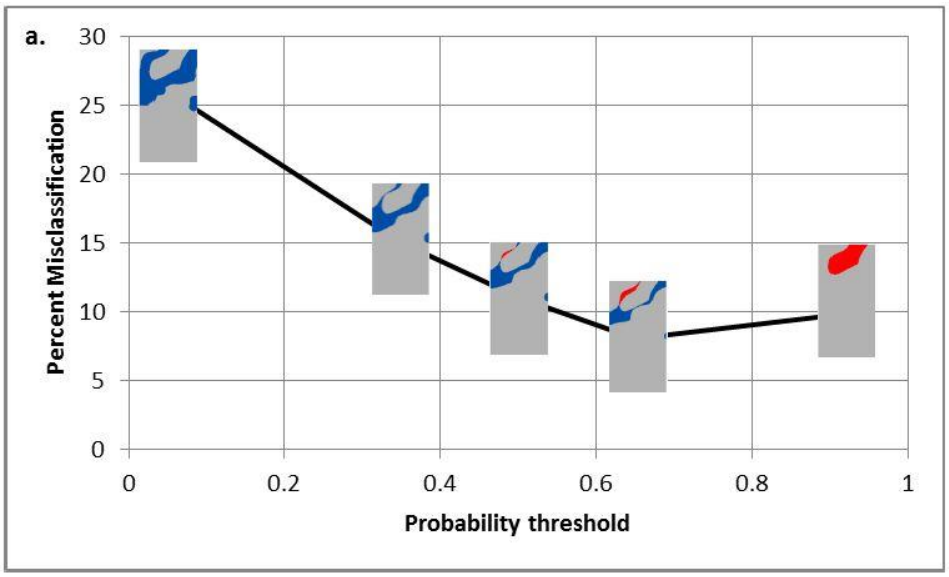

Figure 5.2b

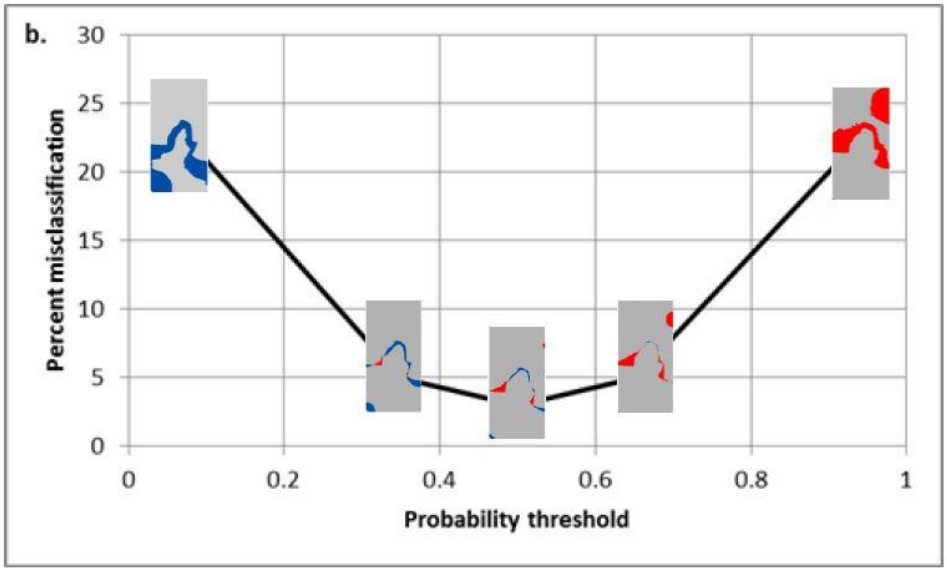

Figure 5.2c

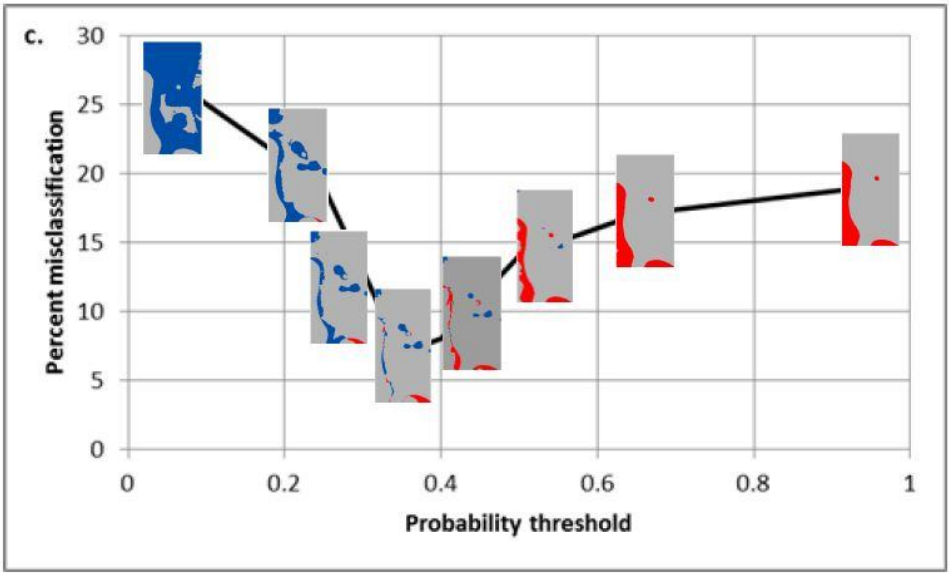

Figure 5.2d

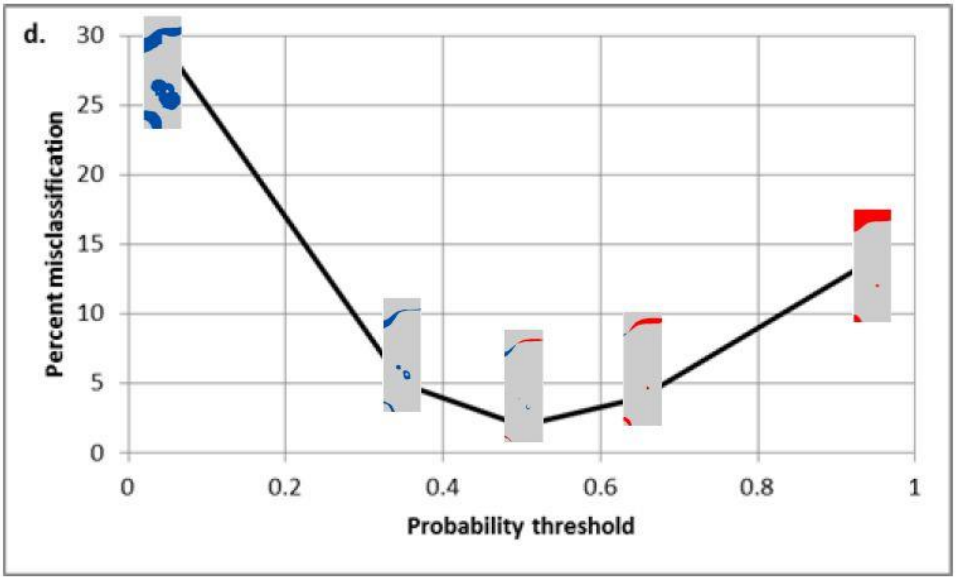

Figure 5.2: Change in distribution of false negative and false positive error with magnitude of total percent misclassification error as a function of probability threshold on: a) Earthworks with a 400 ppm hazard standard, b) Earthworks with a 150 ppm hazard standard, c) Growing Joy Plot #1 with a 150 ppm hazard standard, and d) Growing Joy Plot #2 with a 150 ppm hazard standard

5.4 Study Limitations

A considerable limitation of this study was the small number of sites (three) analyzed. Although adding two additional gardens to the pilot study contributes additional insight into spatial variability on urban garden plots, it does not provide enough information to formulate strict sampling recommendations. Another limitation is the simplifying assumption that the kriging estimates represent an exhaustive 'true' data set. Even if variography and kriging are conducted with extreme care and attention to detail, they are nevertheless models that are subject to uncertainty and potential bias. A further limitation includes the lack of assessment of the effect of sample support and volume on the statistical analyses conducted in this thesis. Larger sample volumes would generate an averaging effect similar to compositing samples, therefore, smaller samples would increase confidence in hotspot detection, especially with respect to smaller sample spacings. Finally, spatial variability in this study was assessed using one meter as the

smallest sample spacing limiting information regarding spatial variability that may exist at scales smaller than one meter. Designing a sampling scheme with smaller sample volumes and finer scale spatial variability would increase confidence in hotspot detection.

5.5 Future Research

Ideally, future research will involve conducting similar analyses as those presented in this thesis at a large number of urban garden plots in Detroit. However, such analyses will require large amounts of time and funding to conduct. A potential solution is the use of field portable x-ray fluorescence (FP-XRF), which has the ability to analyze a large number of soil samples quickly with a tradeoff of decreased sensitivity (Clark et al., 2006; Clark et al., 2008). The problem of decreased sensitivity can be addressed by applying more sensitive laboratory analyses for validation on a subset of the soil samples. Analyzing urban garden plots using FP-XRF could greatly increase the number of sites and metals that could be tested in a smaller amount of time, and at a lower cost after initial equipment purchases.

Additional soil size fraction analyses would also be useful to assess the effect of grain size distributions on spatial variability. Fine-grained particles typically have the highest lead concentrations, however, particles smaller than the 250 micron USEPA sieving recommendation may have the highest soil lead concentration. Future study should involve more detailed analysis of the smaller than 250 micron size fraction to better understand the mechanisms at work and how they might contribute to the spatial variability in lead concentration on urban gardens.

An emerging sampling strategy that also merits future analysis on urban gardens is multi-incremental sampling (ITRC, 2012). Multi-incremental sampling differs from traditional composite sampling in that a site is divided into decision units, with roughly 30 composites taken

per decision unit. This method of compositing is more rigorous, but still includes the benefits of model based sampling, because decision units are adjacent and organized in a regular grid pattern. It would also be useful to determine an optimally sized decision unit for use in multi-incremental sampling on urban garden plots, especially considering that current multi-incremental sampling strategies involve decision units that are typically the size of urban garden lots. Applying multi-incremental sampling strategies to the analyses presented in this thesis would be of considerable interest to the relevant scientific and urban gardening communities.

5.6 Conclusions and Recommendations

Evaluation of thesis hypotheses revealed considerable spatial variability in soil lead concentrations on urban gardens. This inherent spatial variability makes accurate site characterization important from a human health perspective. Specifying of the sampling goal is perhaps the most significant decision affecting subsequent decisions and the sampling campaign as a whole. However, the sampling design, number of samples and subsamples, and choice of soil hazard standard also have a considerable impact on risk associated with sampling at urban gardens.

From a risk analysis perspective, type II error (i.e. failing to detect contamination on a site) on urban garden plots is of greater concern to the health of the general public. In order to minimize type II error and the potential associated human health effects, model-based approaches with minimal, if any, sample compositing are recommended for site characterization of urban garden plots.

Finally, the percent misclassification is not necessarily minimized at a probability close to the marginal probability of contamination as originally hypothesized. The choice of an

acceptable exceedance probability threshold has a considerable impact on the probability of site misclassification, and using an intermediate probability threshold tends to minimize this probability. Analyses of additional urban garden plots, along with the evaluation of alternative sampling strategies such as multi-incremental sampling, are needed to expand upon the results and recommendations presented in this thesis.

APPENDIX A

GSLIB Sample Parameter Files

DECLUS Parameter file:

```
                  Parameters for DECLUS
                  *********************

START OF PARAMETERS:
SANDY.dat                        \file with data
1   2   0   3                 \  columns for X, Y, Z, and variable
-1.0e21     1.0e21            \  trimming limits
SANDY OUT.sum                 \file for summary output
SANDY OUT.out                 \file for output with data & weights
1.0   1.0                     \Y and Z cell anisotropy(Ysize=size*Yanis)
1                             \0=look for minimum declustered mean (1=max)
10  1.0  10.0                 \number of cell sizes, min size, max size
5                             \number of origin offsets
```

NSCORE Parameter file:

```
                 Parameters for NSCORE
                 *********************

START OF PARAMETERS:
SANDY.out                      \file with data
3   5                         \  columns for variable and weight
-1.0e21   1.0e21              \  trimming limits
0                             \1=transform according to specified dist.
                                 \  file with reference dist.
1   2                         \  columns for variable and weight
SANDY.out                     \file for output
SANDY.trn                     \file for output transformation table
```

BACKTR Parameter file:

```
                  Parameters for BACKTR
                  *********************

START OF PARAMETERS:
Tomato_Total.out           \file with data
1                          \  column with Gaussian variable
-1.0e21   1.0e21           \  trimming limits
Tomato_Total_Back.out      \file for output
TOMATO_TOTAL_NSCORE.trn    \file with input transformation table
0.0 300                    \minimum and maximum data value
1    0.0                   \lower tail option and parameter
1   100                    \upper tail option and parameter
```

IK3D Parameter file:

```
                  Parameters for IK3D
                  *******************
START OF PARAMETERS:
1                          \1=continuous(cdf), 0=categorical(pdf)
0                          \option: 0=grid, 1=cross, 2=jackknife
jack.dat                   \file with jackknife data
1   2   0    3             \   columns for X,Y,Z,vr
9                          \number thresholds/categories
61    69    77    88    106   124   137   155   194       \   thresholds /
categories
0.1   0.2   0.3   0.4   0.5   0.6   0.7   0.8   0.9     \   global cdf / pdf
TOMATO_TOTAL.out           \file with data
1   2   0    3             \   columns for X,Y,Z and variable
                           \file with soft indicator input
                           \   columns for X,Y,Z and indicators
-1.0e21   1.0e21           \trimming limits
2                          \debugging level: 0,1,2,3
ik3d_tomato.dbg            \file for debugging output
ik3d_tomato.out            \file for kriging output
150   0.05    0.1          \nx,xmn,xsiz
300   0.05    0.1          \ny,ymn,ysiz
1    0.0    0.1            \nz,zmn,zsiz
3    15                    \min, max data for kriging
20.0  20.0  20.0           \maximum search radii
0.0   0.0   0.0            \angles for search ellipsoid
0                          \max per octant (0-> not used)
0 0.5                      \0=full IK, 1=Median IK(threshold num)
1                          \0=SK, 1=OK
1    0.52                  \One   nst, nugget effect
2    0.48 0.0   0.0   0.0  \      it,cc,ang1,ang2,ang3
         10.0  10.0  10.0  \      a_hmax, a_hmin, a_vert
1    0.39                  \Two   nst, nugget effect
1    0.61  0.0   0.0   0.0 \      it,cc,ang1,ang2,ang3
```

```
         6.0  6.0  6.0     \      a_hmax, a_hmin, a_vert
1    0.36                  \Three nst, nugget effect
1    0.64  0.0   0.0   0.0 \      it,cc,ang1,ang2,ang3
         4.0  4.0  4.0     \      a_hmax, a_hmin, a_vert
1    0.47                  \Four  nst, nugget effect
1    0.53  0.0   0.0   0.0 \      it,cc,ang1,ang2,ang3
         4.0  4.0  4.0     \      a_hmax, a_hmin, a_vert
1    0.43                  \Five  nst, nugget effect
2    0.57 0.0   0.0   0.0  \      it,cc,ang1,ang2,ang3
         5.0  5.0  5.0     \      a_hmax, a_hmin, a_vert
1    0.38                  \Six  nst, nugget effect
2    0.62 0.0   0.0   0.0  \      it,cc,ang1,ang2,ang3
         4.0  4.0  4.0     \      a_hmax, a_hmin, a_vert
1    0.46                  \Seven  nst, nugget effect
2    0.54 0.0   0.0   0.0  \      it,cc,ang1,ang2,ang3
         4.0  4.0  4.0     \      a_hmax, a_hmin, a_vert
1    0.49                  \Eight  nst, nugget effect
2    0.51 0.0   0.0   0.0  \      it,cc,ang1,ang2,ang3
         5.0  5.0  5.0     \      a_hmax, a_hmin, a_vert
1    0.42                  \Nine  nst, nugget effect
1    0.58 0.0   0.0   0.0  \      it,cc,ang1,ang2,ang3
         20.0  20.0  20.0  \      a_hmax, a_hmin, a_vert
```

POSTIK parameter file:

```
                  Parameters for POSTIK
                  *********************

START OF PARAMETERS:
ik3d_sieved.out            \file with IK3D output (continuous)
postik_sieved_150.out      \file for output
2   400                    \output option, output parameter
9                          \number of thresholds
83  95  108  127  154  172  190  237  277          \the thresholds
0   1      0.75            \volume support?, type, varred
cluster.dat                \file with global distribution
3   0    -1.0   1.0e21     \   ivr,  iwt,  tmin,  tmax
0.0    1600                \minimum and maximum Z value
1   1.0                    \lower tail: option, parameter
1   1.0                    \middle    : option, parameter
1   2.0                    \upper tail: option, parameter
100                        \maximum discretization
option 1 = E-type
       2 = probability and mean above threshold(par)
       3 = Z percentile corresponding to (par)
       4 = conditional variance
```

APPENDIX B

Indicator Variogram Model Parameters*

Earthworks	Decile								
	1	**2**	**3**	**4**	**5**	**6**	**7**	**8**	**9**
Nugget	0.04	0.1	0.12	0.11	0.1	0.06	0.035	0	0
Sill Contribution	0.09	0.07	0.11	0.16	0.21	0.23	0.215	0.25	0.15
Scaled Nugget	0.31	0.59	0.52	0.41	0.32	0.21	0.14	0	0
Scaled Sill	0.69	0.41	0.48	0.59	0.68	0.79	0.86	1	1
Range	12	4	7	6	9.4	9.2	9.2	16	19
Model	E (2)	E (2)	E (2)	S (1)	S (1)	S (1)	S (1)	S (1)	S (1)

Growing Joy Garden #1	Decile								
	1	**2**	**3**	**4**	**5**	**6**	**7**	**8**	**9**
Nugget	0.055	0.08	0.08	0.12	0.12	0.1	0.11	0.095	0.05
Sill Contribution	0.05	0.125	0.145	0.135	0.16	0.165	0.13	0.1	0.07
Scaled Nugget	0.52	0.39	0.36	0.47	0.43	0.38	0.46	0.49	0.42
Scaled Sill	0.48	0.61	0.64	0.53	0.57	0.62	0.54	0.51	0.58
Range	10	6	4	4	5	4	4	5	20
Model	E (2)	S (1)	S (1)	S (1)	E (2)	E (2)	E (2)	E (2)	S (1)

Growing Joy Garden #2	Decile								
	1	**2**	**3**	**4**	**5**	**6**	**7**	**8**	**9**
Nugget	0.035	0.12	0.11	0.13	0.13	0.15	0.07	0.02	0.005
Sill Contribution	0.075	0.065	0.13	0.14	0.16	0.25	0.3	0.4	0.23
Scaled Nugget	0.32	0.65	0.46	0.48	0.45	0.38	0.19	0.05	0.02
Scaled Sill	0.68	0.35	0.54	0.52	0.55	0.63	0.81	0.95	0.98
Range	9	9	4.5	3.5	7	20	22	24	26
Model	S (1)	E (2)	E (2)	E (2)	E (2)	S (1)	S (1)	S(1)	S (1)

* The scaled nugget and sill were calculated by scaling the total sill to equal 1.0. The model abbreviations S and E stand for spherical and exponential models, respectively. The corresponding numbers in parentheses are the codes used to represent those models in GSLIB programs.

APPENDIX C

FORTRAN Programs written for Monte Carlo Simulations

EPA2003 program:

```
      USE DFPORT

      IMPLICIT NONE

      INTEGER i, j, k, l, nrec, ARG1, ARG2, ARG
      INTEGER NTRIAL, NSAMPLE
      INTEGER COUNTEXC, COUNTRPD, SAMCNT

      LOGICAL CHECK1

      Real CDF, CONC1, CONC2, SoilPb, Conc, CTOTAL
      REAL*8 SAMP1, SAMP2, SAMP0, RPD, SAMP

      CHARACTER*80 title
      CHARACTER*24 varname

      Dimension CDF(75000,3)
      Dimension SAMP(10000, 10), CONC(10000,10), ARG(10000,10)
      Dimension SoilPb(10000), RPD(10000), SAMCNT(10001)

C     Definition of variables

C     INTEGER VARIABLES

c     i, j, k are count variables.
c     nrec = number of records in the CDF file
c     ARG1, ARG2 = arguments corresponding to random conc values in CDF file
c     ARG = array of arguments corresponding to random conc values in CDF
file
c     NTRIAL = the number of trials (i.e., a random sampling event)
c     NSAMPLE = the number of samples taken in each trial
c     COUNTEXC = number of trials exceeding Target Value (400 ug/g)
c     COUNTRPD = number of trials with RPD > 0.50

C     REAL VARIABLES

C     CDF = Array with 65,131 sorted soil lead concentration values.
c     CDF values were exported from a 0.1m by 0.1m grid of kriged values in
SGeMS
C     CDF array contains 1) concentration, 2) cumulative frequency and
3)frequency

C     SAMP0 is a dummy variable
```

```
c     SAMP1 and SAMP2 are random numbers
c     SAMP = array of sampled values as random numbers
c     CONC1 and CONC2 are concentrations drawn from the CDF            c
      corresponding to SAMP1 and SAMP2
c     RPD is the relative percent difference between CONC1 and CONC2
c     RPD()=array of RPD values for 2 sample trials

c     CONC = array of concentrations drawn from the CDF corresponding  c
      to SAMP
c     CTOTAL = holding variable to sum concentrations before averaging
c     SoilPb = average soil concentration for trial based on NSAMPLE   c
      samples

      NTRIAL = 10000
      NSAMPLE = 6


      OPEN(1, File='C:\Documents and Settings\Lauren\Desktop\New Model

      READ(1,*) nrec    ! read the number of records
      PRINT*, 'NREC = ', nrec

      Do i=1,nrec       ! do loop to read variable names
            READ(1,*) (CDF(i,j), j=1,3)
      EndDo
      CLOSE(1)

      SAMCNT(1) = 0
      CTOTAL=0.0

      DO K=1,NTRIAL

100               DO L=1, NSAMPLE
                        SAMP0=(0)
                        SAMP(K,L)=RANDOM(0)
                        ARG(K,L)=INT(NREC*SAMP(K,L))
                        CONC(K,L)=CDF(ARG(K,L), 1)

                        CTOTAL = CTOTAL + CONC(K,L)
                  ENDDO
            SAMCNT(K) = SAMCNT(K) + 1

            SoilPb(K) = CTOTAL/(NSAMPLE*SAMCNT(K))

            SAMCNT(K+1) = 0
            CTOTAL = 0.0

      ENDDO

      OPEN(10, File='C:\Documents and Settings\Lauren\Desktop\New Model
```

```
      1Monte Carlo\No RPD\6_Samples.dat')


      DO K=1, NTRIAL
            Write (10, 111) K, SoilPb(K), RPD(K), SAMCNT(K)
111         Format(I5, 3x, F8.2, 3x, F6.3, 3x, I5)
      ENDDO

      Write (10,*), 'Total Number of Trials = ', NTRIAL
      Write (10,*), '    With ', NSAMPLE, ' Samples per trial.'
      Write (10,*), 'Total Trials Exceeding 400 ug/g = ', COUNTEXC
      Write (10,*), 'Total Trials with RPD > 50% = ', COUNTRPD

      CLOSE(10)

      PRINT*, 'Normal Program Termination.'

      END
```

EPA2000 program:

```
      USE DFPORT

      IMPLICIT NONE

      INTEGER i, j, k, l, m, nrec, ARG1, ARG2, ARG
      INTEGER NTRIAL, NSAMPLE, NCOMP
      INTEGER COUNTEXC, COUNTRPD, SAMCNT

      LOGICAL CHECK1

      Real CDF, CONC1, CONC2, SoilPb, Conc, CTOTAL, COMPTOT
      REAL*8 SAMP1, SAMP2, SAMP0, RPD, SAMP, COMPAVG

      CHARACTER*80 title
      CHARACTER*24 varname

      Dimension CDF(75000,3), COMPAVG(10)
      Dimension SAMP(10000, 10), CONC(10000,10), ARG(10000,10)
      Dimension SoilPb(10000), RPD(10000), SAMCNT(10001)

C     Definition of variables

C     INTEGER VARIABLES

c     i, j, k, l, m are count variables.
c     nrec = number of records in the CDF file
c     ARG1, ARG2 = arguments corresponding to random conc values in CDF c
      file
c     ARG = array of arguments corresponding to random conc values in  c
      CDF file
c     NTRIAL = the number of trials (i.e., a random sampling event)
c     NSAMPLE = the number of samples taken in each trial
c     NCOMP = the number of composites per sample
c     NREC = number of records in CDF
c     SAMCNT = number of times sampling (and re-sampling) takes place  c
      in each trial
c     COUNTEXC = number of trials exceeding Target Value (400 ug/g)
c     COUNTRPD = number of trials with RPD > 0.50

C     REAL VARIABLES

C     CDF = Array with 65,131 sorted soil lead concentration values.
c     CDF values were exported from a 0.1m by 0.1m grid of kriged      c
      values in SGeMS
C     CDF array contains 1) concentration, 2) cumulative frequency and c
      3)frequency

C     SAMP0 is a dummy variable
```

```
c     SAMP1 and SAMP2 are random numbers
c     SAMP = array of sampled values as random numbers
c     CONC1 and CONC2 are concentrations drawn from the CDF            c
      corresponding to SAMP1 and SAMP2
c     RPD is the relative percent difference between CONC1 and CONC2
c     RPD()=array of RPD values for 2 sample trials

c     CONC = array of concentrations drawn from the CDF corresponding   c
      to SAMP
c     CTOTAL = holding variable to sum concentrations before averaging
c     COMPTOT = holding variable to sum composites before averaging
c     COMPAVG = average of composites
c     SoilPb = average soil concentration for trial based on NSAMPLE   c
      samples

      NTRIAL = 10000
      NSAMPLE = 2
      NCOMP = 5
      COUNTEXC = 0
      COUNTRPD = 0
      CHECK1 = .FALSE.

      OPEN(1, File='C:\Documents and Settings\Lauren\Desktop\Sample.out

      READ(1,*) nrec    ! read the number of records
      PRINT*, 'NREC = ', nrec

      DO i=1,nrec       ! do loop to read variable names
            READ(1,*) (CDF(i,j), j=1,3)
      ENDDO
      CLOSE(1)

      SAMCNT(1) = 0
      CTOTAL=0.0

      DO K=1,NTRIAL
            CHECK1 = .FALSE.
            IF (CHECK1.EQ..FALSE.) THEN

100               DO L=1, NSAMPLE  ! NSAMPLE should always be 2
                        COMPTOT = 0.0
                              DO M=1, NCOMP
                                    SAMP0=(0)
                                    SAMP(L,M)=RANDOM(0)
                                    print*, "SAMP(L,M)=", SAMP(L,M)
                                    ARG(L,M)=INT(NREC*SAMP(L,M))

                                    IF(ARG(L,M).EQ.0) THEN
                                          ARG(L,M)=1
                                    ENDIF
```

```
                                    CONC(L,M)=CDF(ARG(L,M), 1)
                                    COMPTOT = COMPTOT + CONC(L,M)

                               ENDDO

                         COMPAVG(L) = COMPTOT/NCOMP

                         CTOTAL = CTOTAL + COMPAVG(L)
                   ENDDO

                   SAMCNT(K) = SAMCNT(K) + 1

                   IF (NSAMPLE.EQ.2) THEN RPD(K)=(ABS(COMPAVG(1)-
            COMPAVG(2)))/(COMPAVG(1)+COMPAVG(2))*2.0
                   ENDIF

                   IF (RPD(K).LE.0.50) THEN
                   CHECK1 = .TRUE.
                   SoilPb(K) = CTOTAL/(NSAMPLE*SAMCNT(K))
                   ENDIF

                   IF (SoilPB(K).GT.400.0) COUNTEXC = COUNTEXC+1
                         SAMCNT(K+1) = 0
                         CTOTAL = 0.0
                   ENDIF

                   IF (RPD(K).GT.0.50) THEN
                         COUNTRPD = COUNTRPD+1
                         GOTO 100
                   ENDIF
       ENDDO

      OPEN(10, File='C:\Documents and Settings\Lauren\Desktop\New Model
      1Monte Carlo\With RPD\5 subsamples.dat')

      DO K=1, NTRIAL
            Write (10, 111) K, SoilPb(K), RPD(K), SAMCNT(K)
111         Format(I5, 3x, F8.2, 3x, F6.3, 3x, I5)
      ENDDO

      Write (10,*), 'Total Number of Trials = ', NTRIAL
      Write (10,*), '    With ', NSAMPLE, ' Samples per trial.'
      Write (10,*), 'Total Trials Exceeding 400 ug/g = ', COUNTEXC
      Write (10,*), 'Total Trials with RPD > 50% = ', COUNTRPD

      CLOSE(10)
      PRINT*, 'Normal Program Termination.'

      END
```

RANDSAMP program:

```
      USE DFPORT

      IMPLICIT NONE

      INTEGER i, j, k, l, nrec, ARG1, ARG2, ARG
      INTEGER NTRIAL, NSAMPLE
      INTEGER COUNTEXC, COUNTRPD, SAMCNT, DETECT, DETSUM, EXCEED

      LOGICAL CHECK1

      Real CDF, CONC1, CONC2, SoilPb, Conc, CTOTAL
      REAL*8 SAMP1, SAMP2, SAMP0, RPD, SAMP, Prob

      CHARACTER*80 title
      CHARACTER*24 varname

      Dimension CDF(75000,3)
      Dimension SAMP(10001, 51), CONC(10001,51), ARG(10001,51)
      Dimension DETECT(10001)

C     Definition of variables

C     INTEGER VARIABLES

c     i, j, k are count variables.
c     nrec = number of records in the CDF file
c     ARG1, ARG2 = arguments corresponding to random conc values in CDF c
      file
c     ARG = array of arguments corresponding to random conc values in  c
      CDF file
c     NTRIAL = the number of trials (i.e., a random sampling event)
c     NSAMPLE = the number of samples taken in each trial
c     COUNTEXC = number of trials exceeding Target Value (400 ug/g)
c     COUNTRPD = number of trials with RPD > 0.50

C     REAL VARIABLES

C     CDF = Array with 65,131 sorted soil lead concentration values.
c     CDF values were exported from a 0.1m by 0.1m grid of kriged      c
      values in SGeMS
C     CDF array contains 1) concentration, 2) cumulative frequency and c
      3)frequency
C     SAMP0 is a dummy variable
c     SAMP1 and SAMP2 are random numbers
c     SAMP = array of sampled values as random numbers
c     CONC1 and CONC2 are concentrations drawn from the CDF            c
      corresponding to SAMP1 and SAMP2
c     RPD is the relative percent difference between CONC1 and CONC2
```

```
c     RPD()=array of RPD values for 2 sample trials
c     CONC = array of concentrations drawn from the CDF corresponding  c
      to SAMP
c     CTOTAL = holding variable to sum concentrations before averaging
c     SoilPb = average soil concentration for trial based on NSAMPLE   c
      samples

      NTRIAL = 10000
      NSAMPLE = 40

      OPEN(1, File='C:\Users\Lauren\Documents\My Documents\Sample.out')

      READ(1,*) nrec    ! read the number of records
      DO i=1,nrec       ! do loop to read variable names
            READ(1,*) (CDF(i,j), j=1,3)
      ENDDO
      CLOSE(1)

      DO K=1, NTRIAL
      DETECT(K) = 0
            DO L=1, NSAMPLE
                  SAMP0=(0)
                  SAMP(K,L)=RANDOM(0)
                  ARG(K,L)=INT(NREC*SAMP(K,L))
                        IF (ARG(K,L).EQ.0) THEN
                              ARG(K,L) =1
                        ENDIF
                  CONC(K,L)=CDF(ARG(K,L), 1)

                  IF (CONC(K,L).GT.400) THEN
                        DETECT(K)=1
                  ENDIF
            ENDDO
      ENDDO

      OPEN(10, File='C:\Users\Lauren\Documents\MyDocuments\Sample.dat')

      DO K=1, NTRIAL
            Write (10, 111) K, DETECT(K)
111         Format(I5, 3x, I5)
      ENDDO

      Write (10,*), PROB
      Write (10,*), '    With ', NSAMPLE, ' Samples per trial.'
      Write (10,*), 'Total Trials Exceeding 400 ug/g = ', COUNTEXC
      Write (10,*), 'Total Trials with RPD > 50% = ', COUNTRPD

      CLOSE(10)
      PRINT*, 'Normal Program Termination.'
      END
```

GRIDSAMP program

```
      USE DFLIB
      USE DFPORT

      IMPLICIT NONE

      INTEGER i, j, k, l, n, m, x, y, g, h, nrec
      INTEGER NTRIAL, NBLOCK, NSAMPLE, RANDSEED, EXCNT, index
      INTEGER XCOUNT, YCOUNT, THOLD, XYCNT, EXCEED, XC, YC, ZC, DETECT


      Real XYZSURF, CONC, MEANPB, SAMP, DELIN, XIND, YIND
      REAL XCOORD, YCOORD, XRAND, YRAND, CTOTAL

      REAL*8 XDIM, YDIM, XINC, YINC


      CHARACTER*80 title
      CHARACTER INFILE*180, OUTFILE*220
      CHARACTER*24 varname


      Dimension XYZSURF(75000,3), XYCNT(100,3), MEANPB(10001)
      Dimension CONC(200, 400), DELIN(10001), EXCEED(10001,55,5)
      Dimension SAMP(10001,55,5), DETECT(40000)

C     Definition of variables

C     INTEGER VARIABLES

c     i, j, k, l, m, g, h, x and y are count variables.
c     nrec = number of records in the DAT file
c     NTRIAL = the number of trials (i.e., a random sampling event)
c     NSAMPLE = the number of samples taken in each block
c     NBLOCK = number of grid blocks (number samples to take on a grid)
c     XCOUNT and YCOUNT = counter used to position and dimension blocks
c     NREC = number of records in data file
c     XRAND and YRAND = Random number used to place sample within block
c     XIND and YIND = Variable to point X and Y coordinates to         c
      corresponding concentration value in DAT file
c     RANDSEED = Five digit random number for use in Monte Carlo       c
      Simulation
c     EXCEED = Detect flag (all 0 or 1, 0 if below THOLD, 1 if above)
c     THOLD = soil hazard threshold value
c     XYCNT = X and Y count lookup table
c     XC, YC, ZC = Variable used to scale axes before assigning to      c
      ordered array

c     REAL VARIABLES
```

```
c     XDIM and YDIM = dimensions of the site in the x and y direction
c     XINC and YINC = grid spacing in x and y direction
c     XYZSURF = an array holding the x and y location and concentration c
      read from the input file
c     XCOORD and YCOORD = X and Y coordinates of random number within  c
      block
c     MEANPB = the average soil lead concentration per trial
c     CONC = an array containing x location, y location and            c
      concentration, with x and y rescaled
c     SAMP = an array containing the results of the Monte Carlo        c
      Sampling
c     XRAND and YRAND = random number used to point to a specific point c
      in the dataset (random sampling)
c     PROB = array containing the probability of hotspot detection as   c
      calculated from EXCEED


      OPEN(3, File='C:\Users\Lauren\Documents\My Documents\Grid.par')
      READ(3,*) INFILE
      PRINT *, INFILE
      READ(3,*) OUTFILE
      PRINT*, OUTFILE
      READ(3,*) XDIM
      Print*, XDIM
      READ(3,*) YDIM
      Print*, YDIM
      READ(3,*) XINC
      Print*, XINC
      READ(3,*) YINC
      print*, YINC
      READ(3,*) NTRIAL
      READ(3,*) NBLOCK
      READ(3,*) NSAMPLE
      READ(3,*) THOLD
      Print*, "THRESHOLD=", THOLD
      READ(3,*, end=28) RANDSEED
28    CLOSE(3)

      OPEN(1, file=INFILE, status='old')

      READ(1,*) nrec
      DO i=1,nrec       ! do loop to read variable names
            READ(1,*) (XYZSURF(i,j), j=1,3)
      ENDDO
      CLOSE(1)


      XC=INT(XDIM/XINC)+1 !+1 for i start at 1
```

```
      YC=INT(YDIM/YINC)+1  !+1 for i start at 1

      ZC=0
      DO j=1, YC
            DO i=1, XC
                  CONC(I,J) = XYZSURF(i+ZC, 3)
            ENDDO
            ZC=ZC+XC
      ENDDO

OPEN(5, File='C:\Users\Lauren\Documents\My Documents\X and Y count
definitions.dat')

      DO g=1, 50
            READ(5,*) XYCNT(g,1), XYCNT(g,2), XYCNT(g,3)
      ENDDO
      CLOSE(5)

      XCOUNT = XYCNT(NBLOCK, 2)
      YCOUNT = XYCNT(NBLOCK, 3)

      CALL SEED(RANDSEED)


      DO K=1,NTRIAL
            M=0
            DO X=1, XCOUNT
            DO Y=1, YCOUNT
                  M=M+1
                  DO N=1, NSAMPLE
                        XRAND = RANDOM(0)
                        YRAND = RANDOM(0)

                        XCOORD=XRAND*XDIM/XCOUNT+(XDIM/XCOUNT)*(X-1)
                  YCOORD=YRAND*YDIM/YCOUNT +(YDIM/YCOUNT)*(Y-1)

                        XIND = INT(XCOORD/XINC)+1
                        YIND = INT(YCOORD/YINC)+1
                        SAMP(K,M,N) = CONC(XIND,YIND)
                  ENDDO

            ENDDO
            ENDDO

      ENDDO

      DO K=1, NTRIAL
            DETECT(K) = 0
            DO M=1, NBLOCK
                  DO N=1, NSAMPLE
```

```
                        IF (SAMP(K,M,N).GE.THOLD) THEN
                              EXCEED(K,M,N) = 1
                              DETECT(K) = 1
                        ELSEIF (SAMP(K,M,N).LT.THOLD) THEN
                              EXCEED(K,M,N) = 0
                        ENDIF

                  ENDDO
            ENDDO
      ENDDO

      DO K=1, NTRIAL
            CTOTAL=0
            EXCNT=0
            DO M=1, NBLOCK
                  DO N=1, NSAMPLE
                        CTOTAL = CTOTAL + SAMP(K,M,N)
                        EXCNT = EXCNT+EXCEED(K,M,N)
                  ENDDO
            ENDDO
            MEANPB(K) = CTOTAL/(NBLOCK*NSAMPLE)
            DELIN(K)= real(EXCNT)/real(NBLOCK)

      ENDDO

      OPEN(15, File='C:\Users\Lauren\Documents\My Documents\Grid.dat')

      DO K=1, NTRIAL
            Write (15, 111) K, MEANPB(K), DETECT(K), DELIN(K)
111         Format(I5, 3x, F8.2, 3x, I5, 3x, F6.3)
      ENDDO
      CLOSE(15)

      END
```

GRIDSAMP Parameter file:

```
                              GRIDSAMP PARAMETERS

"C:\Documents\Input.dat"      \ input file (XYZ Surfer file)
"C:\Documents\Output.dat"     \output file
17.1                          \site dimension in x direction (XDIM)
32.1                          \ site dimension in y direction (YDIM)
.1005882                      \grid spacing in x direction (XINC)
.1003125                      \ grid spacing in y direction  (YINC)
10000                         \ number of trials (NTRIAL)
3                             \ number of grid blocks (NBLOCK)
1                             \number of samples per grid block(NSAMPLE)
400                           \soil lead concentration threshold (THOLD)
78902                         \random number seed (RANDSEED)
```

APPENDIX D

Soil Lead Concentration Measurements

Earthworks Plot:

Sample ID*	X** Coordinate (m)	Y Coordinate (m)	Unsieved Concentration (ppm)	Sieved Concentration (ppm)	Bioaccessible Concentration (ppm)
D10M-001	0	0	445	197	53
D10M-001-R	0	0	105	160	33
D10M-002	10	0	387	123	16
D10M-003	20	0	426	533	173
D10M-004	0	10	106	98	31
D10M-005	10	10	90	128	15
D10M-005-R	10	10	76	123	14
D10M-006	20	10	191	205	75
D10M-007	0	20	335	308	90
D10M-008	10	20	135	198	31
D10M-008-R	10	20	136	188	16
D10M-009	20	20	456	384	107
D10M-010	0	30	339	269	86
D10M-011	10	30	430	503	109
D10M-012	20	30	219	254	58
D05M-001	5	0	17	35	11
D05M-002	15	0	92	89	21
D05M-003	0	5	118	32	19
D05M-004	5	5	31	54	13
D05M-005	10	5	48	76	11
D05M-006	15	5	57	100	18
D05M-007	20	5	843	620	139
D05M-008	5	10	110	101	21
D05M-009	15	10	179	172	32
D05M-010	0	15	198	185	51
D05M-011	5	15	91	140	28
D05M-012	10	15	32	99	16
D05M-013	15	15	220	288	63
D05M-014	20	15	112	209	41
D05M-015	5	20	214	293	42
D05M-016	15	20	153	242	26
D05M-017	0	25	318	269	44
D05M-017-R	0	25	399	252	50
D05M-018	5	25	890	1,532	182

D05M-019	10	25	382	471	81
D05M-019-R	10	25	374	389	68
D05M-020	15	25	121	144	25
D05M-021	20	25	420	385	105
D05M-022	5	30	232	263	38
D05M-023	15	30	483	317	45
D05M-023-R	15	30	372	383	60
D02M-001	7	10	45	60	21
D02M-002	9	10	90	133	29
D02M-002-R	9	10	86	115	22
D02M-003	11	10	144	154	48
D02M-004	13	10	142	181	43
D02M-005	5	12	160	153	47
D02M-006	7	12	67	87	25
D02M-007	9	12	71	107	23
D02M-008	11	12	110	119	23
D02M-009	13	12	145	185	33
D02M-010	15	12	159	215	42
D02M-010-R	15	12	206	197	38
D02M-011	5	14	106	144	35
D02M-012	7	14	63	106	20
D02M-013	9	14	60	133	16
D02M-014	11	14	127	159	29
D02M-015	13	14	186	249	38
D02M-015-R	13	14	150	189	34
D02M-016	15	14	222	259	45
D02M-017	5	16	158	169	39
D02M-018	7	16	91	86	18
D02M-019	9	16	59	83	15
D02M-020	11	16	137	185	33
D02M-020-R	11	16	139	162	30
D02M-021	13	16	226	238	41
D02M-022	15	16	268	278	64
D02M-023	5	18	170	217	38
D02M-024	7	18	116	156	28
D02M-025	9	18	70	115	17
D02M-025-R	9	18	58	120	17
D02M-026	11	18	114	170	22
D02M-027	13	18	288	238	46
D02M-028	15	18	190	246	40
D02M-029	7	20	173	158	30

D02M-030	9	20	176	167	26
D02M-030-R	9	20	112	178	28
D02M-031	11	20	146	192	24
D02M-032	13	20	193	213	44
D01M-001	8	13	29	97	17
D01M-002	9	13	50	90	17
D01M-003	10	13	46	91	21
D01M-003-R	10	13	40	90	20
D01M-004	11	13	87	154	24
D01M-005	12	13	96	128	27
D01M-006	8	14	37	111	17
D01M-007	10	14	61	106	20
D01M-008	12	14	113	171	32
D01M-009	8	15	26	93	16
D01M-010	9	15	19	89	16
D01M-011	11	15	111	154	34
D01M-012	12	15	195	172	34
D01M-013	8	16	106	75	13
D01M-013-R	8	16	80	83	13
D01M-014	10	16	89	95	19
D01M-015	12	16	205	193	40
D01M-016	8	17	111	144	22
D01M-016-R	8	17	103	84	17
D01M-017	9	17	53	66	10
D01M-017-R	9	17	63	78	13
D01M-018	10	17	91	117	21
D01M-019	11	17	165	163	37
D01M-019-R	11	17	225	171	32
D01M-020	12	17	209	233	41

*Replicate samples are marked with –R after the sample number.

**X and Y coordinates correspond to meters in the horizontal and vertical direction starting from the origin at the lower left corner of the site.

Growing Joy Plot #1:

Sample ID*	X** Coordinate (m)	Y Coordinate (m)	Unsieved Concentration (ppm)	Sieved Concentration (ppm)	Bioaccessible Concentration (ppm)
T05m-001	0	0	298	298	73
T05m-002	5	0	116	99	16
T05m-003	10	0	259	257	46
T05m-004	15	0	138	154	23
T05m-005	0	5	171	190	37
T05m-006	5	5	145	135	32
T05m-006-R	5	5		164	24
T05m-007	10	5	107	96	43
T05m-008	15	5	68	125	21
T05m-009	0	10	168	200	46
T05m-010	5	10	199	76	3
T05m-011	10	10	81	138	21
T05m-012	15	10	128	85	17
T05m-013	0	15	99	275	73
T05m-014	5	15	179	77	13
T05m-014-R	5	15		75	3
T05m-015	10	15	79	151	37
T05m-016	15	15	99	104	25
T05m-017	0	20	121	187	45
T05m-018	5	20	93	133	19
T05m-019	10	20		104	29
T05m-020	15	20		78	3
T05m-021	0	25		130	35
T05m-021-R	0	25		130	39
T05m-022	5	25		115	26
T05m-022-R	5	25		104	14
T05m-023	10	25		43	4
T05m-024	15	25		73	22
T05m-025	0	30		174	44
T05m-026	5	30		46	4
T05m-027	10	30		61	18
T05m-028	15	30		59	4
T02m-001	7	10		70	3
T02m-002	9	10		155	35
T02m-003	11	10		94	29
T02m-004	13	10		80	23
T02m-005	5	12		61	3

T02m-006	7	12		52	3
T02m-007	9	12		114	39
T02m-008	11	12		62	28
T02m-009	13	12		113	34
T02m-010	15	12		127	34
T02m-011	5	14		85	20
T02m-012	7	14		110	31
T02m-013	9	14		69	15
T02m-014	11	14		62	18
T02m-014-R	11	14		63	3
T02m-015	13	14		61	13
T02m-016	15	14		187	50
T02m-017	5	16		83	28
T02m-017-R	5	16		92	29
T02m-018	7	16		77	17
T02m-019	9	16		95	22
T02m-020	11	16		135	33
T02m-020-R	11	16		154	32
T02m-021	13	16		130	47
T02m-022	15	16		88	17
T02m-023	5	18		119	36
T02m-024	7	18		85	15
T02m-025	9	18		260	63
T02m-026	11	18		122	32
T02m-027	13	18		115	29
T02m-028	15	18		66	13
T02m-029	7	20		156	25
T02m-030	9	20		148	28
T02m-031	11	20		108	22
T02m-032	13	20		128	31
T01m-001	8	13		67	3
T01m-002	9	13		63	10
T01m-003	10	13		59	3
T01m-004	11	13		60	13
T01m-005	12	13		71	17
T01m-006	8	14		72	18
T01m-007	10	14		76	15
T01m-008	12	14		63	16
T01m-009	8	15		217	72
T01m-009-R	8	15		260	66
T01m-010	9	15		182	55

T01m-011	11	15		196	67
T01m-012	12	15		194	53
T01m-013	8	16		155	54
T01m-014	10	16		135	36
T01m-015	12	16		159	47
T01m-016	8	17		128	17
T01m-017	9	17		103	35
T01m-018	10	17		150	42
T01m-019	11	17		81	25
T01m-020	12	17		84	7

*Replicate samples are marked with –R after the sample number

**X and Y coordinates correspond to meters in the horizontal and vertical direction starting from the origin at the lower left corner of the site.

Growing Joy Plot #2:

Sample ID*	X** Coordinate (m)	Y Coordinate (m)	Unsieved Concentration (ppm)	Sieved Concentration (ppm)	Bioaccessible Concentration (ppm)
S05m-001	0	0	158	201	59
S05m-001-R	0	0		257	84
S05m-002	5	0	135	125	34
S05m-003	10	0	135	140	39
S05m-004	0	5	109	128	39
S05m-005	5	5	81	125	33
S05m-006	10	5	94	103	23
S05m-007	0	10	56	93	27
S05m-008	5	10	39	65	21
S05m-009	10	10	77	115	20
S05m-010	0	15	76	78	14
S05m-011	5	15	50	59	5
S05m-012	10	15	55	47	6
S05m-013	0	20		50	6
S05m-014	5	20	68	69	11
S05m-015	10	20		76	6
S05m-016	0	25	238	247	59
S05m-017	5	25	98	107	21
S05m-017-R	5	25		71	16
S05m-018	10	25	153	142	21
S05m-019	0	30		152	22
S05m-020	5	30		294	98
S05m-021	10	30		227	58
S02m-001	2	10		51	5
S02m-002	4	10		40	5
S02m-003	6	10		307	75
S02m-004	8	10		112	19
S02m-004-R	8	10		77	5
S02m-005	0	12		84	13
S02m-006	2	12		74	5
S02m-007	4	12		160	24
S02m-008	6	12		67	16
S02m-008-R	6	12		83	15
S02m-009	8	12		58	6
S02m-010	10	12		42	13
S02m-011	0	14		28	6
S02m-012	2	14		54	8

S02m-012-R	2	14		67	11
S02m-013	4	14		87	6
S02m-014	6	14		55	6
S02m-015	8	14		62	6
S02m-016	10	14		33	6
S02m-017	0	16		108	6
S02m-018	2	16		83	6
S02m-019	4	16		59	6
S02m-020	6	16		113	21
S02m-021	8	16		86	11
S02m-022	10	16		88	11
S02m-023	0	18		95	11
S02m-024	2	18		90	14
S02m-025	4	18		71	6
S02m-025-R	4	18		84	11
S02m-026	6	18		56	6
S02m-027	8	18		61	6
S02m-027-R	8	18		70	6
S02m-028	10	18		75	12
S02m-029	2	20		68	5
S02m-030	4	20		108	20
S02m-031	6	20		64	5
S02m-032	8	20		65	5
S01m-001	3	13		54	7
S01m-002	4	13		48	7
S01m-003	5	13		61	7
S01m-004	6	13		78	14
S01m-005	7	13		61	7
S01m-006	3	14		95	7
S01m-007	5	14		83	7
S01m-008	7	14		72	7
S01m-009	3	15		53	7
S01m-010	4	15		72	21
S01m-011	6	15		87	23
S01m-012	7	15		64	17
S01m-013	3	16		62	7
S01m-014	5	16		68	7
S01m-015	7	16		73	7
S01m-016	3	17		60	12
S01m-017	4	17		57	7
S01m-018	5	17		65	7

S01m-019	6	17		61	7
S01m-020	7	17		56	7

*Replicate samples are marked with –R after the sample number.

**X and Y coordinates correspond to meters in the horizontal and vertical direction starting from the origin at the lower left corner of the site.

APPENDIX E

Ordinary Kriging Maps with Control Points

Earthworks Plot Total Lead:

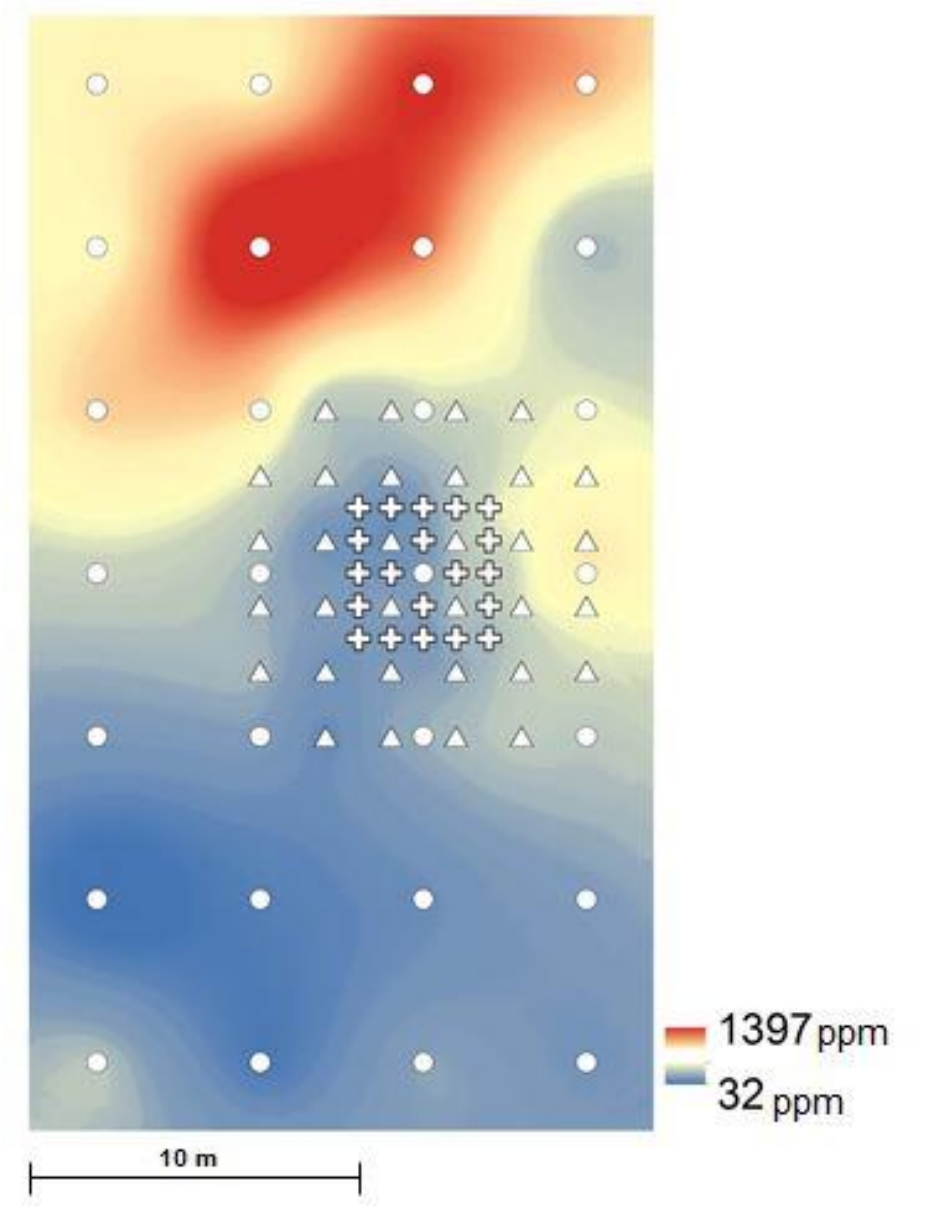

Earthworks Plot Bioaccessible Lead

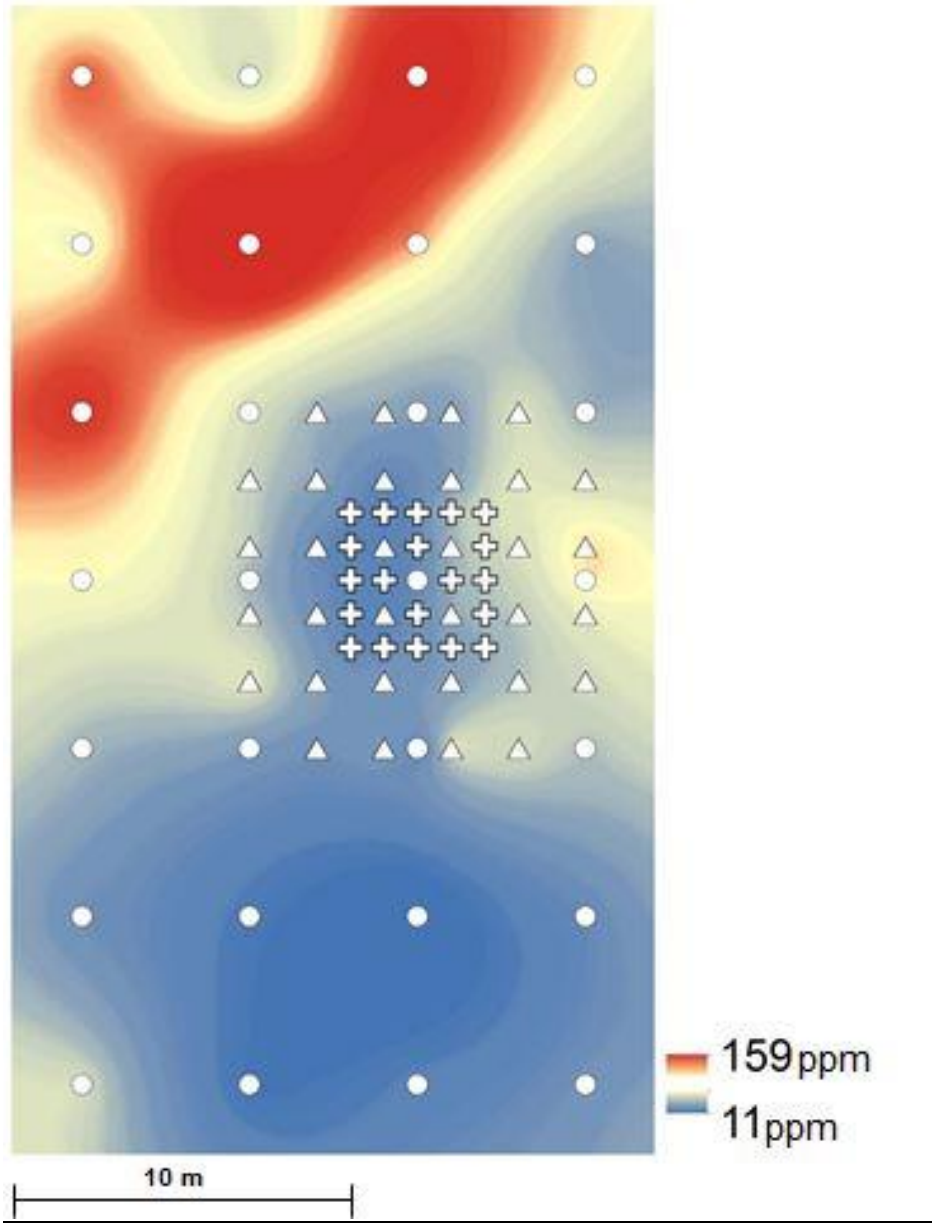

Growing Joy Plot #1 Total Lead

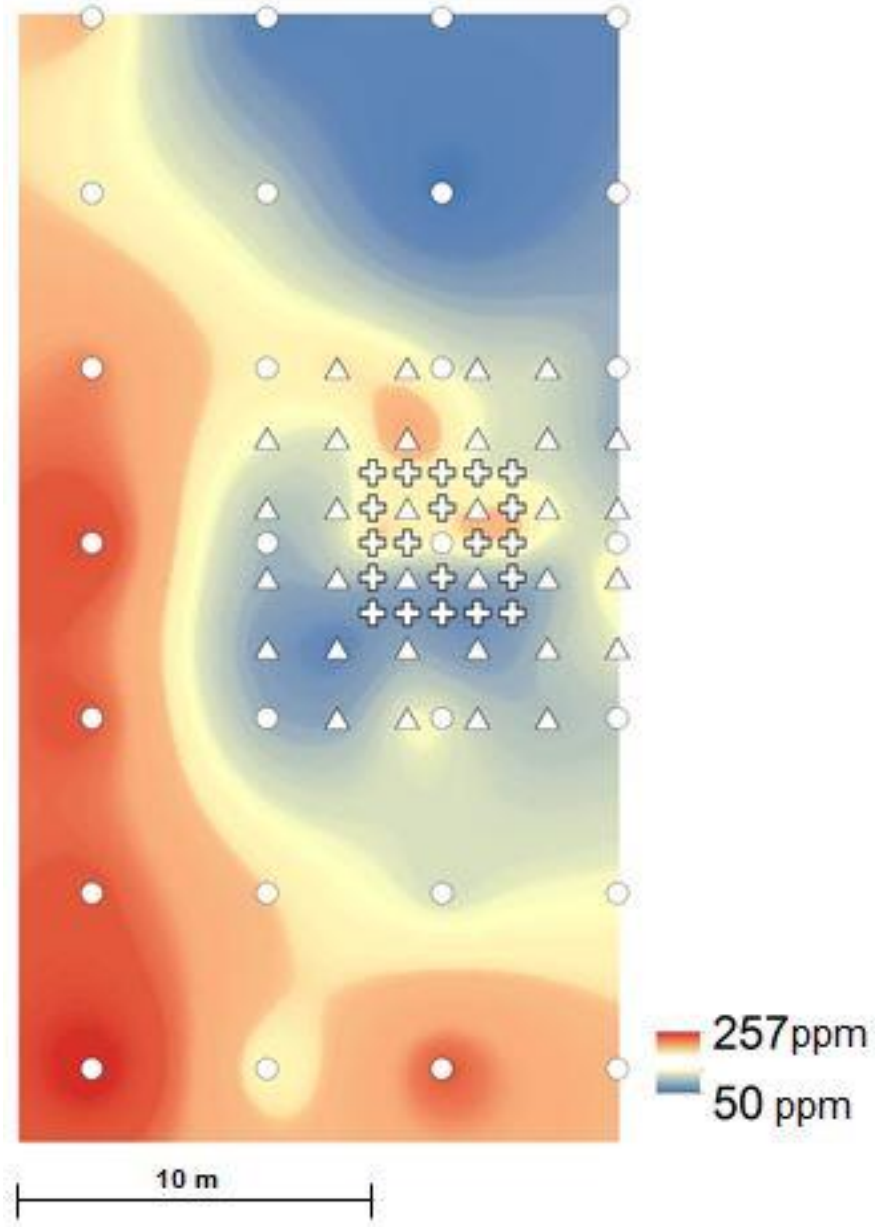

Growing Joy Plot #1 Bioaccessible Lead:

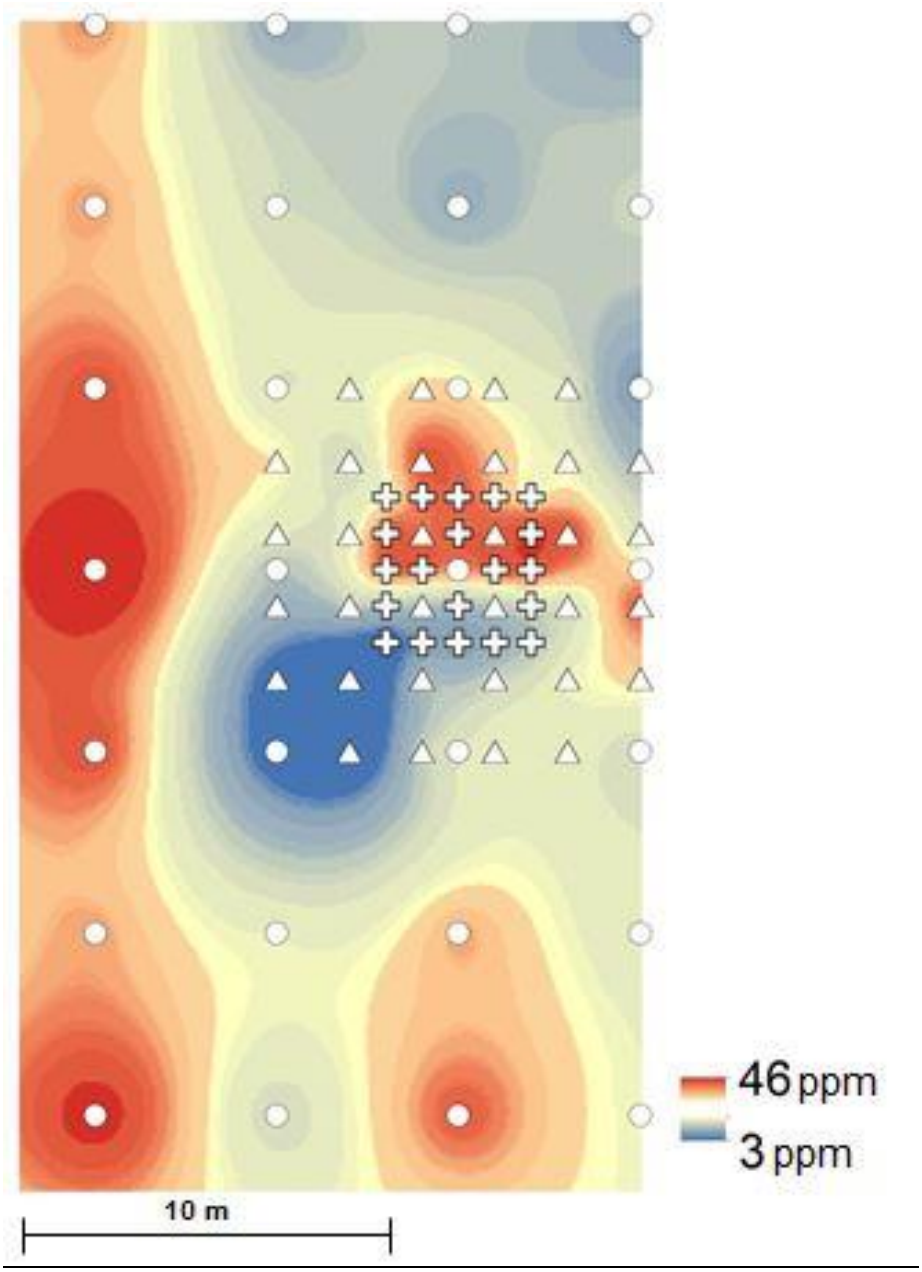

Growing Joy Plot #2 Total Lead:

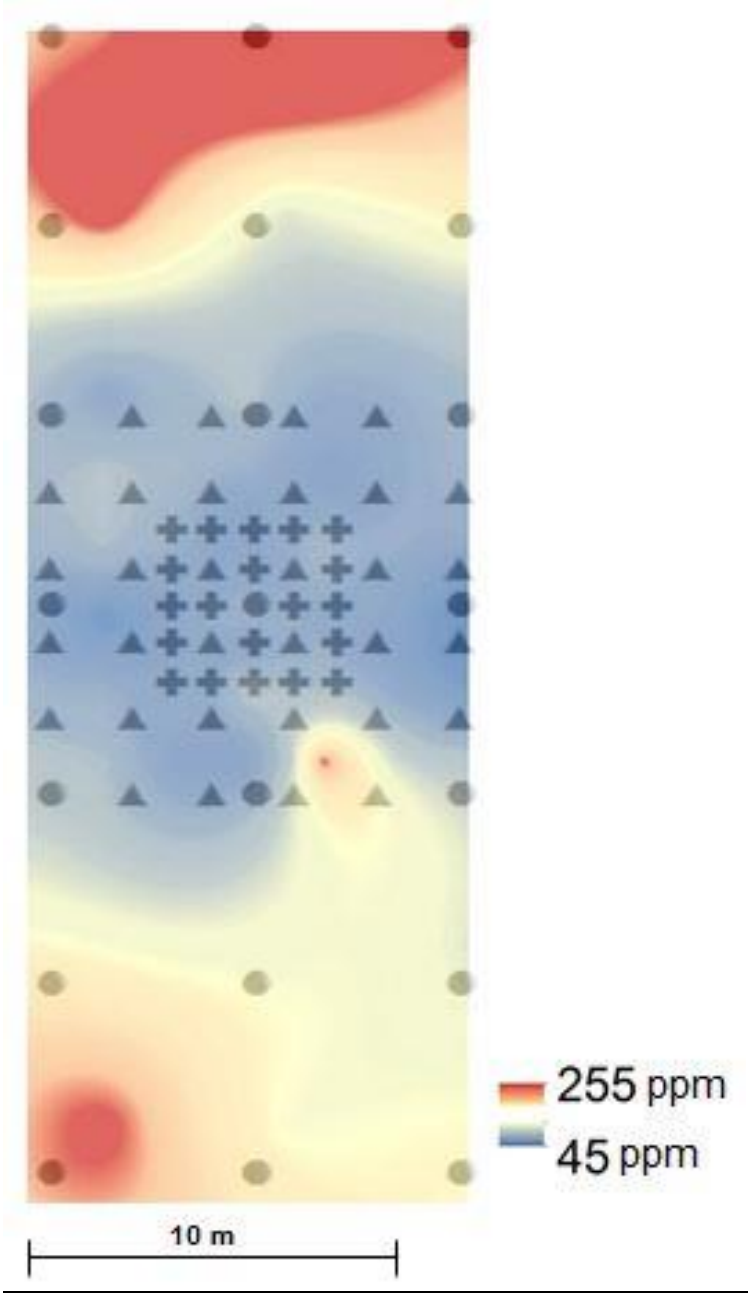

Growing Joy Plot #2 Bioaccessible Lead:

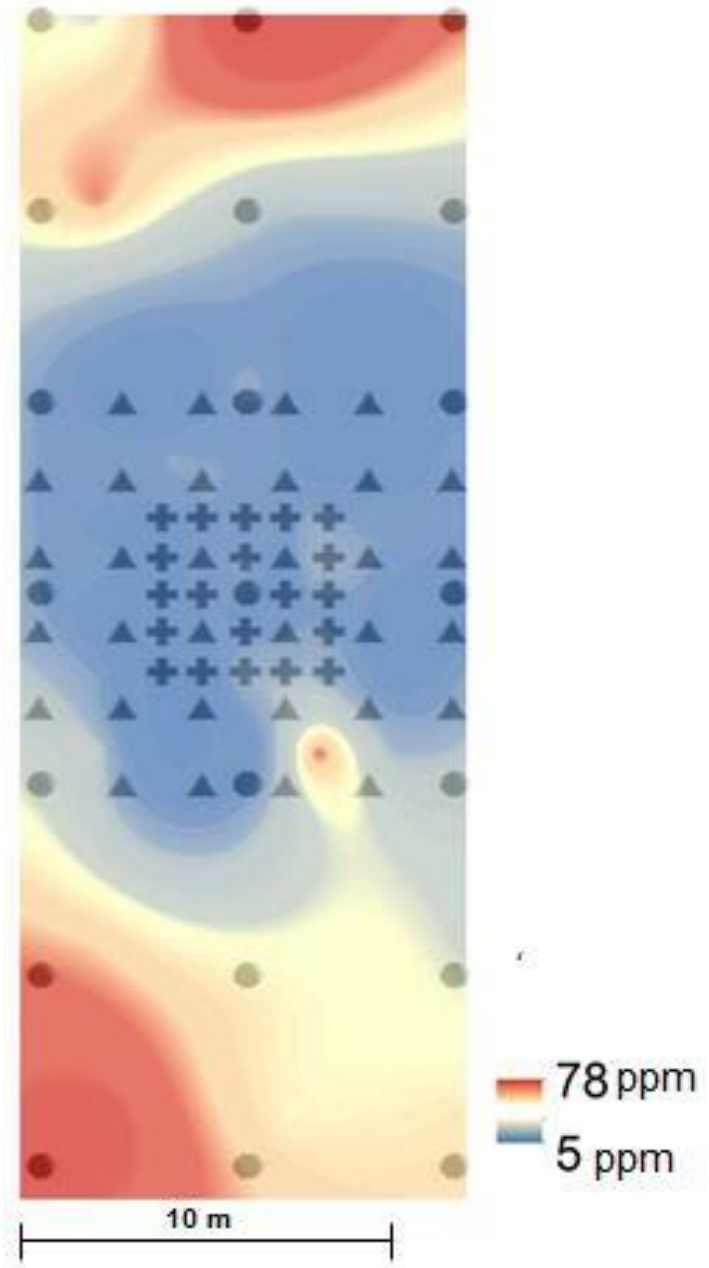

REFERENCES

Abouelnasr, D. M., 2009, The Relationship Between Soil Particle Size and Lead Concentration: Proceedings of the Annual International Conference of Soils, Sediments, Water and Energy, v. 14, no. 8, p. 81-86.

Agency for Toxic Substances and Disease Control (ATSDR), 2007, Lead Fact Sheet, U.S. Department of Public Health and Human Services, Atlanta, GA, CAS # 7439-92-1.

Boudreault, J., Dube, J., Chouteau, M., Winiarski, T., and Hardy, E., 2010, Geophysical characterization of contaminated urban fills: Engineering Geology, v. 116, no. 3-4, p. 196-206.

Bugdalski, L., Lemke, L., and McElmurry, S., 2013, Spatial Variation of Soil Lead in an Urban Community Garden: Implications for Risk-Based Sampling: Risk Analysis, published online April 24, 2013. DOI: 10.1111/risa.12053

Canfield, R. L., Henderson, C. R., Cory-Slechta, D. A., Cox, C., Jusko, T. A., and Lanphear, B. P., 2003, Intellectual Impairment in Children with Blood Lead Concentrations below 10 ug per Deciliter: The New England Journal of Medicine, v. 348, no. 16, p. 1517-1526.

California Office of Environmental Health Hazard Asssessment (OEHHA), 2009, Revised California Human Health Screening Level for Lead. Available at: http://oehha.ca.gov/risk/pdf/LeadCHHSL51809.pdf

Casteel, S. W., Cowart, R. P., Weis, C. P., Henningsen, G. M., Hoffman, E., Brattin, W. J., Guzman, R. E., Starost, M. F., Payne, J. T., Stockham, S. L., Becker, S. V., Drexler, J. W., and Turk, J. R., 1997, Bioavailability of lead to juvenile swine dosed with soil from the Smuggler Mountain NPL site of Aspen, Colorado: Fundamental and Applied Toxicology, v. 36, no. 2, p. 177-187.

Cattle, J. A., McBratney, A. B., and Minasny, B., 2002, Kriging Method Evaluation for Assessing the Spatial Distribution of Urban Soil Lead Contamination: Journal of Environmental Quality, v. 31, no. 5, p. 1576-1588.

Centers for Disease Control (CDC), 2012, CDC Response to Advisory Committee on Childhood Lead Poisoning Prevention Recommendations in "Low Level Lead Exposure Harms Children: A Renewed Call for Primary Prevention". Available at http://www.cdc.gov/nceh/lead/acclpp/CDC_Response_Lead_Exposure_Recs.pdf

Clark, H. F., Brabander, D. J., and Erdil, R. M., 2006, Sources, Sinks, and Exposure Pathways of Lead in Urban Garden Soil: Journal of Environmental Quality, v. 35, no. 6, p. 2066-2074.

Clark, H. F., Hausladen, D. M., and Brabander, D. J., 2008, Urban gardens: Lead exposure, recontamination mechanisms, and implications for remediation design: Environmental Research, v. 107, no. 3, p. 312-319.

Clesceri, L. S., Greenberg, A. E., and Eaton, A. D., 1998, Method 3111 - Metals By Flame Atomic Absorption Spectrometry, Standard Methods for the Examination of Water and Wastewater: Washington, DC, American Public Health Association, American Water Works Association, and Water Environment Federation.

Compaq Computer Corporation, 1999, *Compaq Fortran Language Reference Manual*, Houston, TX.

Coppola, E., Capra, G., Odierna, P., Vacca, S., and Buondonno, A., 2012, Lead distribution as related to pedological features of soils in the Volturno River low Basin (Campania, Italy): Geoderma, v. 159, no. 3-4, p. 342-349.

de Gruijter, J., Brus, D., Bierkens, M., and Knotters, M., 2006, Sampling for Natural Resource Monitoring, The Netherlands, Springer. 332 pp.

Demayo, A., Taylor, M. C., Taylor, K. W., and Hodson, P. V., 1982, Toxic Effects of Lead and Lead Compounds on Human Health, Aquatic Life, Wildlife Plants, and Livestock: CRC Critical Reviews in Environmental Control, v. 12, no. 4, p. 257-305.

Deutsch, C. V.,1989, DECLUS - A FORTRAN-77 PROGRAM FOR DETERMINING OPTIMUM SPATIAL DECLUSTERING WEIGHTS, *Computers & Geosciences, 15*(3), 325-332, DOI: 10.1016/0098-3004(89)90043-5.

Deutsch, C.V. & A.G. Journel, 1998, *GSLIB: Geostatistical Software Library and User Guide*, Oxford University Press, New York, 369 pp.

Drexler, J. W., and Brattin, W. J., 2007, An in vitro procedure for estimation of lead relative bioavailability: With validation: Human and Ecological Risk Assessment, v. 13, no. 2, p. 383-401.

Ersoy, A., Yunsel, T. Y., and Cetin, M., 2004, Characterization of Land Contaminated by Past Heavy Metal Mining Using Geostatistical Methods: Archives of Environmental Contamination and Toxicology, v. 46, p. 162-175.

Filippelli, G. M., and Laidlaw, M. A. S., 2010, THE ELEPHANT IN THE PLAYGROUND: Confronting lead-contaminated soils as an important source of lead burdens to urban populations: Perspectives in Biology and Medicine, v. 53, no. 1, p. 31-45.

Finster, M. E., Gray, K. A., and Binns, H. J., 2003, Lead levels of edibles grown in contaminated residential soils: a field survey: Science of the Total Environment.

Gallagher J, 2010, Reimagining Detroit: Opportunities for Redefining an American City. Wayne State University Press, Detroit, MI. 166 pp.

Goovaerts, P, 1997, *Geostatistics for Natural Resource Evaulation*, Oxford University Press, New York, 483 pp.

Gustafsson, J., Tiberg, C., Edkymish, A., and Kleja, D., 2011, Modelling lead(II) sorption to ferrihydrite and soil organic matter: Environmental Chemistry, v. 8, no. 5, p. 485-492.

Isaaks, E.H., & Srivastava, R. M., 1989, *An Introduction to Applied Geostatistics*, Oxford University Press, New York, 561 pp.

ITRC (Interstate Technology & Regulatory Council). 2012, *Incremental Sampling Methodology*. Interstate Technology & Regulatory Council, Incremental Sampling Methodology Team, Washington, D.C., ISM-1.

Jusko, T. A., Henderson, C. R., Lanphear, B. P., Cory-Slechta, D. A., Parsons, P. J., and Canfield, R. L., 2008, Blood lead concentrations < 10 mu g/dL and child intelligence at 6 years of age: Environmental Health Perspectives, v. 116, no. 2, p. 243-248.

Lanphear, B. P., Hornung, R., Khoury, J., Yolton, K., Baghurstl, P., Bellinger, D. C., Canfield, R. L., Dietrich, K. N., Bornschein, R., Greene, T., Rothenberg, S. J., Needleman, H. L., Schnaas, L., Wasserman, G., Graziano, J., and Roberts, R., 2005, Low-level environmental lead exposure and children's intellectual function: An international pooled analysis: Environmental Health Perspectives, v. 113, no. 7, p. 894-899.

Maddaloni, M., Lolacono, N., Manton, W., Blum, C., Drexler, J., and Graziano, J., 1998, Bioavailability of soilborne lead in adults, by stable isotope dilution: Environmental Health Perspectives, v. 106, p. 1589-1594.

McBridge, M., Mathur, R., and Baker, L., 2011, Chemical Extractability of Lead in Field-Contaminated Soils: Implications for Estimating Total Lead: Communications in Soil Science and Plant Analysis, v. 42, p. 1581-1593.

McClintock, N., 2012, Asessing soil lead contamination at multiple scales in Oakland, California: Implications for urban agriculture and environmental justice Applied Geography, v. 35, p. 460-473.

McKillup, S., and Dyar, M. D., 2010, *Geostatistics Explained: An Introductory Guide for Earth Scientists*, Cambridge University Press, Cambridge, United Kingdom. 396 pp.

Mielke, H. W., Laidlaw, M. A. S., and Gonzales, C. R., 2011, Estimation of leaded (Pb) gasoline's continuing material and health impacts on 90 US urbanized areas: Environment International, v. 37, no. 1, p. 248-257.

Mielke, H. W., and Reagan, P., 1998, Soil is an Important Pathway of Human Lead Exposure: Environmental Health Perspectives, v. 106, p. 217-229.

Milillo, T., Sinha, G., and Gardella, J. A., Jr., 2012, Use of geostatistics for remediation planning to transcend urban political boundaries: Environmental pollution (1987), v. 170, p. 52-62.

NIST (National Institute of Standards and Technology), 2008, Stadnard Reference Material 2585: Trace Elements in Soil Contianing Lead from Paint. Gaithersburg, MD.

Paustenbach, D. J., Finley, B. L., and Long, T. F., 1997, The Critical Role of House Dust in Understanding the Hazards Posed by Contaminated Soils: International Journal of Toxicology, v. 16, p. 339-362.

Que Hee, S. S., Peace, B., Clark, C. S., Boyle, J. R., Bornschein, R. L., and Hammond, P. B., 1985, Evolution of efficient methods to sample lead sources, such as house dust and hand dust, in the homes of children: Environ Res, v. 38, no. 1, p. 77-95.

Raymond, R. E., Tarr, H., and Tufts, M., GIS Collaboration leads to a better understanding of the impact of elevated blood lead levels on student achievement, *in* Proceedings ESRI Health GIS Conference, Denver, CO, 2010. http://proceedings.esri.com/library/userconf/health10/docs/gis_collaboration.pdf

Reis, A. P., Da Silva, E. F., Sousa, A. J., Matos, J., Patinha, C., Abenta, J., and Fonseca, E. C., 2005, Combining GIS and stochastic simulation to estimate spatial patterns of variation for lead at the Lousal mine, Portugal: Land Degradation & Development, v. 16, no. 2, p. 229-242.

Remy, N., Boucher, A., and Wu, J., 2009, *Applied Geostatistics with SGeMS: A User's Guide*, Cambridge University Press, New York, 263 pp.

Ruby, M. V., Davis, A., Schoof, R., Eberle, S., and Sellstone, C. M., 1996, Estimation of lead and arsenic bioavailability using a physiologically based extraction test: Environmental Science & Technology, v. 30, no. 2, p. 422-430.

Ruby, M., Schoof, R., and W, B., 1999, Advances in evaluating the oral bioavailability of inorganics in soil for use in human health risk assessment: Environmental Science & Technology, v. 33, no. 21, p. 3697-3705.

Saito, H., and Goovaerts, P., 2002, Accounting for measurement error in uncertainty modeling and decision-making using indicator kriging and p-field simulation: application to a dioxin contaminated site: Environmetrics, v. 13, no. 5-6, p. 555-567.

Schwarz, K., Pickett, S. T. A., Lathrop, R. G., Weathers, K. C., and Pouyat, R. V., 2012, The effects of the urban built environment on the spatial distribution of lead in residential soils: Environmental pollution (1987), v. 163, p. 32-39.

Shinn, N. J., Bing-Canar, J., Cailas, M., Peneff, N., and Binns, H. J., 2000, Determination of Spatial Continuity of Soil Lead Levels in an Urban Residential Neighborhood: Environmental Research, v. 82, p. 46-52.

Stanek, E. J., Calabrese, E. J., and Xu, B., 2012, Meta-Analysis of Mass-Balance Studies of Soil Ingestion in Children: Risk Analysis, v. 32, no. 3, p. 433-447.

TRW (Technical Review Workgroup), 2000, Short Sheet: TRW Recommendations for Sampling and Analysis of Soil at Lead (Pb) Sites, Washington, DC 20460, EPA #540-F-00-010.

Turner A.H., 2009, Urban Agriculture and Soil Contamination: An Introduction to Urban Gardening. University of Louisville, Louisville, KY. 20 pp.

U.S. EPA, 1994, Guidance Manual for the Integrated Exposure Uptake Biokinetic Model for Lead In Children, U.S. Environmental Protection Agency, Washington, D.C., EPA/540/R-93/081, PB93-963510.

U.S. EPA, 1994b, Technical Support Document: Parameters and Equations Used in the Integrated Exposure Uptake Biokinetic Model for Lead in Children (v. 0.99d), United States Environmental Protection Agency, Washington D.C.

U.S. EPA, 1997a, Exposure Factors Handbook-Fruit and Vegetable Intake, United States Environmental Protection Agency, Washington D.C. http://www.epa.gov/ncea/efh/pdfs/efh-chapter09.pdf

U.S. EPA, 1997b, Exposure Factors Handbook: Soil Ingestion and Pica, United States Environmental Protection Agency, Washington D.C. http://www.epa.gov/ncea/efh/pdfs/efh-chapter05.pdf

U.S. EPA, 1998, Sources of Lead in Soil: A Literature Review, United States Environmental Protection Agency, Washington D.C, EPA 747-R-98-001a.

U.S. EPA, 2000, Region VIII Superfund Program Residential Soil Lead Sampling Guidance Document, United States Environmental Protection Agency, Denver, CO 80202-2466.

U.S. EPA, 2001, Lead; Identification of Dangerous Levels of Lead; Final Rule, United States Environmental Protection Agency, Washington D.C., 40 CFR Part 745.

U.S. EPA, 2003, Superfund Lead-Contaminated Residential Sites Handbook, United States Environmental Protection Agency, Washington D.C., OSWER 9285.7-50.

U.S. EPA, 2007, Estimation of Relative Bioavailability of Lead in Soil and Soil-like Materials Using *In Vivo* and *In Vitro* Methods, United States Environmental Protection Agency, Washington D.C, OSWER 9285.7-77

U.S. EPA, 2007b, Method 3051A - Microwave Assisted Acid Digestion of Sediments, Sludges, Soils, and Oils, U.S. Environmental Protection Agency, Washington, D.C.

U.S. EPA, 2010, Revisions to Lead Ambient Air Monitoring Requirements; Final Rule, United States Environmental Protection Agency, Washington, D.C., 40 CFR Part 58.

U.S. EPA, 2013, America's Children and the Environment, 3rd edition, United States Environmental Protection Agency, Washington, D.C., EPA 240-R-13-001.

Zia, M. H., Scheckel, K. G., and Chaney, R. L., 2010, Fractional Bio-Accessibility: A New Tool with Revised Recommendations for Pb Risk Assessment for Urban Garden Soils and Superfund Sites, 2010 International Annual Meetings, Green Revolution 2.0: Food+Energy and Environmental Security: Long Beach, CA, ASA, CSSA, and SSSA

ABSTRACT

QUANTIFYING THE RISKS OF SOIL LEAD IN URBAN COMMUNITY GARDENS: SAMPLING TO ACCOUNT FOR SPATIAL VARIABILITY

by

LAUREN E. BUGDALSKI

August 2013

Advisor: Dr. Lawrence D. Lemke

Major: Geology

Degree: Master of Science

Urban gardening has recently gained popularity as a way to provide fresh produce and income to urban residents; however, finding suitable sites for urban gardens is challenging because of historical soil lead contamination particularly in post- industrial cities like Detroit, Michigan. Soil lead measurements from three Detroit gardens were modeled using geostatistical techniques to assess risk and alternate sampling strategies. General sampling recommendations for urban gardens were developed based on results of Monte Carlo simulations and associated risk assessment. Variograms and kriged concentration maps indicate spatial variability at scales as small as one meter, with site specific variability in spatial patterns. Sampling plans designed to detect hotspots are found to be more protective of human health than plans designed to determine a representative or global mean concentration. Additional recommendations include sampling with a grid-based design and taking more than two samples with minimal, if any, compositing of samples.

AUTOBIOGRAPHICAL STATEMENT

I, Lauren Bugdalski, was born and raised in southeastern Michigan. I graduated from L'Anse Creuse High School-North in 2007 and began my undergraduate studies at Wayne State University soon after. My initial academic interest was in applying to pharmacy school, but I soon realized that I was not very passionate about the subject. In my sophomore year of college, I befriended a student who was enrolled in the Environmental Science program at Wayne State, and after taking only one of the program's core classes, I decided to change my major. I earned a Bachelor's of Science in Environmental Science in May of 2011, with plans to begin graduate studies at Wayne State in the fall of 2011. During the summer of 2011, I was an intern for RTI Laboratories, an environmental chemistry lab. I had developed an interest in numerical modeling and geostatistics during my undergraduate coursework and research and pursued this interest further in graduate school. After completion of my Master of Science in Geology, I will begin employment with AMEC Earth and Infrastructure, an engineering consulting firm, as an Environmental Geologist.